ABSTRACT

Title of Thesis:	THE PROBIOTICS OF BIOFUEL: A METAGENOMIC STUDY OF MICROALGAE GROWN FOR FUEL PRODUCTION
	Samuel Russell Major, Master of Science, 2018
Thesis Directed By:	Dr. Russell T. Hill, Professor, Institute of Marine and Environmental Technology, University of Maryland Center for Environmental Science

Ponds in Frederick, MD were fertilized with chicken manure to increase the nutrient load in the water and stimulate microalgal growth. Nutrient analyses indicate that fertilization results in significant increases in the DOC, TDN, and TDP. The bacterial and eukaryotic microalgal communities were analyzed using 16S and 18S rRNA gene sequencing, respectively. Communities were analyzed pre-fertilization and for 15 days following fertilization. Molecular data reveals a decrease in diversity as microalgal blooms form. The microalgal density increased following fertilization, with enrichment for the *Chlamydomonadales* order. Prior to fertilization the bacterial communities were dominated by five phyla: *Actinobacteria*, *Bacteroidetes*, *Cyanobacteria*, *Proteobacteria*, and *Verrucomicrobia*. Dominant bacterial genera post-fertilization included *Flavobacterium*, *Limnohabitans*, and *Polynucleobacter*. Bacteria isolated from the ponds were screened for effects on *Scenedesmus* sp. HTB1

to identify bacteria that either enhance or inhibit microalgal growth. The growth-promoting bacteria were closely related to bacteria found to be enriched during microalgal bloom formation.

THE PROBIOTICS OF BIOFUEL: A METAGENOMIC STUDY OF MICROALGAE GROWN FOR FUEL PRODUCTION

by

Samuel Russell Major

Thesis submitted to the Faculty of the Graduate School of the
University of Maryland, College Park, in partial fulfillment
of the requirements for the degree of
Master of Science
2018

Advisory Committee:
Professor Russell T. Hill, Chair
Professor Feng Chen
Associate Professor Yantao Li

Dedication

I would like to dedicate this work to my mother and father for their unwavering support for all my endeavors. To the beautiful Carolyn for her dedication, sacrifice, and keeping me filled with donuts and cookies during my research. And to my brother and his family; hopefully the world will be a little bit better and cleaner when Chase and Olivia can read this.

Acknowledgements

I would like to thank my advisor Dr. Russell Hill for taking a chance and granting me the opportunity to become a better scientist. His patience and advice has pushed me to learn new skills I never imagined I would learn. Thank you to my committee members Dr. Feng Chen and Dr. Yantao Li for their guidance through the microalgal world. My kindest regards go out to Dr. Ryan Powell and all of Manta Biofuel for allowing us to perform the research. A giant thanks to all my interns Ema Pagliaroli, Deanna Stephens, Lily Xiao, and Bryanna Sanders for their aid in executing experiments and tolerating my teaching style as I tried to teach them the intricacies of molecular biology. Also, I would like to acknowledge the patience and assistance of IMET's all-star bioinformaticians: Tsetso Bachvaroff, Ryan McDonald, and Amanda Maggio. The entire Hill lab, Hanzhi Lin, Daniela Tizabi, Lauren Jonas, Taylor Carter, Billie Beckley, and Jan Vincente, all deserve an extra slice of cake as well for listening to my terrible jokes, even worse singing, and I'm sorry if you ever caught me dancing.

Table of Contents

List of Tables

List of Figures

List of Abbreviations

TDN Total Dissolved Nitrogen

TDP Total Dissolved Phosphorus

DOC Dissolved Organic Carbon

CFB Cytophaga-Flavobacterium-Bacteroides group

HTB1 *Scenedesmus* sp. HTB1

CC503 *Chlamydomonas reinhardtii* CC503

RAI5 *Desmodesmus* sp. RAI5

Chapter 1: Microalgae: from their evolution to an energy revolution

1.1 Algae evolution, diversity, and current technological uses

Prior to the evolution of cyanobacteria, a young planet Earth was nearly devoid of oxygen. This changed during the "Great Oxidation Event" that occurred 2.4 billion years ago (1). The earliest stages of the Great Oxidation Event may have begun more than a billion years prior to the deduced timing of the observed event (2–5). The increase in molecular oxygen allowed for the proliferation of ancient life forms that were able to adapt to this dramatic change in the ocean's biogeochemistry. The diversity of the surviving prokaryotic life forms provided the first steps to creating ancient eukaryotic algae. The endosymbiosis of an *Alphaproteobacteria* by another prokaryote to form an early heterotrophic protist is estimated to have happened 1,200 million years ago (6). The first lineages of photosynthetic eukaryotic organisms are theorized to have occurred in a singular evolutionary event (termed primary endosymbiosis) when heterotrophic protists captured cyanobacteria and integrated them within their cells as plastids to make the first eukaryotic algae (7–10).

Through molecular, phylogenetic, and ultra-structural studies of algal plastids, the algal lineage has been determined to be a diverse monophyletic group (5, 7, 11–13). The first plastid acquired by a protist is aptly named the "primary plastid" and is found in three lineages with unique characteristic plastids: the glaucocystophytes, the red-algae, and the green algae and plants (9, 14–16). As the algae became increasingly abundant, further endosymbiotic events occurred, creating a remarkable

diversity within the "algal" lineages, eventually including multicellular macro alga such as the kelps.

These subsequent evolutionary events, termed "secondary endosymbiosis", involved the ingestion of a green or red alga by another eukaryote to create the chlorarachniophyta and the cryptomonads, respectively. Upon ingestion, the cells inherited four organellar genomes: a plastid, a nucleus, mitochondria, and a remnant of the ancestral endosymbionts' nucleus called a nucleomorph (17, 18). Several taxa, including euglenoids, heterokonts, diatoms, and haptophytes, do not contain a nucleomorph, but still are thought to be derived from secondary endosymbiosis as their plastids are closely related to green and red algae (19–21). To further advance the endosymbiotic route of evolution, some dinoflagellates (particularly ancestral *Karenia brevis*) have been shown to contain the plastid from haptophytes producing peridinin, which subsequently became replaced with an accessory pigment, fucoxanthin, through another tertiary symbiosis (22, 23). Though the plastid is of a monophyletic origin in the Archaeplastida group; the remarkable diversity and succession of endosymbiotic events has resulted in microalgae becoming a deeply branched set of polyphyletic organisms (17), as a result of the complex series of endosymbiosis events as illustrated in figure 1.

Given the diversity of the algal lineage, algae have evolved numerous mechanisms that allow them to both survive and proliferate under a wide range of environmental conditions. Many of these evolutionary traits that have enabled microalgae to become resilient around the world have also resulted in great human interest for ways to use algae, culminating in the current interest in algal

biotechnology. The first recorded use of microalgae dates to a famine in China 2,000 years ago when humans consumed *Nostoc*, a cyanobacterium, in order to survive (24). It is now common to eat other types of algae to either augment our foods as in the use of seaweeds with sushi, or as dietary supplements such as those comprised of *Spirulina*. Current research examining the high lipid content of eukaryotic microalgae extends their use as a potential source of cooking oil that may be cheaper than conventional plant oils and with added health benefits (25).

Beyond the use of algae as a food product, algae have additional desirable characteristics that make them suitable for production of other useful commodities. For example, some algae have a high concentration of carotenoids with antioxidative properties which have shown to have applications in human medicine (26–28). Physiologically, the carotenoids in algae and in higher plants act both to harvest light energy as well as protect the chloroplast light-harvesting antennae from photo-oxidative damage (29–31). Microalgae also produce large quantities of lipids, making them not only a suitable source of nutrition for both agricultural and human purposes, but also the high accumulation of lipids make microalgae an attractive source for biofuels (32–39).

Microalgae are one of the oldest and most diverse groups of organisms on the planet, with evidence tracing their ancestry to the pre-Cambrian era (more than 540 million years ago). Fossil fuels mined from China contained compounds that are similar to hydrocarbons produced by modern algal species (40). The combustion of these fossil fuels powers our vehicles, but consequently releases CO_2 into the environment, contributing to global climate change (32). Alternative energy sources,

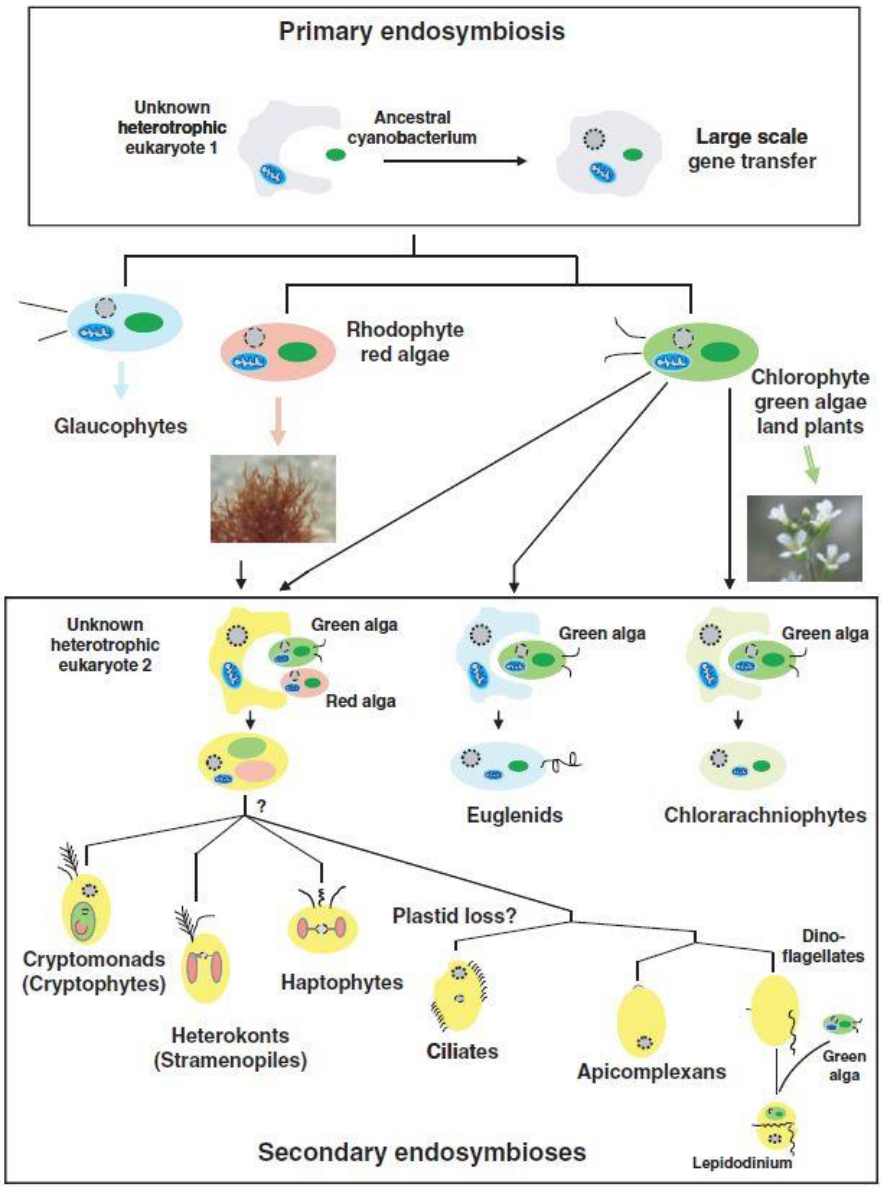

Figure 1.1: Schematic diagram summarizing the endosymbiotic events resulting in algal diversity. Primary endosymbiosis involved the engulfment of a cyanobacterium by a heterotrophic aerobic bacterium resulting in the Glaucophytes, the Rhodophytes (red algae), and the Chlorophytes (green algae and land plants). The resulting red and/or green algae were further engulfed by another heterotrophic green algae in a secondary endosymbiotic event leading to the Diatoms (heterokonts) and the diatoms (5).

such as wind and solar power, continue to grow in popularity, but they also have their own technical issues and infrastructure problems. Wind energy requires large investments to expand the infrastructure to cities in low wind areas. These large wind turbines have also been to blame for affecting wildlife, namely killing birds and bats who fly into the turbines (41) (https://energy.gov, accessed May 2017). Solar energy is becoming more attractive for small roofs, but the solar panels themselves are large, expensive, and not efficient enough to power large communities without sacrificing usable land (https://understandsolar.com, accessed May 2017). As an alternative to traditional fossil fuels that require drilling and increased risks of oil spills, microalgal-derived biofuels can be generated in virtually any environment with minimal impact on wildlife and can utilize the already established petroleum-based infrastructure.

1.2 Algae as a biofuel

In 1978, President Jimmy Carter and the U.S Department of Energy's Office of Fuels Development created the Aquatic Species Program, whose focus was to produce biodiesel from algae grown in outdoor ponds using CO_2 waste from coal burning power plants. Though the program was terminated in 1996, research was not abandoned (32). The U.S Department of Energy continued to recognize the potential efficiency of algal-derived biofuels over terrestrial-plant based biofuels (41, 42). Bioenergy from algal feedstocks provides several advantages over traditional biofuels from crops such as corn or sugar cane: 1) Microalgae can grow in ponds on non-arable land, and therefore do not compete with food crops for fertile land; 2) Algae can grow in wastewater for the dual purpose of mitigating the effects of agricultural runoff contamination; 3) Microalgae can double their biomass much faster than their

terrestrial plant counterparts; and 4) They are carbon neutral, meaning the carbon released from the combustion of the biofuel was directly fixed from CO_2 in the atmosphere (32–34, 43).

Land based biofuels such as corn, soy, or palms are estimated to require 24% of the United States' cultivable land to meet 50% of the U.S fuel needs. The conversion of previously undisturbed ecosystems to crop-land for biofuel production would result in greater release of CO_2 than a given crop can fix, creating a counterproductive practice (44, 45). Alternatively, microalgae would only require 1-3% of cultivable land and can be maintained in a dedicated culturing vessel as opposed to being subjected to crop rotations like many other terrestrial biofuel-producing plants (33, 43, 46).

Microalgae are useful indicators to the health or trophic state of aquatic environments (47–52). It has been well established that microalgal growth and diversity are tightly correlated with the concentration of available phosphorous (53–57). Models relating algal biomass to the total phosphorus in ponds have been used as a proxy for potential productivity (55, 57, 58). However, phosphorous is not the only limiting factor for algal growth, but rather their growth obeys Liebig's Law of the Minimum (59, 60). Regression analyses on chlorophyll *a* with total phosphorus and total nitrogen found that both nutrient concentrations were significantly related with the chlorophyll *a* biomass proxy (61). Redfield (1958) defined a ratio of carbon-to-nitrogen-to-phosphorus (106:16:1) that is required to maintain growth of microalgae. Large ratios indicate that phosphorus is the limiting nutrient; smaller ratios imply that carbon or nitrogen is a limiting factor. When the nutrient concentrations in a water

source increases, the water source is said to undergo eutrophication; it becomes eutrophic. Anthropogenic interactions with these water sources have been identified as the major contributor of both nitrogen and phosphorus to marine, estuarine, and freshwater systems (62). The eutrophication of these aquatic environments creates a suitable habitat for microalgae which can result in a bloom. The ability of microalgae to proliferate in eutrophic waters make them a suitable tool for mitigating wastewater run-off (63–65). Industrial by-products including flue gas have also been used to supply microalgae cultures with CO_2 for the dual purpose of enhancing growth of the culture and mitigating CO_2 output from a power-plant (66–68).

Though fossil fuels have been the driving force behind industrial proliferation, the byproducts from their combustion have silent and long-lasting effects. Traditional fossil fuels have been heavily implicated in global climate change, primarily by releasing greenhouse gases such as CO_2. It has been estimated that the energy sector is responsible for approximately 70% of anthropogenic effects due to the production of greenhouse gases from the expenditure of non-renewable fossil fuels (69). The emission of CO_2 presents a long-standing problem; a portion of the released greenhouse gas has been shown to decay within 3-4 years, but the larger portion has been modeled to decay much slower, lasting more than 200 years. It should be noted that these models are often complicated by some confounding factors such as plant biomass and gas exchange with the ocean surface (70). The danger of consuming such high quantities of fossil fuels like coal, oil, or natural gas is the release of long sequestered carbon sources into the atmosphere which in turn have been correlated with global climate change and ocean acidification (71, 72). This is where the

advantage of algal biofuels would play a crucial role to halt the accumulation of CO_2 in the atmosphere. Because they are photosynthetic organisms, they acquire carbon from the atmosphere to generate biomass. When the biomass of the algal feedstock is converted into a combustible fuel source, only the carbon fixed from their growth is released back into the atmosphere, earning this process the label "carbon-neutral."

1.3 Biofuel production

The advantage of photobioreactors and the construction of raceway ponds to grow algae *en masse* has allowed researchers to manipulate cultures of microalgae to experiment with and identify industrially useful strains, particularly those that produce a variety of fatty acids, or lipids (34, 41, 42). Biodiesel is traditionally derived from the transesterification of linear chain fatty acids (73), which many algae are capable of creating in a form called triacylglyceride (TAG). TAG is a product from the diacylglycerol acyltransferase (DGAT) genes. Typically, lipid synthesis is induced by stressing a microalgal culture with light, pH, or nutrient starvation. The culture is then harvested and dried to produce an algal paste, after which chemical-based lipid extraction is performed to harvest the lipids for conversion to biofuel (33, 37, 74).

However, problems with mass production paired with laborious methods needed to extract lipids and convert them into biofuel has made this strategy cost prohibitive (75). Transesterification requires the use of an organic solvent at a minimum ratio of 3:1 moles of solvent to TAG, but is often used in excess to favor the formation of methyl esters (33, 76). Other co-products from processes that extract high-value products via transesterification and fermentation can be used in a number of

industries (77). Alternative methods to generate biocrude, a mix of different sized hydrocarbons, such as liquefaction, bypasses the need for a solvent extraction step. This reduces the cost for expendables and re-focuses the priority on the efficiency of fuel conversion. For this reason, multi-fraction processing studies have been performed to produce the maximum energy from a culture of algae and to study what is required for microalgal-derived biofuels to become a viable product (78, 79). In 2010, Ross *et al.* showed that different types of microalgae can be converted into biocrude oil through a process called hydrothermal liquefaction (HTL) (80). Subsequently, Zhou *et al.* (2013) introduced the "Environmental- Enhancing Energy" (E^2-Energy) system that locally recycles nutrients from wastewater and continuously converts low-oil, mixed algal-bacterial biomass into biocrude using HTL (78). Using a mathematical model, Zhou *et al.* predicted that E^2-Energy operations could amplify the biomass and biofuel production using wastewater by up to 10 times (78).

HTL is a process that treats biological materials with high temperature and pressure to convert any biomass, including carbohydrates, proteins, and lipids into biocrude (81). HTL has become a more attractive route for biofuel production due to its non-discriminating method of converting organic compounds into biocrude (82). Biocrude production via HTL relies on the amount of biomass available, reducing the need to manipulate the algae's metabolic physiology and instead focusing on how to optimize biomass production. It should be noted that having a high-quality lipid-containing feedstock may yield higher quantities of alga-derived biofuels after hydrothermal liquefaction (83–85). The mass production of algal biofuels will likely be achieved in large outdoor ponds rather than closed photobioreactors due to the

high capital associated with closed systems (86). It is impossible to maintain axenic (bacteria-free), or even uni-algal cultures during the growth phases of microalgae in large open ponds. Although, it has been found that highly-diverse microalgal communities (known as polycultures) are more efficient at nutrient utilization, produce more biomass, and contain a higher carbon content compared with monocultures (57, 87, 88). Algal biomass and lipid content has been shown to be positively associated with communities rich in species diversity (87, 89, 90). Interestingly, eutrophication has been shown to reduce the species diversity, indicating a selection process for species that are more suited to thrive in nutrient rich conditions (91–94). When algae are grown in large open ponds, the culture is subject to invasion by microalgal-predators such as *Daphnia* species and can cause the cultures to "crash" or die (95, 96). Efficient open pond cultures will require a thorough understanding of how blooms of microalgae develop, how they interact with their associated bacterial communities, and how this may affect the biocrude end-product (43).

1.4 Bacteria to improve algae-derived biofuels

From a biological standpoint, the symbiotic relationship between algae and bacteria that leads to a successful bloom is a "black box" that is little studied and poorly understood. As an algal bloom develops, the community composition of the associated bacteria changes dynamically; the interactions between the algae and the bacteria change due in part to environmental conditions (97). Several studies have shown that approximately 50% of microalgae are dependent on bacteria for vitamin B_{12} (98–100), suggesting the existence of specific algal-bacterial associations. One

meta-analysis showed that 101 bacterial isolates from 40 macro- and microalgae only represented six phyla of bacteria (101, 102). Marine diatom species have also been shown to be associated with specific bacterial species (101, 103). A study of bacterial host specificity associated with freshwater phytoplankton revealed differences between the attached and free-living bacterial communities, suggesting that algal-bacterial associations are varied and complex (103, 104) .

A metagenomic analysis on the bacterial community associated with *C. sorokiniana* cultures in a photobioreactor identified a fungus as well as the actinobacteria *Microbacterium trichotecenolyticum*, to promote the growth of the microalga (105). Numerous studies have revealed that individual bacterial isolates can promote microalgal growth in communities, with mechanisms of the interactions ranging from the bacteria fixing nitrogen to sharing bioactive compounds (105–108). Specifically, a bacterium, *Azospirillum* sp., produces an auxin called indole-3-acetic acid (IAA) that is proposed to be transferred to *Chlorella* cells, promoting growth (109–111). This has been shown to be a reciprocal relationship; microalgal cells release oxygen along with carbon sources to promote bacterial growth which, in turn, produce the two compounds required for the bacteria to produce IAA (105, 112–114).

The harvested microalgal biomass used for HTL conversion inevitably includes the bacterial community associated with the algae growing in an open pond. It should be noted that Stockenreiter *et al*. (2012) demonstrated that polycultures of microalgae exhibited increased lipid production in both natural and laboratory cultures (90). Though the diversity of microalgae may influence lipid production, no bacterial enumeration or identification was performed on the cultures.

To date, no studies have performed experimental metagenomic analyses on the impact that the microalgal microbiome has on the diversity of microalgae in open-pond systems. Therefore, the following research proposes to characterize the bacterial and microalgal communities that simultaneously change in the days following eutrophication. The ponds were fertilized with chicken manure which resulted in significant increases in the nutrient concentrations. Next generation sequencing methods were employed to molecularly distinguish the bacterial and microalgal communities using the 16S rRNA and 18S rRNA genes. Changes in the communities were tracked pre- and post-fertilization, with the aim of identifying dominant microalgae and bacteria that cohabitate the same space. The bacterial communities were also cultured to screen individual isolates for symbiotic interactions between the two domains.

Chapter 2: Diversity of bacterial communities associated with microalgae grown for biofuel production in man-made ponds following artificial eutrophication

2.1 Abstract

In the natural environment microalgae live in symbiosis with bacterial partners and that can have variable effects on each other's growth. In the present study, three artificial ponds filled with five million liters of water from a local stream were each fertilized with five tons of chicken manure to stimulate a bloom of microalgae. The bacterial community diversity was determined by 16S rRNA gene-based sequencing over a period of 15 days to track temporal community changes. Each pond contained an innate characteristic bacterial community prior to the fertilization. Introduction of the fertilizer inoculated the ponds with bacteria present in the manure, though these taxa were not capable of persisting in the pond environment. Fertilization of the ponds significantly increased the total dissolved nitrogen and total dissolved phosphorus in pond water. The most predominant changes in the bacterial communities occurred within the autochthonous populations rather than as a result of bacteria introduced with the manure. Analysis of the genera that rose to dominance post fertilization showed enrichment of bacterial lineages associated with the algal phycosphere.

2.2 Introduction

It has long been understood that the health and fitness of multicellular plants are affected by the bacterial symbionts that colonize the soil around the roots, called the rhizosphere (115). Similarly, within the aquatic environment, bacteria that reside in the area immediately adjacent to phytoplankton are said to be within the "phycosphere" (116). The bacteria that reside in these areas that are associated with green algae and plants have been referred to as plant growth promoting rhizobacteria (PGPR) or plant growth promoting bacteria (PGPB) (117–119). Contributions of the bacteria to the plants or algae can include producing phytohormones (auxins), dissolving organic rock phosphate, producing vitamins, and creating antibiotics to ward off pathogens (98, 110, 114, 120–126). It is worth noting that these relationships are not limited to the bacteria working for the algae but can be a mutual interaction. Cho *et al*. (2015) not only showed that an artificial microalgal-bacterial consortium produced higher lipid content and quality, but that the consortium of bacteria and microalgae may be able to switch from commensal symbiosis to mutual symbiosis depending on the growth phase (127). This type of change in the symbiotic relationship is referred to as the continuum model (128). Recently, researchers have proposed engineering the microbiomes of plants and animals with the aim of improving their growth, productivity, and overall health (129).

The word "algae" is a colloquial term referring to a general group of polyphyletic primary producers typically associated with bodies of water but are also found in soils and in symbiosis with fungi (i.e: lichens) (130, 131). Algae are one of the oldest and most diverse groups of organisms on the planet with evidence tracing

their ancestry to the pre-Cambrian era (more than 540 million years ago). Fossil fuels mined from China were analyzed for their composition and revealed compounds that are similar to hydrocarbons produced by modern algal species (40). These hydrocarbons are the result of photosynthesis; the process that converts atmospheric CO_2 to oxygen. Algae and cyanobacteria are responsible for approximately 75% of the primary production on the planet. The ability of micro algae to produce lipids has provided the world's economy with such products as DHA, β-carotene, and various plastics (132). Solazyme, a major producer of algae-based products, has released a high oleic acid cooking oil produced from algae (133).

Along with generating fossil fuels, algae also produce triacylglycerols that can be harvested and transformed into biofuels that provide an alternative to mined petroleum fuels (37). However, problems with mass production, lipid extraction, and converting the lipids to a useable fuel source has made this strategy cost prohibitive (75). Research continues in efforts to make algal-derived biofuels economic because, unlike other plant-based biofuel sources, algae can be grown relatively quickly in wastewater and on non-arable land, making optimization of these processes key to placing algae at the forefront of biofuel production. Experimental yields of oil from biomass has demonstrated that high-yield oil terrestrial crops would require 24% of the United States' cultivable land to meet 50% of the US transportation fuel demands, whereas microalgae would require only 1-3% of cultivable land to provide 50% of U.S fuel needs (33, 43).

The process of hydrothermal liquefaction can be used to turn algal biomass into biocrude oil, regardless of the lipid content, although having a higher proportion

of lipids to proteins will increase the yield of the resulting biocrude (83, 84). To produce algae at a large enough scale to make the production financially feasible, culturing methods using large raceway ponds or open fertilized ponds have been proposed. These types of culturing methods are not conducive to axenic (bacteria-free) or maintaining unialgal cultures which make the growth of microalgae a dynamic process and rather unpredictable, though some bacteria are often required for healthy algal growth. Several studies have shown that approximately 50% of microalgae are dependent on bacteria for vitamin B_{12} and that a species of *Chlorella* will grow more quickly when co-cultured with various bacterial isolates, and even a fungus (98, 105). Specifically, an *Azospirillum* species has been described that produces an auxin called indole-3-acetic acid (IAA) that has been proposed to be transferred from the bacteria to *Chlorella* cells to promote growth (110, 125). The microalgal cells release carbon sources for bacterial growth along with two compounds required for the bacteria to produce IAA (113). However, until recently, the evidence for the exchange of these metabolites has been "circumstantial".

In this study, multiple ponds were fertilized with a high nutrient manure and the microalgal and bacterial communities in ponds were monitored prior to and post fertilization using high-throughput sequencing and 16S ribosomal RNA gene sequencing identification techniques. The monitoring of the nutrient concentrations in conjunction with studying the microbial ecology in the ponds provides insights into the co-occurring bacterial communities that are present with the microalgae that are grown in open-pond polycultures. Detailed analyses of the bacteria associated with microalgal blooms provides insights into those bacteria specifically associated with

microalgae as well as bacteria that have beneficial or deleterious effects on microalgal growth.

2.3 Methods

2.3.1 Sample collection and processing

In the summer of 2016, pond 1 (labeled 1_F16) and pond 5 (5_F16) about 1 acre each, in Frederick, MD, were filled with approximately 5 million liters of freshwater water from a nearby stream. Each pond was then fertilized with 5 tons of chicken manure to stimulate blooms of microalgae. Fertilizer was introduced into the ponds on Day 0 after sample collection. The first sample collection of fertilized water occurred on Day 1, approximately 24 hours post-fertilization. Different nutrient dispersal strategies were used in each of the two ponds in 2016. In 1_F16, an active nutrient dispersal system utilized an out-board motor to circulate the water and fertilizer as the manure was dumped into the pond. In 5_F16, a passive nutrient dispersal strategy was used in which the manure was placed onto the edge of the pond and a hose was used to spray masses of manure into the pond. This strategy relied on the natural movement of the pond water to spread the nutrient throughout the pond over time. Fertilization of each pond occurred 17 days apart. A third, unfertilized pond, pond 2 (2_F16), was also sampled at the end of the experiment in October of 2016 to assess community variability between ponds. In 2017, pond 1 (1_F17) was filled and fertilized again using the same active nutrient dispersal method. The same unfertilized pond was sampled in parallel to the fertilized pond in 2017 (2_F17) (Table 2.1).

Replicate water samples from the center and at either pole of each pond were collected from the top six inches of the water of each pond (Fig. A2.1). Samples were collected with sterile carboys covered with a 200 µm mesh to eliminate large particles

Table 2.1: The sampling scheme of the experiment. Sampling site, treatment, dispersal methods, and number of replicates is provided. Control treatment refers to a pond that had never been fertilized. Two dates in the control pond, 2_F16, are not listed and were sampled on October 4, 2016 and October 6, 2016.

				Day of Experiment						
ID	**Site (Year)**	**Treatment**	**Dispersal Method**	**-6 (NT)**	**-1 (NT)**	**0 (NT)**	**1 (CM)**	**6 (CM)**	**12 (CM**	**15 (CM)**
1_F16	Pond 1 (2016)	Fertilized	Active	(NA)	N = 2	N = 2	N= 2	N = 2	N = 2	N = 2
5_F16	Pond 5 (2016)	Fertilized	Passive	(NA)	N = 2	N = 2	N= 2	N = 2	N = 2	N = 2
1_F17	Pond 1 (2017)	Fertilized	Active	N = 3	N = 3	N = 3	N = 3	N = 3	N = 3	N = 3
2_F17	Pond 2 (2017)	Control	none	N = 3 (NT)	N = 3 (NT)	N = 3 (NT)	N = 3 (NT)	N = 3 (NT)	N = 3 (NT)	N = 3 (NT)

and detritus. Collection occurred on the day prior to fertilization, the day of fertilization-immediately before fertilization, the day after fertilization, and then on days 6, 12, and 15 post fertilization. A seventh timepoint six days prior to fertilization was included in 2017 to monitor the stability of the native communities in the ponds (Table 2.1). All samples were stored on ice until processing. Two liters of water from each sample was aliquoted after mixing by swirling then serially filtered through 6 µm and 1 µm filters to collect microalgae and their closely associated bacterial assemblages. From this filtrate, the small and free-living bacteria were captured on 0.22 µm Sterivex^{TM} filters. The resulting filtrate was collected for quantification of the dissolved organic carbon (DOC), total dissolved nitrogen (TDN), and total

dissolved phosphate (TDP) in the ponds. The nutrient analysis was performed by the Nutrient Analytical Services Laboratory at the Chesapeake Biological Laboratory, University of Maryland Center for Environmental Science. pH values were taken from the samples collected in 2017.

Water from each sample was serially diluted and plated on R2A plates to enumerate culturable bacterial communities pre- and post-fertilization. Plates were incubated at 27^{o}C for 48 hours, until visible colonies appeared, at which point they were counted. Unfiltered water from the mixed carboy sample was diluted 1:1 in 4% formaldehyde (2% formaldehyde, final concentration), allowed to fix overnight at 4^{o}C, stained with 300 µM of DAPI, and filtered onto 0.1 µm black polycarbonate filters. Epifluorescence microscopy was used to enumerate the bacteria; chlorophyll autofluorescence was used to count the photosynthetic microbes.

An analysis of the bacterial communities within chicken manure from three sources was performed to assess the bacterial communities inoculated into the ponds upon fertilization with chicken manure. The chicken manure samples were designated A1, A2, and Manta17. Samples A1 and A2 were sourced from egg laying hens in 2017 and 2016 respectively, from a farm in Hydes, MD. Manta17 was sourced in 2017 from egg laying hens housed in chicken houses from a farm in Thurmont, MD.

2.3.2 DNA extraction, sequencing, and data processing

DNA was extracted from each sample using Qiagens DNeasy® PowerWater® (with alternative lysis steps, i.e: heating) and PowerWater® Sterivex™ kits. Duplicate DNA extractions for each filter type were performed and DNA samples from the 1 µm and 6 µm filters were pooled prior to sequencing. Each DNA sample

was normalized to 5 ng/mL prior to pooling to ensure equal representation of each of the filter fractions' community. Prior to submission for next generation sequencing, each sample had the V4 region of the16S gene amplified by PCR with 515F (5'-GTCCCAGCMGCCGCGGTAA-3') and 806R (5'-GGACTACVSGGGTATCTAAT-3') to confirm that the DNA was of sufficient quality to serve as a substrate for PCR amplification. The bacterial communities were classified based on the filter size on which they were captured; large bacteria/aggregates/close algal symbionts were collected on the 6 µm and 1 µm filters sample (x >1 µm); small/free-living/loosely associated symbionts were collected on the 0.22 µm filter (1 µm >x > 0.22 µm).

Bacterial communities were characterized by sequence analysis of the V3-V4 hypervariable region of the 16S rRNA gene using the primer pair S-D-Bact-0341-b-S-17, (5'-CCTACGGGNGGCWGCAG-3'), and S-D-Bact-0785-a-A-21 (5'-GACTACHVGGGTATCTAATCC-3') (134, 135). All sequencing was conducted on the Illumina MiSeq platform at the BioAnalytical Services Laboratory (BAS Lab) at the Institute of Marine and Environmental Technology, Baltimore, MD.

To assess the relative quantitative accuracy of the next generation sequencing platform, our bioinformatic pipeline, and our DNA extraction methods, a synthetic mock community was created with five bacterial isolates from two phyla, the *Bacteroidetes* including *Cloacibacterium normanense* IMET F and *Rudanella* sp.; and the *Proteobacteria*, including *Gemmobacter* sp., *Serratia* sp., and *Rhodobacter* sp. All cells were inoculated into 2 L of sterile deionized water in equal proportions of 1.92×10^8 cells of each bacterium. totaling 9.6×10^8 bacteria quantified by

fluorescent DAPI staining. Each bacterium included in the synthetic mock community had the DNA extracted from pure cultures using MoBio's UltraClean® Microbial DNA Isolation kit. The 16S rRNA genes were sequenced using Sanger sequencing technology with the primer pair 27F (5'-AGAGTTTGATCMTGGCTCAG-3') and 1492R (5'-TACGGYTACCTTGTTACGACTT-3'). The resulting sequences were appropriately trimmed and aligned to create the full length 16S gene sequence. NCBI BLAST was then used to extract the sequences from the five top scored matches (if available) with 97% sequence identity. These representative sequences were used as the reference database for the artificial mock community OTU picking.

The output from the MiSeq platform generated forward and reverse sequences 300 nucleotides in length for the 16S rDNA gene. Sequences were pre-processed using the CLC Genomic Workbench by importing the data as paired-end reads, quality trimming, merging overlapping pairs, and trimming all sequences to a fixed length; bacterial 16S rRNA gene sequences yielded 420 nucleotides. The resulting high-quality sequences were exported into the Quantitative Insights into Microbial Ecology (QIIME) program (136) for open reference operational taxonomic unit (OTU) picking and taxonomic classification using Uclust (137) with the Silva 128 database (138). Alignments of the representative sequences were created using Python Nearest Alignment Space Termination (PyNAST) for each OTU and were used to produce nearest-neighbor Newick formatted, mid-point rooted trees with FastTree for downstream phylogenetic analyses. Taxonomic identities were defined as having a 97% identity to the reference sequences. To account for the presence of

16S rRNA genes derived from the chloroplast and mitochondrial genomes within eukaryotic microbes, sequences that identified as either chloroplast or mitochondria were removed prior to analyses of bacterial communities.

Divisions based on the treatment type were performed and the distribution of OTU counts against the number of OTUs present were plotted. The core diversity of the communities within each treatment was defined by identifying spurious OTUs as those that did not occur 10 or more times in two samples of similarly treated ponds on the same filter size (Fig. A2.2). Uneven sampling depth was accounted for by rarefying to an even depth of 4,900 sequences per sample. Singletons were removed from the control communities and then rarefied to an even depth of 21,000 sequences.

2.3.3 Diversity and statistical analyses

All diversity analyses were performed using R and the *phyloseq* package (139). Prior to subsampling to an even depth for statistical analyses, the relative abundance of the phyla present in each pond was determined for OTUs whose relative abundance was greater than 0.1%. Uneven sampling was corrected by rarifying each sample to an even depth of 4,900 sequences per sample. After rarifying the data to an even depth, alpha-diversity was determined with the total number of observed OTUs to represent the richness, the Shannon diversity index, and Pielou's evenness index. Kruskal-Wallis tests were performed to test the alpha-diversity for statistical differences between days. Nemenyi-tests were performed *post hoc* to identify which days were most different. Three methods were used to elucidate the beta-diversity of the communities within the ponds, the treatments (fertilized or untreated), and the communities found on the filter cut-offs. Principal coordinate

analyses/multidimensional scaling plots created with Bray-Curtis dissimilarity (140) unweighted, and unweighted UniFrac (141) distance matrices were generated from the rarefied bacterial OTUs. Bray-Curtis dissimilarity uses the abundance of each of the OTUs in the samples to generate a dissimilarity matrix, whereas the weighted and unweighted Unifrac distances consider the phylogenetic distance as well as the abundance or the presence/absence of an OTU, respectively. Welch's two sample t-test was used to compare the differences between the two treatments. Due to the non-normal nature of the environmental nutrient parameters, significance between non-treated water and fertilized water as well as between each pond was tested with the Wilcoxon rank-sum test. To assess the innate natural differences and the influence of the treatment on the bacterial communities, permutational analysis of variance (PERMANOVA) was performed with the R package *vegan* using the *adonis* function (142). Analysis of similarity (ANOSIM) was used to determine the similarity between the treatments according to their Bray-Curtis dissimilarity distances. Similarity percentages (SIMPER) were then used to determine the OTUs which contribute most to the similarities within each sampling timepoint. Except where indicated, all replicate data were merged together to generate the whole pond community. Canonical correspondence analysis (CCA) was performed to correlate the influence of the nutrient data on each of the microbial communities. The significance of the nutrient data on the microbial communities was confirmed by performing Mantel tests on the microbial communities and the nutrient analyses.

2.4 Results

2.4.1 Sequence processing and control communities

Pre-processing and OTU picking resulted in a total of 11,725,950 sequences representing 271,802 OTUs. After removing the mitochondrial and chloroplast sequences from the total pool of 16S rRNA genes, 10,898,995 sequences remained (~7% reduction in sequences) with 189,927 OTUs (~30% reduction in observed OTUs). Removal of OTUs defined as spurious resulted in 9,748,049 remaining sequences and 5,445 OTUs in 144 samples, reducing the sequences and OTUs further by ~11.5% and ~97%, respectively (Fig. A2.2).

The quality of the sequencing run was assessed by including three additional samples of a mock community containing five genera processed in the same way as other samples. Quality filtering resulted in 172,005 sequences; picking OTUs against the generated representative sequences, and removing singletons reduced the data to 142,136 sequences representing 12 OTUs. All the diversity measures of the replicates fell within the same range indicating consistency between samples in the sequencing run (Fig. A2.3). The most dominant genera sequenced were the *Cloacibacterium* and *Serratia*, together making up over 90% of the community. *Rudanella* was also detected but was severely under represented, as with the other taxa that was not detected at a 0.1% community cut-off (Fig. A2.4). Rarefying the control sample to 21,000 sequences per sample yielded rarefaction curves approaching its complete sampling depth (Fig. A2.5).

2.4.2 Chicken manure bacterial communities

A survey of the bacteria in chicken manure performed on three different manure samples resulted in a total of 161,048 sequences with 18 phyla, 298 identifiable genera and 7,004 OTUs. Singletons and doubletons were removed. The four dominant phyla were the *Actinobacteria*, *Bacteroidetes*, *Firmicutes*, and the *Proteobacteria* (Fig. A2.6). While the bacterial community composition was similar, of the 7,004 OTUs detected between all three samples, only 75 OTUs belonging to 31 genera were shared between all three samples. The most abundant genera in the shared taxa were *Jeotgalicoccus*, *Corynebacterium*, *Atopostipes*, and *Peptoclostridium*. OTUs that were shared between the manure and the experimental ponds represented less than 1% of the community prior to fertilization and peaked immediately after fertilization when they made up an average of 6.8% of the community and continued to become less prolific over time, being below 2% at day 6 and beyond (Fig. 2.1). As was expected, pond 1_F17 had the highest fraction of shared OTUs with manure because the manure sample originated from the source manure used to fertilize that pond. The passive nutrient dispersal method had the smallest fraction of shared OTUs but followed the same pattern.

2.4.3 Nutrient analysis

In 2016, two different dispersal systems were used to disseminate manure within two ponds which displayed varying patterns of nutrient concentration over time (Fig. 2.2). An active nutrient dispersal system was used in Pond 1 in both 2016 and 2017 to spread the nutrient. This resulted in a large spike in the TDN and the TDP immediately after fertilization of the ponds which was followed by a progressive

decline in TDN but stable concentrations of TDP. A passive nutrient dispersal method was used in Pond 5 in 2016 and resulted in gradual increases in both the TDN and TDP, with these nutrients reaching their peaks on day 15. DOC concentrations did not appear to follow any expected pattern as the mean peak of pond 1_F16 and pond 1_F17 appeared prior to their fertilization, on days -1 and -6, respectively. However, Welch's two sample t-tests did not show a significant difference in any of the measured nutrient levels between the two ponds with different nutrient dispersal systems in 2016 (DOC: $t = -0.288$, $p = 0.777$; TDN: $t = 1.271$, $p = 0.222$; TDP: $t = -0.957$, $p = 0.354$). Wilcoxon rank-sum tests were also performed between the two experimental ponds in 2016 and the experimental pond in 2017 to reveal that there were also no differences in the nutrient levels between years within the experimental ponds (DOC: $W = 262$, $p = 0.097$; TDN: $W = 274$, $p = 0.452$; TDP: $W = 208$, $p = 0.442$). Furthermore, all nutrient concentrations were significantly different between the fertilized water and the untreated water (DOC: $W = 621.5$, $p = 0.005$; TDN: $W = 882.5$, $p = 1.842 \times 10^{-8}$; TDP: $W = 972$, $p = 3.479 \times 10^{-14}$). The two ponds sampled in parallel in 2017 showed identical patterns in their water temperature, as would be expected. In 2016, the two experimental ponds were sampled 17 days apart and had reciprocal temperature fluctuations. Canonical correspondence analyses (CCA) were done to visualize the degree of influence of each measured variable on the bacterial community (Fig. 2.3). CCA analysis showed that the communities in untreated water clustered very tightly to each other, compared to the communities in fertilized water**,** which appear to have no clustering effect. The bacterial communities were equally influenced by the total dissolved phosphorus and the total dissolved nitrogen (TDP:

CCA1 = -0.994, CCA2 = -0.031; TDN: CCA1 = -0.681, CCA2 = -0.709), and the DOC had a minimal effect on the clustering of the communities (CCA1 = -0.211, CCA2 = -0.028). To augment the CCA, Mantel tests were performed to assess the strength of the correlation of each of the measured environmental parameters. There was a very weak positive correlation between the DOC and the bacterial community (ρ_s = 0.079, p = 0.026) as well as with the water temperature (ρ_s = 0.131, p = 0.002). The community showed the strongest positive correlations with TDN and TDP (ρ_s = 0.524, p = 0.001; ρ_s = 0.472, p = 0.001), respectively corroborating the CCA results.

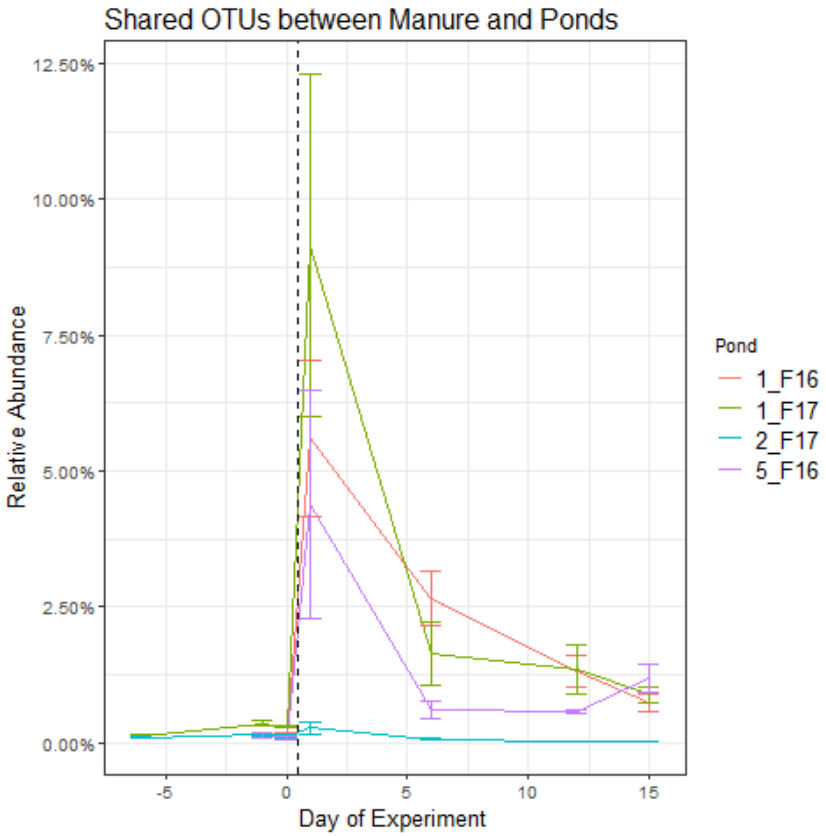

Figure 2.1: **The relative abundance of OTUs in the ponds that identified to OTUs present in the manure.** The black vertical dashed-line represents the time of fertilization into ponds 1_F16, 5_F16, and 1_F17.

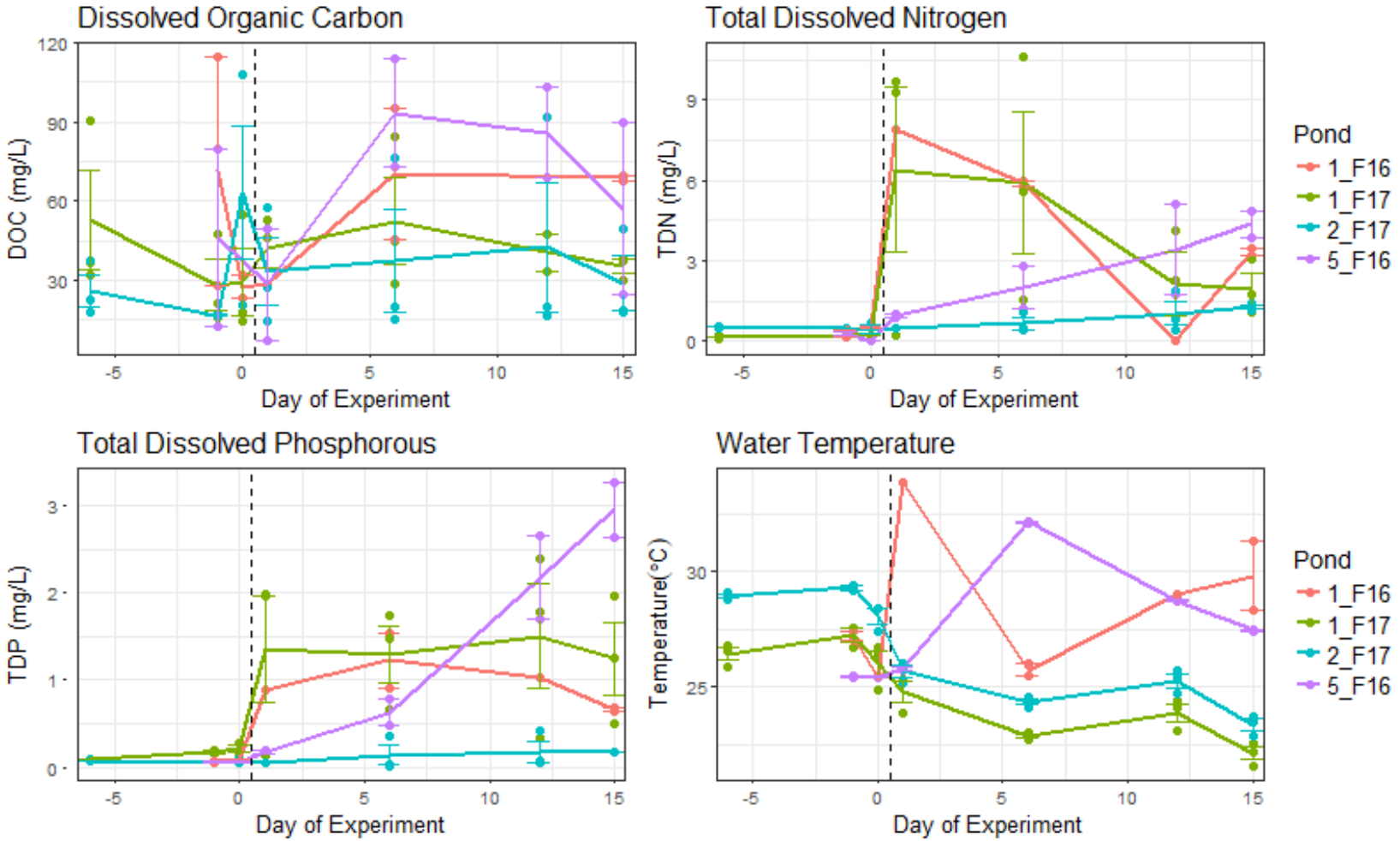

Figure 2.2: Mean environmental variable by day for each pond. Error bars represent the standard error of the mean. The black vertical dashed-line represents the time of fertilization into ponds 1_F16, 5_F16, and 1_F17.

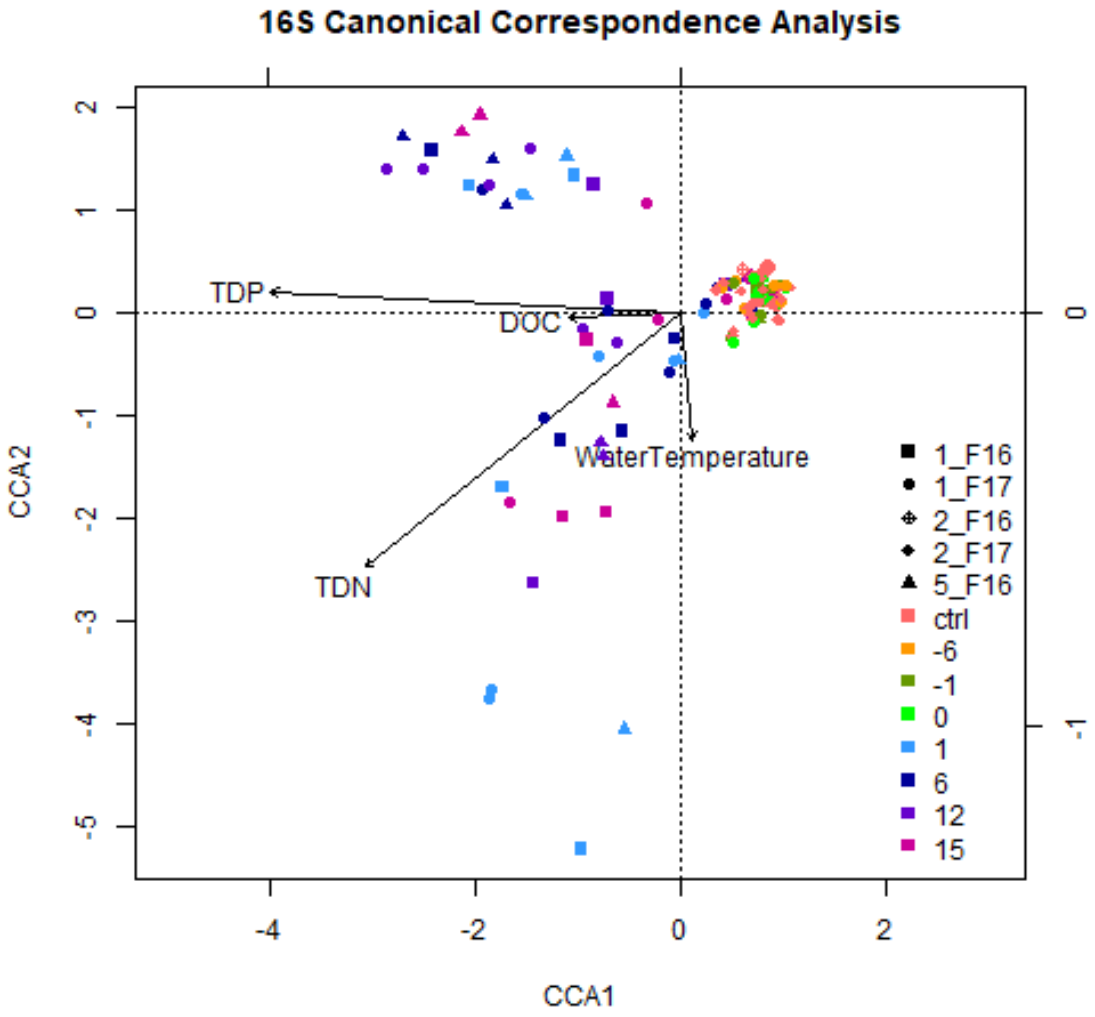

Figure 2.3: Canonical Correspondence Analyses of the 18S rRNA gene communities. Vectors represent the degree of correlation provided by the measured variable.

2.4.4 Taxonomy and diversity analyses

The 12 most prevalent phyla found in all ponds comprised the *Actinobacteria*, *Bacteroidetes*, *Chlorobi*, *Chloroflexi*, *Cyanobacteria*, *Fibrobacteres*, *Firmicutes*, *Parcubacteria*, *Planctomycetes*, *Proteobacteria*, *Spirochaetae*, and the *Verrucomicrobia* (Fig. 2.4). From the 5,445 OTUs representing 9,748,049 sequences in the dataset, these 12 phyla represented 5,337 OTUs with 9,715,466 sequences

(99.7%). Representatives of the *Actinobacteria* and the *Proteobacteria* were found in 143 samples of 144. OTUs that were the most prevalent did not necessarily represent those that had the greatest abundance. For example, the most abundant OTU was a *Terrimicrobium sp*. that appeared in 87 samples with 403,439 sequences (OTU: KP686956.1.1447).

All unfertilized ponds show a similar distribution of the phyla within each pond with the *Actinobacteria*, *Bacteroidetes*, *Cyanobacteria*, *Proteobacteria*, and *Verrucomicrobia* being the most dominant phyla while the *Armatimonadetes*, *Chlorobi*, *Chloroflexi*, *Firmicutes*, *Parcubacteria*, *Planctomycetes*, and *Spirochaetae* are the minor phyla (Fig. 2.5). The control pond samples from 2016 and 2017 originated from the same pond in two different years and showed similar distributions of the most dominant phyla for each year. The control pond in 2017 was sampled for longer (in parallel to the experimental pond in 2017) and portrayed a temporal variability of the previously mentioned phyla. As the *Verrucomicrobia* became more dominant, the *Cyanobacteria* and *Bacteroidetes* dominance decreased. Divisions of the communities from each pond based on the filter size was similar to the whole community (Fig. A2.7). However, the *Cyanobacteria* were almost exclusively detected on the x>1 μm fraction.

After fertilization, *Cyanobacteria* and *Verrucomicrobia* 16S rRNA gene sequences were nearly undetectable. The *Cyanobacteria* and the V*errucomicrobia* mean relative abundance before fertilization was 14.1% (SEM = 2.1%) and 14.8% (SEM = 2.3%), respectively. After fertilization those communities dropped to 1.6% (SEM = 0.5%), and 1.1% (SEM = 0.4%). *Proteobacteria* became the single most

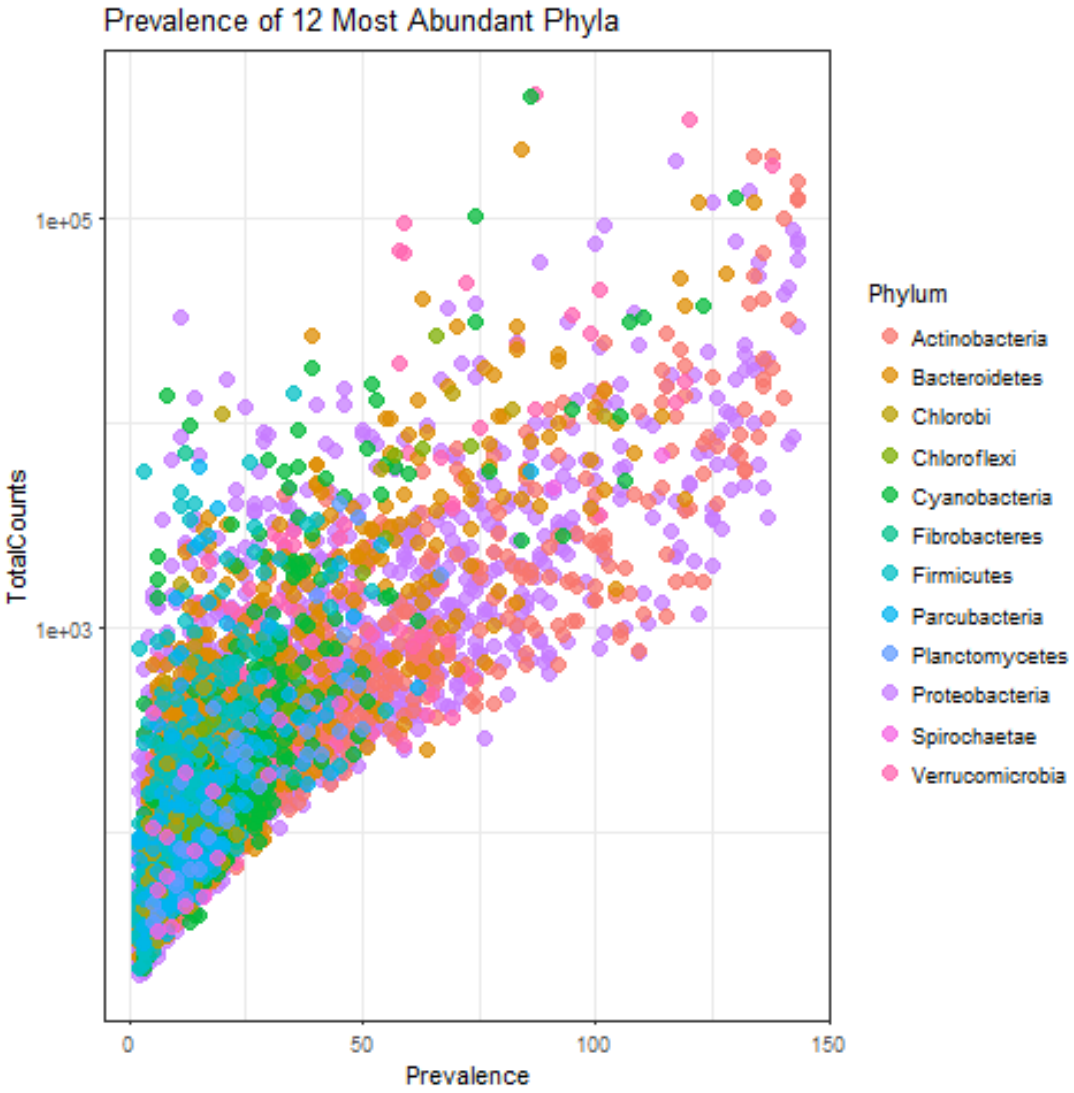

Figure 2.4: Prevalence of the 12 most dominant phyla. The horizontal axis represents the number of samples an OTU occurs in; the y-axis shows the abundance of each individual OTU.

dominant phylum in all fertilized ponds on the day following fertilization and on subsequent days. Other major changes at the phylum level include the proliferation of the *Firmicutes* after fertilization. The *Actinobacteria* and the *Bacteroidetes* were largely unaffected by the fertilization (*Actinobacteria*: 21.2% ± 2.5% and 18.4% ± 2.9%; *Bacteroidetes*: 15.9% ± 1.4% and 15.8% ± 1.6%).

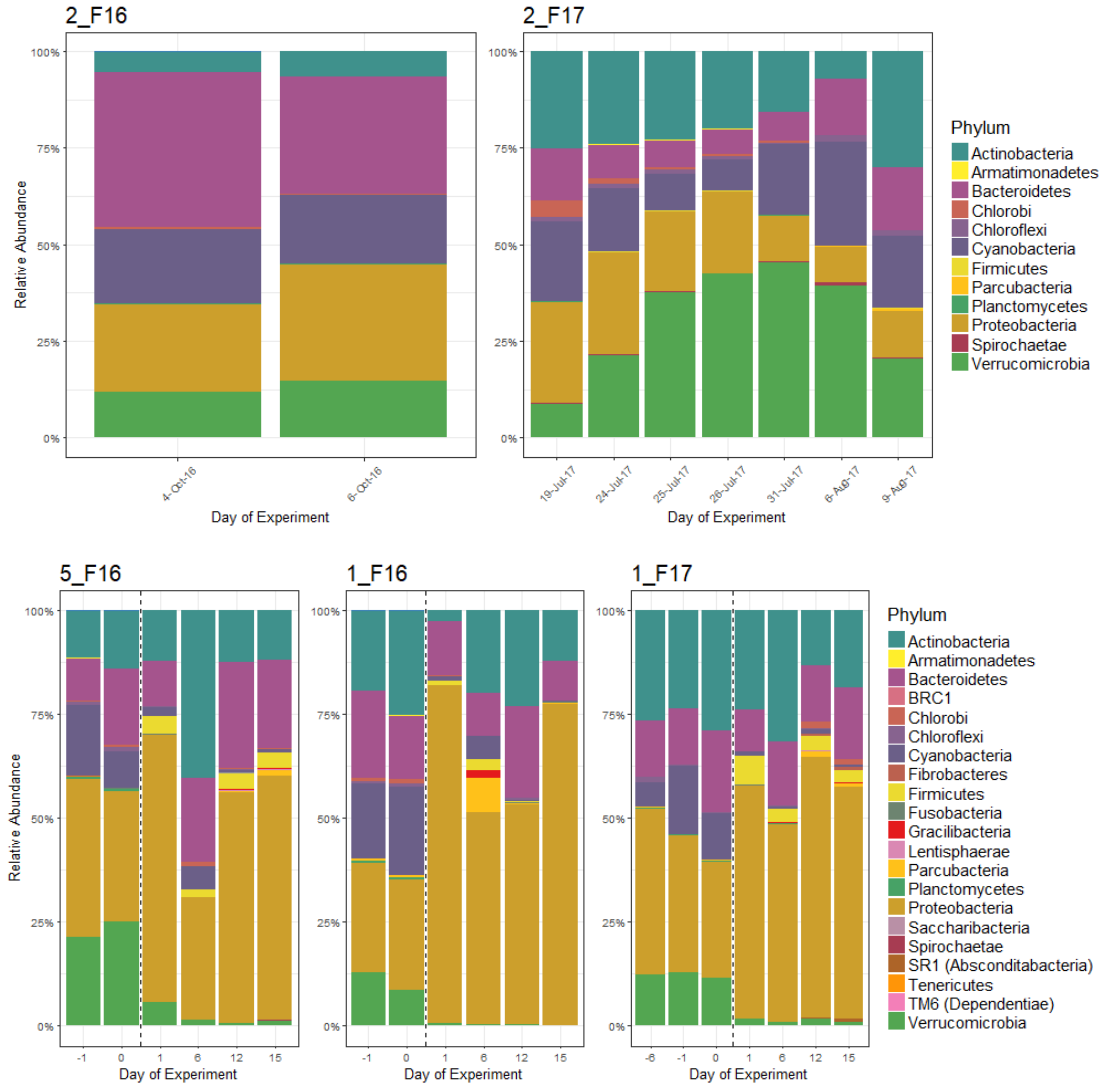

Figure 2.5: Relative abundance of the most dominant phyla. Phyla that represent a minimum of 0.1% of the community in each pond. Charts 2_F16 and 2_F17 represent control ponds that were never fertilized. The date of sampling is provided with percent of the community contributed by each phylum. Experimental ponds are shown in the bottom graphs and the black vertical line represents the time of fertilization.

Rarifying the samples to an even depth of 4,900 sequences/sample removed one sample and 84 OTUs from the analysis. The rarefaction plot does not show a plateau of the curves indicating that more sampling depth would be required to obtain the entire community (Fig. 2.6). Richness, diversity, and evenness measures (observed OTUs, Shannon, and Pielou's J indices) plotted through the progression of the experiment showed a trend towards a reduction in richness and evenness in all ponds; including the control pond (whole community: Fig. 2.7; filter size fractions: Fig. A2.8). Kruskal-Wallis rank sum tests on the treated ponds indicated that there were significant differences in the richness, the diversity, and the evenness within the samples according to sampling day of the experimental ponds as well as the dates within the control ponds (Table A2.1). Pairwise *post hoc* Nemenyi tests show there are no significant differences between each day in the fertilized ponds. The control ponds, however, had significant difference in the number of observed OTUs between day 1 and 12 ($\chi^2 = 13.9$, $p = 0.03$), and in Pielou's J evenness index between day -6 and 6 ($\chi^2 = 14.7$, $p = 0.02$), day -6 and 12 ($\chi^2 = 25.4$, $p = 0.0003$) and day -1 and 12 ($\chi^2 = 18.3$, $p = 0.005$). Each of the communities were further explored by separating the different fraction sizes. In the experimental ponds, Kruskal-Wallis tests showed there were no statistical differences in the day of treatment from the communities captured on the 1μm filter, while there were for the communities smaller than 1 μm but larger than 0.22 μm. Though, there were no significant differences in the pairwise tests. Contrary to the experimental ponds, the control pond (2_F17) showed statistical differences in each of the diversity measures for both fraction sizes. *Post hoc* tests showed that statistical differences lay in the Pielou's J

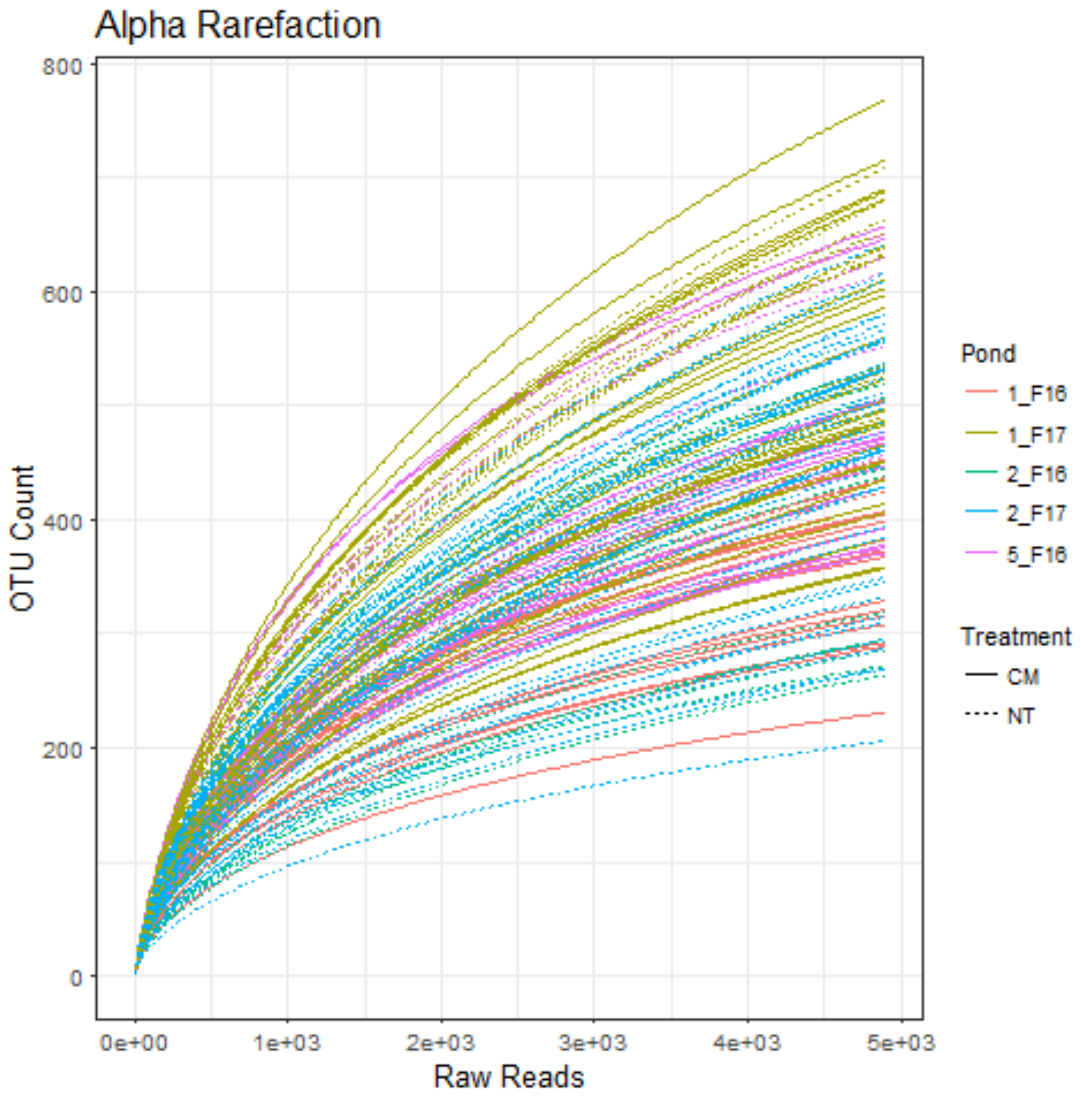

Figure 2.6: Rarefaction of the bacterial communities. Colored lines indicate the pond and year from which the sample was collected. Line types indicate the if the sampled water was collected after fertilization (CM) or before fertilization (NT).

evenness measure between day -6 and 12 for the x>1 μm (χ^2= 12.6, p = 0.05) and the 1 μm>x>0.22 μm (χ^2 = 12.6, p = 0.05) (Table A2.2, Table A2.3).

The Bray-Curtis dissimilarity distance matrix, unweighted UniFrac distance, and weighted UniFrac distance matrices were generated to elucidate the differences between samples in multi-dimensional space. Each method showed nearly identical

patterns discerning the clustering effect of the communities within the treatment categories and the individual ponds (Fig. 2.8). The Bray-Curtis dissimilarity metric and the weighted Unifrac distance showed similar patterns no matter how the community groupings were defined. Considering the phylogenetic distance and the abundance of OTUs with weighted Unifrac distance, there were more similarities between the fertilized waters (CM) with the untreated water (NT) than when only accounting for OTU abundance with the Bray-Curtis dissimilarity. The opposite is true when investigating the community differences based on the filter size on which an OTU was captured. The unweighted Unifrac distance metric shows nearly complete separation between those communities that were present in the fertilized water samples and those that were present in samples from untreated water, as well as complete separation in the phylogenetic distances of bacterial communities retained on different filter sizes. The three distance metrics' patterns of individual pond's separation revealed similar patterns in that communities in all the fertilized water in the experimental ponds cluster closely with each other and the control pond communities cluster with the communities in pretreatment timepoints of the fertilized ponds. After the addition of the fertilizer, each ponds' bacterial community began to disperse from its innate community structure. Weighted Unifrac metrics show the greatest percent variation explained (axis 1: 24.9%; axis 2: 18.1%) compared to the Bray-Curtis (axis 1 14.4%; axis 2: 10.3%) or the unweighted Unifrac (axis 1: 14.2%; axis 2: 11.7%).

2.4.5 Statistical similarities

The PERMANOVA test (ADONIS) revealed that the ponds sampled accounted for more of the differences whether the pond was fertilized or not (Table 2.2). However, the ANOSIM test results showed that the similarities between ponds and the similarities between the treatments were approximately equivalent. Further analyses comparing the individual ponds and the years within a treatment category exposed differences between the naturally occurring bacterial communities between each pond more so than the differences between each year (ADONIS: pond R^2 = 0.354, p = 0.001; year R^2 = 0.193, p = 0.001). It is notable that ANOSIM tests between the years of the natural bacterial communities were more similar (R = 0.530, p = 0.001) than between each pond (R = 0.945, p = 0.001). The high degree of dissimilarity within each pond's natural community may indicate that each pond has its own unique community. The experimental ponds were parsed out from the control pond to determine the overall similarities within the ponds and showed the day of treatment described the greatest reason for the variability in the ponds (ADONIS: R^2 = 0.214, p = 0.001). ANOSIM results confirmed that the days of treatment explained that there was more dissimilarity compared with the year or treatment type (R = 0.389, p = 0.007) but the greatest differences were still between the individual ponds. Within the fertilized water, neither the year, pond, nor the day of treatment strongly explained the reason for the changes in the communities (ADONIS, year R^2 = 0.193, p = 0.002; pond R^2 = 0.145, p = 0.016), although the dissimilarities between the two sampling years were greater than between the ponds (ANOSIM: year R = 0.300, p = 0.043; pond R = 0.494, p = 0.001).

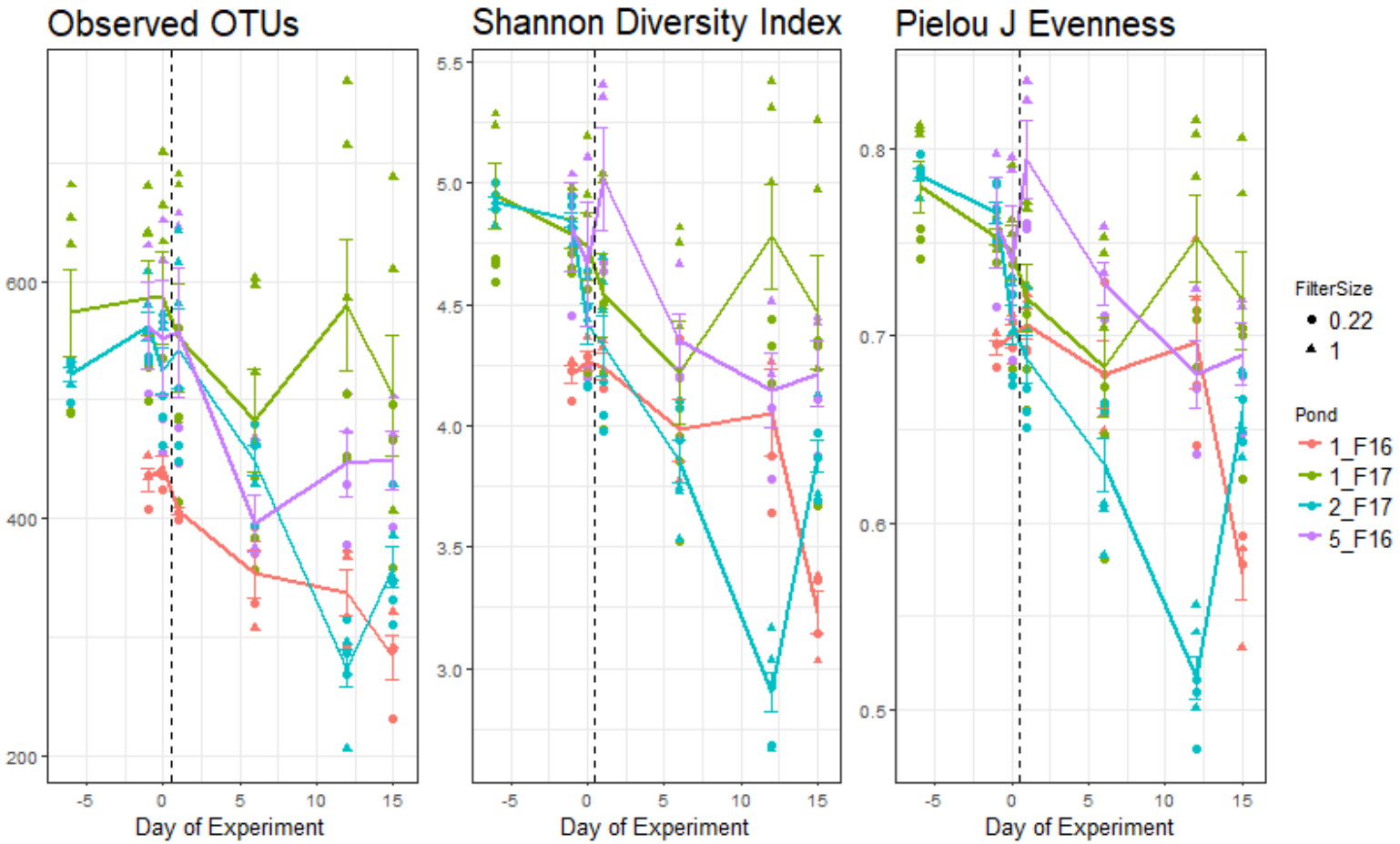

Figure 2.7: Mean alpha diversity measures of the algal community of each pond over time. Pond 2_F17 was never fertilized. Error bars indicate the standard error of the mean of each measure. The black vertical dashed-line represents the time of fertilization into ponds 1_F16, 5_F16, and 1_F17.

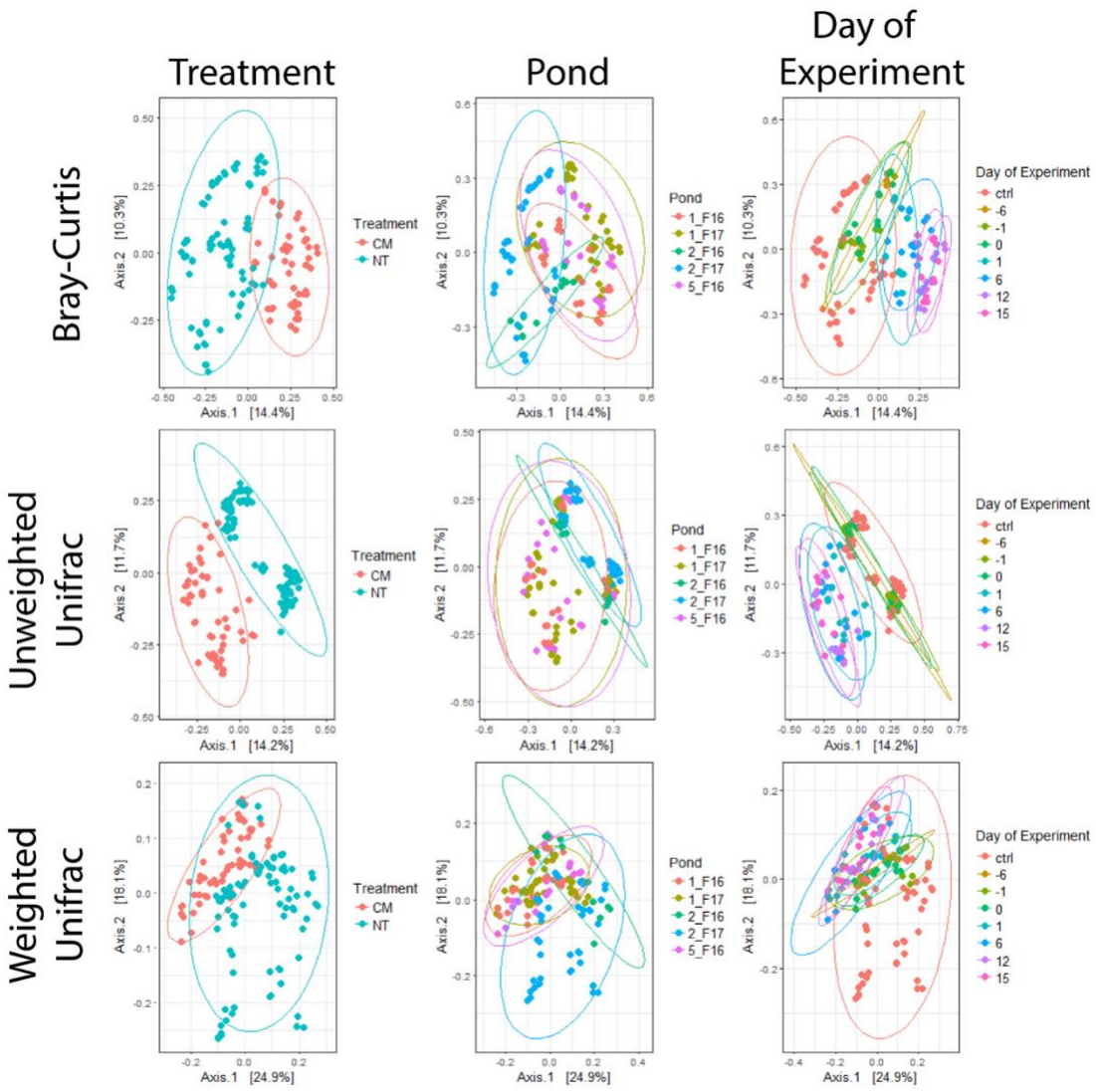

Figure 2.8: Multidimensional scaling/principal coordinate analyses of bacterial communities. The top row is distinguished by the Bray-Curtis dissimilarity metric; the middle row shows separation based on unweighted UniFrac distances; the bottom row shows weighted UniFrac distances. Ellipses represent the 95% confidence.

Table 2.2: ADONIS and ANOSIM tests describing the explanation of variation in the bacterial communities. ANOSIM values describe the similarity between ponds; R values range from 0-1, 1 representing no similarities between the ponds and 0 representing identical communities. * = replicates were not combined due to lack of sample size within comparisons.

All Pond Water			Untreated Water*			Fertilized Water		
ADONIS	**R^2**	**P**	**ADONIS**	**R^2**	**P**	**ADONIS**	**R^2**	**P**
Pond	0.303	0.001	**Pond**	0.354	0.001	**Pond**	0.145	0.016
Year	0.134	0.001	**Year**	0.193	0.001	**Year**	0.193	0.002
Treatme	0.182	0.001	**Date**	0.372	0.001	**Day**	0.200	0.001
ANOSIM	**R**	**P**	**ANOSIM**	**R**	**P**	**ANOSIM**	**R**	**P**
Pond	0.581	0.001	**Pond**	0.945	0.001	**Pond**	0.494	0.001
Year	0.351	0.002	**Year**	0.530	0.001	**Year**	0.300	0.043
Treatme	0.58	0.001	**Date**	0.408	0.001	**Day**	0.262	0.061

Experimental Ponds		
ADONIS	**R^2**	**P**
Pond	0.119	0.011
Year	0.169	0.001
Treatme	0.177	0.001
Day	0.214	0.001
ANOSIM	**R**	**P**
Pond	0.506	0.001
Year	0.343	0.005
Treatme	0.374	0.004
Day	0.389	0.007

The dissimilarities between the total bacterial communities in the three experimental ponds ranged from 76.1% to 86.9%, as described by SIMPER analyses. There was a total of 73 OTUs within these ponds that explained 50% of the differences between communities in each of the ponds. These OTUs represented seven different phyla; *Actinobacteria*, *Bacteroidetes*, *Cyanobacteria*, *Firmicutes*, *Parcubacteria*, *Proteobacteria*, and *Verrucomicrobia*, with the *Proteobacteria*,

Bacteroidetes, and the *Actinobacteria* being the most represented. These seven phyla represent the most variable bacterial OTUs between the ponds. To further elucidate the variable OTUs that are most affected by fertilization, samples from each experimental day within the ponds were compared, and OTUs contributing to the first 50% of the cumulative dissimilarity were identified for each day.

Dissimilarity between the experimental days for both years ranged from 54.2% between the two untreated days (day -1 and day 0) to 88.1% between the sampling date six days prior to treatment and the final day of the experiment (day -6 and day 15). A total of 104 OTUs were the most variable, contributing to 50% of the community differences between each day making up 255,045 of 436,100 sequences. These represented the same seven phyla containing 17 classes and 37 genera. Prior to the fertilization event, the ponds were dominated by the *Actinobacteria*, *Bacteroidetes, Proteobacteria*, and the *Verrucomicrobia* (Fig. 2.5). Immediately following fertilization, the ponds experienced a brief increase in the *Epsilonproteobacteria*, and *Gammaproteobacteria* of ~2% from day 0 to day 1. As the experiment progressed, *Betaproteobacteria* steadily increased dominance in the ponds making up greater than 10% of the communities by day 15, whereas it only comprised of less than 5% of the community pre-fertilization (day -1 and 0). The *Actinobacteria* peaked on day 6 and dropped to its lowest level on day 15. The *Flavobacteria* proliferated to be the third most dominant class by day 6 and fluctuated to fifth and fourth most dominant on days 12 and day 15. The spike in the *Epsilonbacteria* and the *Gammabacteria* were short lived and steadily declined as the experiment progressed. Interestingly, the *Alphaproteobacteria* maintained a steady

presence throughout the experiment until it reached a peak on day 15 (Fig. 2.9). Two alternative patterns in the variable classes of the community arise in the different filter fractions. Communities captured on the 1 μm filter show the *Betaproteobacteria* emerge as a dominant class of bacteria along with the *Alphaproteobacteria* by steadily doubling their presence from pre-fertilization (< 2.5%) to day 15 (>5%). The *Flavobacteriia* also showed enrichment six days post-fertilization when the mean presence began to decrease. Similarly, communities smaller than 1μm and larger than 0.22 μm also showed almost a three-fold increase in the *Betaproteobacteri*. No other bacterial class showed clear enrichment in the communities captured on the 0.22 μm filter. Both communities revealed a two-fold spike in the *Actinobacteria* on day six before dropping below pre-fertilization abundances (Fig. A2.9).

2.5 Discussion

Three man-made ponds were fertilized with chicken manure over two successive years, with the aim of stimulating blooms of phytoplankton that could be harvested for biofuel production. The bacterial communities free-living in the pond water and closely associated with the microalgae were characterized by 16S rRNA gene sequencing. By studying the bacterial communities in the water and closely associated with microalgae, we aimed to gain insights into the symbiotic cohort of bacteria associated with micro-algal blooms that resulted from the artificial eutrophication. Understanding how the bacterial communities develop in parallel with the microalgae will provide greater insights into what bacteria a healthy, productive bloom of microalgae contain versus which bacteria may be present that results in a

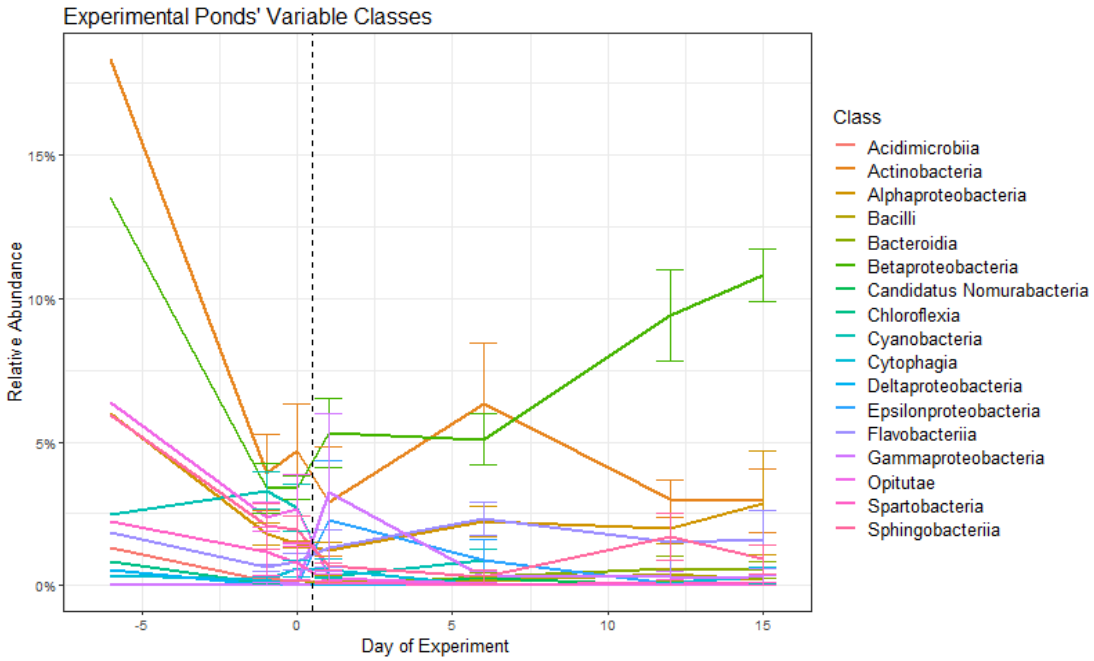

Figure 2.9: Change in relative abundance of the most variable classes. Classes that explain 50% of the differences between each day plotted over time to show temporal variation in the communities. The percent of the community is based on the normalized sum of each days' community abundance. The data are from the experimental ponds; 1_F16, 5_F16, and 1_F17. Error bars represent the standard error of the mean.

bloom crash. This is the first study of its kind in freshwater ponds in which intermittent samplings were used to track the natural short-term oscillation of bacterial communities in response to nutrient addition.

Three synthetic control communities were created using five strains of bacteria from two phyla at equal concentrations, *Bacteroidetes* and *Proteobacteria*, originating from the ponds. The Illumina MiSeq sequencing run output three highly similar communities with little variation between samples. Only three out of the five genera were detected using a custom-made database, revealing a shortcoming in either A) the DNA extraction methods, or B) bias in the PCR amplification.

Klindworth *et al*. (2013) evaluated 175 forward and reverse primers and concluded that the primer pair S-D-Bact-0341-b-S-17 and S-D-Bact-0785-a-A-21 had the greatest coverage of phyla compared to others tested and, if one mismatch is tolerated, the total coverage can be increased to 64.6% for archeae; 94.5% for bacteria; and 0.1% for eukaryotes (135). While performing these evaluations, pre-described communities of bacteria from a marine environment were experimented with again and found similar results that were determined not to be an artifact of the sequencing. While these studies confirm the efficiency and accuracy of the primers and sequencing platform, it does not evaluate the efficiency of DNA extraction protocols. This leads to the alternative conclusion that the DNA extraction protocol was insufficient to lyse all representative bacteria in the environmental samples. Although the DNA protocol may not have been able to extract DNA from all genera, the precision of the sequencer provides valuable insights into the relative changes of the communities most affected by the experiment.

The bacterial communities in the control ponds that were not fertilized were dominated by five phyla that comprised greater than 90% of the community in all the samples: *Actinobacteria*, *Bacteroidetes*, *Cyanobacteria*, *Proteobacteria*, and *Verrucomicrobia*. The presence of these phyla is consistent with findings of a meta-analysis of 68 papers describing freshwater lake 16S rRNA gene sequences (143). Consistent with other studies, there was a significant presence of the genus *Flavobacterium*. Also, the hgcl clade, *Sphingomonas, Polynucleobacter,* and *Limnohabitans* genera were found which are often associated with blooms of cyanobacteria (144–148). Interestingly, it has previously been reported that

Flavobacterium is well adapted to the cyanobacterial phycosphere and is often found to be abundant during blooms of cyanobacteria as it may be able to efficiently break down *Microcystis* hepatotoxins. The genus *Flavobacterium* occurred abundantly in the water of unfertilized ponds (1.1% to 35.1%). More importantly, however, the class *Flavobacteriia*, the parent group of the *Flavobacterium*, briefly becomes the most abundant taxa on the 1 μm filter on the sixth day post-fertilization. Conversely, *Bdellovibrio* and *Peredibacter* are reported to be bacteriovores, preying on *Microcystis* or other bacteria (149–152). *Peredibacter* appeared only in a single pond at only 0.59% of the community and *Bdellovibrio* was present but represented less than 0.1% of the community indicating that bacteriovorus bacteria are not likely to be playing a major role in controlling the cyanobacterial communities.

Chicken manure sourced from three different locations and times was dominated by similar bacterial groups, with the *Actinobacteria*, *Bacteroidetes*, *Firmicutes*, and *Proteobacteria* making up greater than 80% of the communities. This is consistent with other poultry microbiome studies (153). Variation within the chicken manure biome is likely due to the individual samples storage condition, source, and age. To assess whether the bacteria present in the chicken manure contaminated the bacterial communities in the ponds following fertilization, identified bacterial OTUs within the ponds were compared with manure-associated OTUs to determine relative abundance of OTUs contributed from the manure. The proportion of contaminating OTUs derived from chicken manure within the ponds spiked immediately after fertilization up to 17.8% of the total sequences with an average of 6.8%. The five most abundant manure-derived genera found in the ponds were the

Mycobacterium, *Lactobacillus*, *Corynebacterium*, *Acinetobacter*, and the *Atopostipes*. These genera are all commonly found in agriculture manure (154–159). However, the contaminants did not persist in the pond environment (Fig. 2.1). Reduction in the manure-derived bacteria could be explained by several factors including the water temperature, salinity, exposure to UV light, or the competition with the bacterioplankton already in the ponds that are presumably well adapted to that environment (160, 161).

After inoculation of the chicken manure fertilizer into the ponds, there was an immediate spike in the *Proteobacteria* in all three of the fertilized ponds, along with decreases in the *Verrucomicrobia* and the *Cyanobacteria* (Fig. 2.5). The *Firmicutes* also increased, most notably in 5_F16 and 1_F17. It was found that while 222 OTUs were shared between the ponds and the chicken manure, these OTUs only represented a total of 1% of the total sequences, peaking right after fertilization and diminishing in subsequent days. The communities that were shared between the manure and the ponds consisted mainly of the phyla *Firmicutes*, *Actinobacteria*, and *Proteobacteria*. This helps explain the sudden increase in the *Firmicutes* and *Proteobacteria* in the fertilized water immediately post-fertilization.

The ponds' communities became more similar to each other after fertilization compared with the communities in the pre-fertilized ponds. Suggesting that even though these ponds are within 100 m of each other and filled with the same source water, the community within each pond is unique. This characteristic became less apparent after the ponds were fertilized. The communities displayed a mean decline in richness and diversity post-fertilization. The largest differences in the community

diversity occurred between the dates prior to and post fertilization, but the control pond also showed the diversity fluctuating over time. These ponds are "closed" systems without any inflow or outflow of water during the experimental period; changes in the control pond cannot be explained by fluxes in the salinity which has previously been recognized to be the most important factor contributing to community structure and function (162, 163). It should be noted that a total of 0.69 inches of precipitation fell during the sampling period in 2017, according to Weather Underground (www.wunderground.com, accessed March 2018). Increases in the ponds' water level would affect the nutrient concentrations throughout the pond, but this effect is expected to be negligible due such high nutrient concentrations introduced from the manure.

Despite the unexpected change in the community diversity in the control pond even with lack of manipulation, beta-diversity analyses showed that the introduction of the chicken manure clearly resulted in a change in taxa in the treated ponds. Most importantly, communities from the fertilized water in any pond clustered tightly with each other indicating a selection process induced by the introduction of the nutrient. Whereas, the relatively low nutrient concentrations prior to fertilization showed a more phylogenetically diverse community with varying abundances between ponds.

Only 21 taxa were shared between the 7,004 taxa in the chicken manure and the 3,426 taxa in the waters prior to fertilization. However, nutrient enrichment by addition of chicken manure was a clear driver of bacterial community structure between treated and untreated ponds (Fig. 2.3). Eiler *et al.* (2003) showed that the bacterial growth rate and community composition was dictated by the DOC

concentrations (164). It has been well documented that different clades from various phyla show disparate growth responses and competitive abilities to changing nutrient availability (145, 164–171). Mantel tests along with the canonical correspondence analysis showed positive correlations between all measured parameters (DOC, TDN, TDP, and water temperature). The largest correlation was found to be between the TDN and TDP ($\rho_s = 0.524$, $p = 0.001$; $\rho_s = 0.472$, $p = 0.001$) and the weakest correlation was with the DOC ($\rho_s = 0.079$, $p = 0.026$). Previous studies showed that some *Betaproteobacterial* lineages had a negative correlation with the DOC:total phosphorus ratio and clades within the *Actinobacteria* are more common in acidic lakes with high DOC concentrations (143). In 2017, pH was measured in the control pond (2_F17) and an experimental pond (1_F17). The pH increased in the unfertilized pond but remained constant in the fertilized pond. It is worth noting that correlations to environmental parameters by higher taxonomic classifications like phylum level is uncommon, but rather a higher resolution of taxonomic grouping should be considered (172). To address the relative significance of community changes in the experimental ponds, a similarity percentages analysis was performed to describe the OTUs that explained the greatest differences, contributing to the first 50% of the cumulative difference between each day. 104 OTUs made up greater than 50% of the total number of sequences in the subsampled ponds, comprising 37 genera. All identified taxa that contributed to the differences between days in the experiment were present in the ponds prior to fertilization, with the exception for a member of the *Acinetobacter* genus originating from the manure, indicating that all other changes in this community can be attributed to autochthonous populations. Several ecologically

important genera that are associated with freshwater were also identified as dominant post-fertilization; *Flavobacterium*, *Limnohabitans*, and *Polynucleobacter* accompanied by members of the *Betaproteobacteria*, clade 12up and the *Actinobacteria*, *Alpinimonas* (Fig. 2.9).

As previously mentioned, the *Flavobacterium* genus has been implicated in co-occurring with phytoplankton blooms and degrading organic materials produced by microalgae (144, 145, 173–175). Numerous other studies have described several species that are psychrophilic and psychrotolerant. More broadly, members of the class *Flavobacteria* have often been found associated closely with algae of different lineages as well as coral (173, 174, 176). A genome sequenced and annotated in 2013 revealed that the *Flavobacteria* species *Formosa agariphila* KMM 3901^T contained the highest densities of carbohydrate active enzymes that was capable of degrading polysaccharides generated by a broad range of algal lineages (177). Though very few cyanobacterial 16S rRNA gene sequences were identified, the purpose of fertilization was intended to facilitate microalgal blooms. Occurrence of the *Flavobacteria* may be indicating the formation of euakaryotic microalgal blooms.

Members of the *Betaproteobacterial* lineage *Limnohabitans, Polynucleobacter*, and the 12up clade tend to be more versatile in their lifecycles and tolerate a range of trophic conditions. The genus *Limnohabitans* grows quickly in response to nutrient pulses and have been reported to be proxies for low-molecular-weight algal-derived substrates, though their populations can be countered by their susceptibility to grazing (178–180). Draft genomes of two strains of *Limnohabitans* have showed their potential to partake in photosynthesis, CO_2 fixation, as well as

ammonia and sulfur oxidation (181). Members belonging to the *Polynucleobacter* have been described as aerobic chemoorganotrophs but could also function as facultative anaerobes (143). A recent study investigated the quality and quantity of organic matter from three genera of algae (a Cryptophyte and two Chlorophytes) and found that *Limnohabitans* and *Polynucleobacter* were able to grow on organic matter from the Chlorophyte *Coelastrum* but only *Limnohabitans* could grow off the metabolic byproducts from both the Cryptophyte and the Chlorophytes (182). Similar to the *Polynucleobacter*, the 12up clade is capable of functioning as a facultative anaerobe and it has been reported to be involved in the phosphorus removal from wastewater. The abundance of the 12up clade may be indicative of a highly polluted and potentially anoxic environment (163, 183). Contrary to the indications of the 12up clade, the *Actinobacteria* genus *Alpinimonas* was originally described as a psychrophilic species that will not grow under anaerobic conditions; therefore**,** the abundance of this bacterium suggests that the experimental ponds were not anoxic, as suggested by the presence of the 12up clade (184). Due to the stagnant nature of the ponds, it is possible that there are both anoxic and oxic microniches in the ponds.

Separation of the communities based on the filter-fraction size reveals two unique communities. At the phylum level, *Cyanobacteria* were largely removed by the 1 μm filter while the remainder of the phyla remained consistent with the whole community analysis. The 1 μm filter cut-off was used as an intermediate step to collect microalgae (eukaryotic algae and cyanobacterial algae) along with their close symbionts while the 0.22 μm filter was used as a final filtration step to collect the free-living or planktonic bacteria in the water. Diversity analyses showed that the x>1

μm fraction generally had a more even and diverse community as compared with the 1 μm>x>0.22 μm fraction. This could either be explained by particulate matter and fowl excrement indiscriminately trapping a variety of bacteria; or, this may be a result of preferential bacterial-algal assemblages formed during bloom formation. To explore what the most likely explanation is, the OTUs that cumulatively explained 50% of the differences on each filter fraction between each day in the experimental ponds were tracked over time. The most variable OTUs within the 1 μm>x>0.22 μm fraction comprised mainly of the classes *Betaproteobacteria* and *Actinobacteria*. However, the x>1 μm fraction showed a more interesting pattern. Both the *Betaproteobacteria* and *Actinobacteria* were in agreement with the smaller fraction size, but there was also clear enrichment for members of the *Alphaproteobacteria* and the *Flavobacteriia* classes. This data corroborates others' findings that the *Flavobacteriia* (*Flavobacterium* in particular) has previously been implicated to be frequently co-occurring with phytoplankton. Due to the relative absence of this bacteria on the 0.22 μm fraction, two conclusions could be made; 1) this class of bacteria is larger than 1 μm; or 2) this is a true algal associate bound to algal cells.

Changes in the *Alphaproteobacteria* class were also almost exclusive to the x>1 μm community fraction. The *Alphaproteobacteria* is a ubiquitous class of bacteria that displays plasticity in its genome and is hypothesized to be the endosymbiont that generated the first eukaryotic cell (143). This characteristic is a likely explanation to their roles of endosymbionts or intracellular parasites (185). These bacteria have been known to form filaments or aggregates when their abundance increases, aiding them in defense against grazing, and providing a top-

down control mechanism that favors the *Alphaproteobacteria* (143, 186, 187). It could be surmised that these characteristics are the reason why the *Alphaproteobacteria* were most abundantly found on the 1 μm filters. *Alphaproteobacteria* are also known to be able to degrade recalcitrant organic compounds and are competitive for scarce resources. Eiler *et al*., (2003) found that the *Alphaproteobacteria* were exclusively found in natural communities with low concentrations of DOC, and that the DOC in their experiments were determined to be the growth rate limiting factor in their mesocosms. Nutrient data in the current experiments show a relatively constant concentration of DOC post-fertilization compared with the TDN; showing a dramatic decrease after an initial spike in both nutrients. The DOC concentrations in this data have not been determined to be instrumental in the organization of the bacterial communities. However, we see the enrichment for these bacteria peak by day 15 post-fertilization, shortly after the TDN of the ponds reached its lowest concentration. A group of bacteria called the rhizobia are a generic name for soil-living bacteria that have a mutualistic symbiosis with plants in which the bacteria fix N_2 for use by the plants while the plant produces growth substrates for the bacteria (188–190). This group of bacteria is largely populated by members of the *Alphaproteobacteria*, which, as previously described, preferentially infects plant root hairs and is provided molecular cues from the plant to induce an infection (191). With this knowledge and enrichment of these bacteria in the ponds on the 1μm filter, in conjunction with the reduction in TDN in the actively dispersed nutrient ponds, shows strong support for mutualistic interactions between primary producers and the *Alphaproteobacteria*.

2.6 Conclusions

Man-made ponds that are filled with water from a local stream contained bacterial communities dominated by *Actinobacteria*, *Bacteroidetes*, *Cyanobacteria*, *Proteobacteria*, and *Verrucomicrobia*. Despite being located within proximity to each other, each pond had a characteristic community that differed from that in neighboring ponds. When fertilized with high nutrient chicken manure, the allochthonous bacterial communities from the manure were unable to persist in the pond environment. The bacterial communities become more phylogenetically similar to each other, though less diverse, following the fertilization. Artificial eutrophication of the ponds was induced with the intent of stimulating blooms of microalgae for biofuel production. Interestingly, the most notable changes in the communities happened within genera that have been previously reported to commonly appear within the algal phycosphere, consistent with a shift in the environment to be more conducive for healthy algal-blooms.

Chapter 3: Microalgal 18S rRNA gene community dynamics in agricultural ponds fertilized to stimulate blooms for biofuel production

3.1 Abstract

Growth, harvesting and processing of microalgae for the production of biofuels is a difficult and often cost prohibitive process. For microalgal derived biofuels to be a feasible alternative to fossil fuels, production, harvesting, and conversion to a bio-crude product must be done economically. Alternative methods of biofuel conversion, such as hydrothermal liquefaction (HTL), are not dependent on the internal contents of an algal cell, rather the process is dependent on the biomass input. Thus, the primary goal for HTL fuel conversion strategies is to produce and harvest the maximum amount algal biomass in the smallest amount of time. In this study, artificial man-made ponds were filled with water from a nearby stream and fertilized with chicken manure to stimulate blooms of microalgae. Chicken manure contains high concentrations of total dissolved nitrogen (TDN) and total dissolved phosphorous (TDP). The addition of these nutrients in high concentrations induces a eutrophic environment conducive to the growth of a select group of microalgae. Molecular data indicates an enrichment for the *Chlamydomonadales* class of microalgae. Microscopic counts show increased algal density demonstrating that our approach resulted in an improved production of algal biomass. Ratios of bacteria-to-autofluorescent cells show a trend to return to cell numbers present prior to fertilization, after six days. Unweighted UniFrac PCoAs showed that eutrophication

changes the composition of the rare-taxa in each pond, with the emergence of a sub-set of phylogenetically distinct populations. Weighted UniFrac metrics showed that dominant taxa in each of the ponds were phylogenetically related. Diversity indices all show a reduction in the richness and evenness of the algal communities in all the ponds over the course of the experiment, likely caused by a selection process by competition and blooms of specific microalgae species.

3.2 Introduction

Microalgae are a group of polyphyletic organisms ranging from the communal *Volvox* genus of the Chlorophytes to the *Cyanobacteria* phylum within the Bacteria kingdom. All algae and subsequently all higher plants that evolved from algae are the product of the endosymbiosis of an ancient cyanobacterium in a non-photosynthetic protist to form the plastid used for photosynthesis (Chapter 1, 7, 192, 193). The proliferation of modern plants has resulted in the enzyme ribulose bisphosphate carboxylase/oxygenase (RuBisCO) being the most abundant protein on Earth (194). All plants, including algae, use the RuBisCO enzyme to take CO_2 from the surrounding environment to ultimately make glucose as a substrate for starch and oil production. (7, 68, 195).

In ponds, bicarbonate is the preferred source of CO_2 for cyanobacteria and eukaryotic algae. Because CO_2 is the rate limiting substrate in photosynthesis and carbon fixation, microalgae have developed an energy-dependent system to concentrate inorganic carbon called the CO_2-concentrating mechanisms (CCM) (196–198). However, the generation of the 5-carbon sugar substrate required for RuBisCO to fix CO_2 is inhibited in the presence of oxygen. Oxygen causes RuBisCO to

undergo an oxygenase reaction which ultimately releases a CO_2 molecule through a process called photorespiration (68). Photorespiration has been shown to reduce carbon fixation efficiency by up to 30% (199). In a similar respect, nitrogen fixing cyanobacteria also require a low concentration of oxygen due to the nitrogenase enzyme being irreversibly inhibited in the presence of oxygen (200, 201). Since the hallmark of photosynthesis is the generation of oxygen, this clearly becomes physiologically problematic when blooms of microalgae occur. In the natural environment these blooms will not occur free of heterotrophic bacteria but rather the microalgae are dependent on the bacteria for a multitude of purposes, such as consuming oxygen and providing CO_2 to their plant cohorts (202).

The microalgal-bacterial consortium has been shown to be a dynamic relationship in which the bacteria and the algae can work together to support each other's growth. As previously discussed, problematic oxygen concentrations can be reduced by heterotrophic bacteria to increase the efficiency of nitrogen fixation, photosynthetically derived carbon fixation, and provide CO_2 back to the algae. Croft *et al*. (2005) demonstrated that 50% of microalgae are also auxotrophic for vitamin B_{12}, which is provided by their symbiotic bacteria (98). A great example of B_{12} dependency can be seen in the mutualistic relationship between *Lobomonas rostrata* (phylum *Chlorophyta*) and *Mesorhizobium loti* (phylum *Proteobacteria*). In this relationship the bacteria supply vitamin B_{12} to the microalgae and in exchange the bacteria have access to a carbon source from the algae derived from photosynthesis (100). Conversely, the consortium that occupy the same microenvironment are in competition for other nutrients to sustain their own growth. Low phosphorous

concentrations limit algal growth at times of high light intensity because their bacterial cohorts have a stronger affinity for phosphorous, out-competing the algae (203). However, in the context of producing microalgae *en masse* for biofuel generation, it is unlikely that macronutrients, like nitrogen or phosphorous, will be limiting factors for algal growth because of the biofuel conversion process called hydrothermal liquefaction (HTL). HTL depends on a high quantity of biomass thus nutrient limitation would need to be avoided as to not restrict algal growth (81, 82).

For HTL to be an effective method for generating biofuels, algal biomass needs to be produced quickly with minimal costs. Conveniently, microalgae have been proven to be efficient at treating wastewater or sewage, a common cause of eutrophication, making nutrient enrichment cheap and accessible (63–65). Flue gas from power-plants has also been proposed as a source of CO_2 and has been shown to be 30% more productive than supplementation with pure CO_2 alone, but is costlier to implement (66–68). Financial considerations demand that culturing microalgae, particularly for biofuel generation, be done with minimal energy input. Established industrial production of microalgae for purposes other than biofuel production use tubular or flat-paneled photobioreactors (204). These photobioreactors can use sunlight or LED light to yield 8,000 kg/ha or 245,000 kg/ha of algae respectively. Alternatively, open pond systems can be used to produce 5,000 kg/ha of algae at an eighth of what it would cost to use an LED light photobioreactor (205). The reduced cost in the open pond production of microalgae outweighs the consequence of reduced production (41). Even though open ponds provide a more economic option for microalgal production, they also offer less control. They are limited in the type of

microalgae that can be grown, have a lower efficiency of light utilization, poor gas transfer, no temperature control, and are susceptible to culture-crash contamination (206–208). Despite these limitations, Jorquera *et al*. (2010) performed a net energy ratio analysis, defined as the ratio of the total energy produced by the microalgae over the energy input into the cultivation system, between open raceway ponds and photobioreactors and found that the raceway ponds exceeded the photobioreactors in oil production and total biomass (209).

Open-pond cultivation systems are open to the surrounding environment and are not specifically designed to keep out foreign algae that may be carried by wind or animals to create a microalgal polyculture. High-diversity microalgal communities have been found to be more efficient at nutrient utilization and can produce more biomass and contain a higher carbon content per unit of limiting nutrient compared with monocultures (57, 87, 95). Algal biomass and lipid content has been shown to be positively associated with communities rich in species diversity (87, 89, 90). However, these ponds are also subject to invasion by microalgal-predators such as *Daphnia* species and can cause the cultures to "crash" or die (95, 96). Due to the low costs of construction and operation along with the advantages of ecological diversity, open-pond cultivation systems will likely be the strategy for biofuel production.

In the present study, man-made open ponds were fertilized with raw chicken manure to stimulate blooms of native microalgal communities. Changes in the microalgal community structure were monitored by microscopic and molecular identification techniques; a parallel study to track the bacterial community changes were also performed (Chapter 2). The microalgal community shifts and

corresponding changes were determined to understand the dynamic diversity of the microbial community associated with blooms of microalgae.

3.3 Methods

3.3.1 Sample collection and nutrient analysis

In the summer of 2016, two man-made ponds designated 1_F16 and 5_F16 (Fig. A3.1), about 1 acre each, in Frederick, MD, were filled with approximately 5 million liters of freshwater from a nearby stream. Each pond was then fertilized with 5 tons of chicken manure to stimulate blooms of microalgae. Different nutrient dispersal strategies were used in each of the two ponds in 2016, 17 days apart (Chapter 2). A third, unfertilized pond designated 2_F16 was also sampled at the end of the experiment in October of 2016 to assess community variability between fertilized and unfertilized ponds. In 2017, one pond that was fertilized in 2016 was filled and fertilized again (1_F17). The same unfertilized pond (2_F16) was sampled in parallel to the fertilized pond in 2017 and designated 2_F17. The two unfertilized ponds act as a control to the three treated ponds 1_F16, 1_F17, 5_F16 (Chapter 2: Table 2.1; Fig. A2.1).

Replicate water samples located in the center and at either pole of each pond. Water was collected from the top six inches into a sterile carboy through a 200 µm mesh to remove detritus. Samples were collected on the day prior to fertilization, the same day immediately before fertilization, the day after fertilization, and then on days 6, 12, and 15 post fertilization (Table 2.1). A seventh sample was included six days prior to fertilization in 2017 to monitor the stability of the native, un-manipulated

communities in the ponds. All samples were stored on ice until processed upon return to the laboratory. Two liters of water from each sample was serially filtered through 6 µm and 1 µm filters to collect microalgae and their closely associated bacterial assemblages. The resulting filtrate was collected for quantification of the dissolved organic carbon (DOC), total dissolved nitrogen (TDN), and total dissolved phosphate (TDP) in the ponds. The nutrient analysis was performed by the Nutrient Analytical Services Laboratory at the Chesapeake Biological Laboratory, a part of the University of Maryland Center for Environmental Science. pH values were taken from the samples collected in 2017. Unfiltered water from ponds 1_F17 and 2_F17 was fixed in 2% formaldehyde overnight at 4^{o}C, stained with 300 µM of DAPI, and filtered onto 0.1 µm black polycarbonate filters. Epifluorescence microscopy was used to enumerate the bacteria and chlorophyll autofluorescence was used to count the primary producing microbes. Microscopy was performed with a Zeiss AxioPlan microscope. DAPI-stained cells were visualized with Zeiss filter set 49 (G: 365; FT: 395; BP: 445/50). Photosynthetic microalgae were counted on the basis of their morphologyand autofluorescence, visualized using Zeiss filter set 43 (BP: 545/20; FT: 570; BP: 605/70).

3.3.2 DNA extraction, sequencing, and data processing

DNA was extracted from each sample using Qiagen DNeasy® PowerWater® kits. Communities captured on the 6 µm and 1 µm filters were pooled to capture the communal DNA in a single sample. Each DNA fraction was normalized to 5 ng/mL prior to pooling. Prior to next generation sequencing, each DNA sample had the 18S rRNA gene sequences amplified by PCR to check that the DNA sample was suitable

for PCR amplification. Microalgal 18S rRNA genes were sequenced using P73F (5'-AATCAGTTATAGTTTATTTGRTGGTACC-3') and P47R (5'-TCTCAGGCTCCCTCTCCGGA-3') (210).

To assess the efficiency of the relative quantitative accuracy of the next generation sequencing platform, and our bioinformatic pipeline, a mock community was created with three eukaryotic microalgae in 2 L of sterile deionized water and consisted of a total of $1.12x10^8$ cells of three strains, *Chlamydomonas reinhardtii* CC503, and *Scenedesmus* sp. HTB1, and *Desmodesmus* sp. RAI-5 (isolated from the sampling location; Chapter 4), counted with a Neubauer counting chamber. Strains HTB1 and CC503 each consisted of $4.48x10^7$ cells, each making up 40% of the community. Strain RAI-5 made up the remaining 20% with $2.24x10^7$ cells. The cell suspension was filtered directly through a 1 μm filter and DNA was extracted as previously described.

The output from the MiSeq platform generated forward and reverse sequences 300 nucleotides in length. Sequences were pre-processed using the CLC Genomic Workbench by importing the data as paired-end reads, quality trimming, merging overlapping pairs, and trimming all sequences to a fixed length resulting in 18S rRNA gene sequences of 284 nucleotides. Control communities were processed independently of the samples and yielded gene sequences 294 nucleotides in length. The resulting high-quality sequences were exported into the Quantitative Insights into Microbial Ecology (QIIME) program (136) for open reference operational taxonomic unit (OTU) picking and taxonomic classification using Uclust (137) with the Silva 128 database (138). The top five BLAST alignments with identical scores were

extracted and used as a reference, along with the P73F-P47R amplicon of each strain, to identify the control communities with Uclust. Alignments of the representative sequences were created using Python Nearest Alignment Space Termination (PyNAST) for each OTU and were used to produce nearest-neighbor Newick formatted, mid-point rooted trees with FastTree for downstream phylogenetic analyses. Taxonomic identities were defined as having a 97% identity to the reference sequences.

To retain any 18S rRNA gene sequences that are classified as primary producers, only the *Archaeplastida*, *Cryptophyceae*, *Centrohelida*, *Ochrophyta*, and *Dinoflagellata* were retained. Divisions based on the treatment type were performed and the distribution of OTU counts against the number of OTUs present were plotted. The core diversity of the communities within each treatment was defined by identifying spurious OTUs as those that did not occur five or more times in two samples of similarly treated ponds (Fig. A3.2). Uneven sampling depth was accounted for by rarefying to an even depth of 22,000 sequences per sample. Singletons were removed from the control communities and then rarefied to an even depth of 66,200 sequences.

3.3.3 Diversity, statistical, and similarity analyses

All diversity analyses were performed using R and the *phyloseq* package (139). Prior to subsampling to an even depth for statistical analyses, the relative abundance of the phyla present in each pond was determined for OTUs whose relative abundance was greater than 0.1%. Uneven sampling was corrected by rarifying each sample to an even depth of 22,000 sequences per sample. After

rarifying the data to an even depth, alpha-diversity was determined with the total number of observed OTUs to represent the richness, the Shannon diversity index, and Pielou's evenness index. Kruskal-Wallis tests were performed on the diversity measures to test statistical differences between days and Nemenyi-tests were performed *post hoc* to identify which days were most different. Beta-diversity was examined with principal coordinate analyses/multidimensional scaling plots created with Bray-Curtis dissimilarity (140) unweighted, and unweighted UniFrac (141) distance matrices generated from the rarefied data. Due to the non-normal nature of the environmental nutrient parameters, significance between treatments and each pond was tested with the Wilcoxon rank-sum test. Wilcoxon rank-sum tests were performed to determine if significant changes to the diversity occurred throughout the experiment. To assess the innate natural differences and the influence of the treatment on the microalgal communities, permutational analysis of variance (PERMANOVA) were performed with the R package vegan using the *adonis*() function (142). Analysis of similarity (ANOSIM) was also used to determine the similarity between the treatments according to their Bray-Curtis dissimilarity distances. Similarity percentages (SIMPER) were then used to determine the OTUs which contribute most to the similarities within each date. The resulting data was used to extract which OTUs contribute to the first 50% of the differences between each experimental pond and plotted to observe the OTUs that are most variable over time. Except where indicated, all replicate data were merged together to generate the whole pond community. Canonical correspondence analysis (CCA) was performed to correlate the influence of the nutrient data on each of the microbial communities. The influence

of the nutrient data on the microbial communities was confirmed by performing Mantel tests on the microbial communities and the nutrient analyses.

3.4 Results

3.4.1 Sequence processing and control communities

After assembling, quality filtering, and OTU picking, the 18S rRNA gene sequences resulted in 52,855 OTUs with a total of 18,369,903 sequences. Maintaining the Archaeplastids, Cryptophyceae, Centrohelida, Ochrophyta, and Dinoflagellates kept 38,847 OTUs (~26.5% reduction in observed OTUs) and 16,081,783 sequences (~12.9% reduction in sequence). Removal of spurious OTUs resulted in 15,929,430 sequences and 2,071 OTUs in 72 samples, reducing the sequences and OTUs by a total of ~0.05% and ~95%, respectively.

The control communities generated 441,235 sequences after quality trimming and contained 416,306 sequences and 13 OTUs post-OTU picking. Rarefaction also showed that each of the communities contained between 10 and 13 OTUs. Based on the plateau of each replicates curve, the entire community in the controls were accounted for (Fig. A3.2). The HTB1 (*Scenedesmus* sp.) and CC503 (*Chlamydomonas* sp.) strains equally made up a total of 80% of the community prior to sequencing, but the *Chlamydomonas reinhardtii* representative sequences were over-represented, making up about 60% of the community in each replicate. In contrast, HTB1 representative sequences from closely related *Scenedesmus* sp. composed of only 20% of the communities, along with the *Desmodesmus* sp. RAI5 (Fig. A3.3).

3.4.2 Fluorescent cell counts

For 2017 samples, cell counts of autofluorescence, accounting for photosynthetic organisms, displayed a four-fold increase immediately after fertilization on Day 1. The bacterial counts increased nearly seven-fold within 1_F17, the fertilized pond. On the sixth day post-fertilization the bacterial counts were reduced from $6.5x10^7$/mL to less than $3x10^7$/mL and was then comparable to those in the control pond. DAPI counts of the bacterial abundance of 1_F17 reflect an identical pattern to the abundance of the contaminating 16S rRNA gene sequences introduced by the manure (Fig. 3.1). The autofluorescent cells in 1_F17 displayed a steady increase in the cell count until day 12, after which there was a reduction to the level of the control pond. Interestingly, the mean bacterial concentrations showed identical patterns in the changes (Chapter 2, Fig. 2.1). Kruskal-Wallis tests showed that there was a statistical difference between the microscopic counts in the days for both ponds. However, *post hoc* Nemenyi tests for 1_F17 only showed significance between day -6 and 12 for the algal and bacterial:algal ratio counts ($p = 0.039$) and day -6 and 1 for the bacterial counts ($p = 0.025$) (Table A3.1). The unfertilized 2_F17 only showed significant differences for the bacterial:algal ratio between day -6 and 6 ($p = 0.04$)

3.4.3 Nutrient analyses

In 2016, two different dispersal systems were used to disseminate nutrient within two ponds (1_F16 and 5_F16) which displayed varying patterns of nutrient concentrations over time (Fig. 3.2). The active nutrient dispersal system was used to disperse nutrients within 1_F16 and 1_F17. This resulted in a large spike in the TDN

and the TDP immediately after fertilization, 1_F16 Day 0 mean TDN ± sd: 0.54 mg/L ± 0.028; mean TDP: 0.075 mg/L ± 0.025; 1_F16 Day 1 mean TDN ± sd: 7.87 mg/L; mean TDP: 0.88 mg/L; 1_F17 Day 0 mean TDN ± sd: 0.21 mg/L ± 0.023; mean TDP: 0.21 mg/L ± 0.072; 1_F17 Day 1 mean TDN ± sd: 6.41 mg/L ± 5.33; mean TDP: 1.35 mg/L ± 1.06. The nutrient spike was followed by a progressive decline in TDN but stable concentrations of TDP. A passive nutrient dispersal method was used in pond 5_F16 and showed gradual increases in both the TDN and TDP, reaching their peaks on day 15 (mean TDN ± sd: 4.36 mg/L ± 0.67; mean TDP: 2.96 mg/L ± 0.45). DOC did not appear to follow any expected pattern as the mean peak of 1_F16 and 1_F17 appeared prior to their fertilization, days -1 and -6 respectively. However, Welch's two sample t-tests did not show a significant difference in any of the measured nutrient levels between the ponds with different nutrient dispersal systems in 2016 (DOC: $t = -0.288$, $p = 0.777$; TDN: $t = 1.271$, $p = 0.222$; TDP: $t = -0.957$, $p = 0.354$). Wilcoxon rank-sum tests were also performed between the two experimental ponds in 2016 and the experimental pond in 2017 to reveal that there were also no differences in the nutrient levels between years within the experimental ponds (DOC: $W = 262$, $p = 0.097$; TDN: $W = 274$, $p = 0.452$; TDP: $W = 208$, $p = 0.442$). Furthermore, all nutrient concentrations were statistically significantly different between the fertilized water and the untreated water (DOC: $W = 621.5$, $p = 0.005$; TDN: $W = 882.5$, $p = 1.842 \times 10^{-8}$; TDP: $W = 972$, $p = 3.479 \times 10^{-14}$). The two ponds sampled in parallel in 2017 showed identical patterns in their water temperature, as would be expected. In 2016, the two experimental ponds were sampled 17 days apart and showed independent patterns in the temperature fluctuations.

Canonical correspondence analyses (CCA) were done to visualize the degree of influence that each measured variable had on the microalgal communities (Fig. 3.3). The untreated pond communities clustered tightly with each other compared to the microalgal communities in the fertilized pond samples, which showed little clustering in response to nutrient variables. The TDP (CCA1 = -0.797, CCA2 = -0.498) and water temperature (CCA1 = 0.524, CCA2 = -0.725) showed the greatest degree of influence on the eukaryotic communities followed by the DOC (CCA1 = 0.041, CCA2 = -0.642). The correspondence of the TDN (CCA1 = -0.323, CCA2 = -0.387) in the eukaryotic community was approximately half that of the TDP.

To augment the CCA, Mantel tests were performed to assess the strength of the correlation of each of the measured environmental parameters. Even though the DOC showed a strong degree of influence on the community structure, Mantel tests did not indicate a statistically significant correlation with the microalgae ($\rho_s = 0.021$, $p = 0.28$). Weak but positive correlations were found to be associated with the concentrations of TDP and TDN (TDN: $\rho_s = 0.261$, $p = 0.002$; TDP: $\rho_s = 0.326$, $p = 0.001$). Although, according to the CCA water temperature was one of the strongest influencers of the microalgal community, it had the weakest correlation ($\rho_s = 0.189$, $p = 0.001$).

3.4.4 Taxonomy and diversity analyses

The 12 most prevalent taxa mainly belonged to the chlorophytes and included representatives of the classes *Trebouxiophyceae* and *Chlorophyceae* as well as the orders *Chlamydomonadales*, *Chlorellales*, *Dolichomastigales*, *Pedinomonadales*, and

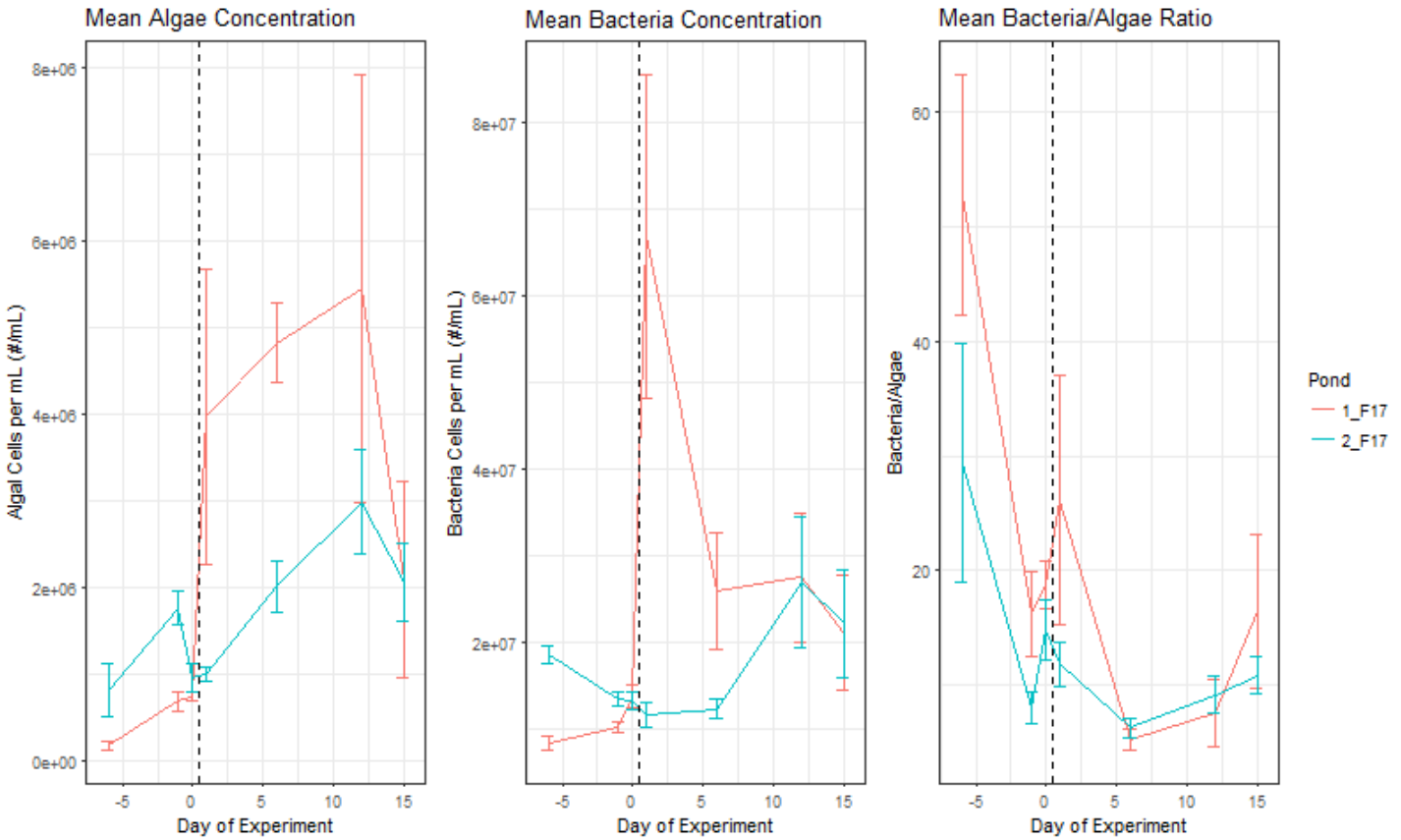

Figure 3.1: **Epifluorescent counts of the mean algal (autofluorescence), bacterial, and the bacteria:algal ratio (respectively).** Error bars represent the standard error of the mean. Pond 1_F17 was fertilized immediately after the Day 0 sampling time. Samples from Day 1 were collected approximately 24 hours after fertilization. The black vertical dashed-line represents the time of fertilization into pond 1_F17. Pond 2_F17 was not fertilized

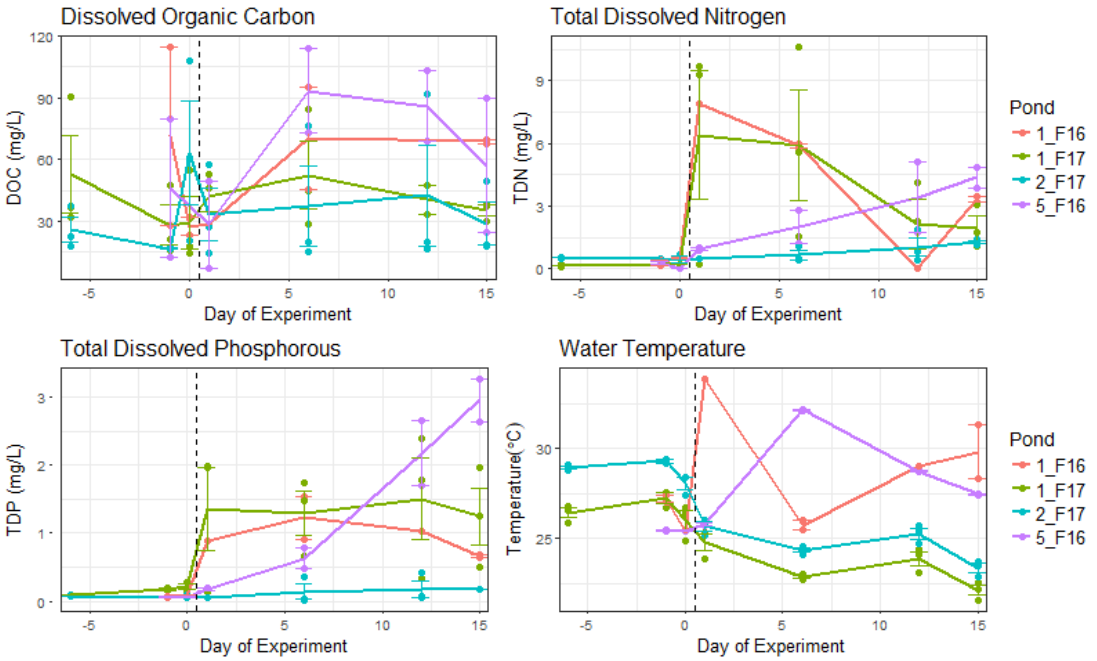

Figure 3.2: Mean environmental variable by day for each pond displaying the change of DOC, TDN, TDP, and water temperature over time. Error bars represent the standard error of the mean. The black vertical dashed-line represents the time of fertilization into ponds 1_F16, 5_F16, and 1_F17.

Sphaeropleales. Representatives of two ochrophytes (heterokonts) were also prevalent belonging to the class *Chrysophyceae* and the order *Synurales* (Fig. 3.4). A single charophyte belonging to the *Desmidiales* order was also present. These 12 taxa represented 1,977 OTUs and 15,860,680 sequences of the 2,071 OTUs and 15,929,430 sequences present in the ponds; 776 of these OTUs were identified as ambiguous taxa or were unable to be identified and these categories contained 3,003,388 sequences. There were five OTUs that were present in all the ponds corresponding to the orders of *Trebouxiophyceae* and *Chlorophyceae*. Three of these OTUs were also the most dominant (OTU FR865536.2.2159, *Chlorophyceae*, 7,734,583 sequences; OTU FM205840.1.2097, *Trebouxiophyceae*, 815,687

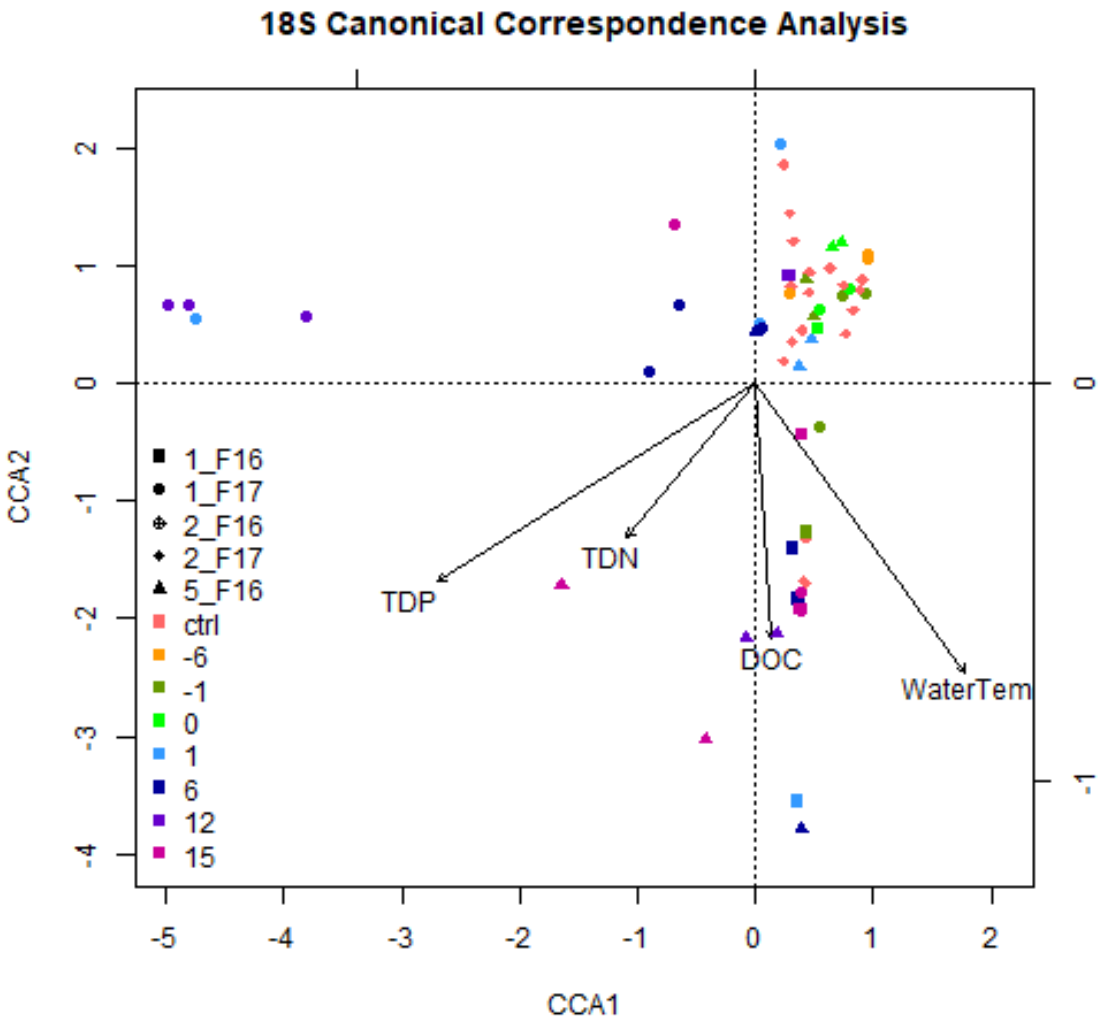

Figure 3.3: Canonical Correspondence Analyses of the 18S rRNA gene communities. Vectors represent the degree of correlation provided by the measured variable.

sequences; OTU JX101905.1.1706, *Chlorophyceae*, 591,306 sequences). Representative sequences from these OTUs were aligned with the BLAST database from NCBI and identified as *Gonium sp.*, *Micractinium sp.*, and *Vitreochlamys sp.*, respectively.

The relative abundance of taxa making up a minimum of 0.1% of the pond communities identified to the fifth level of taxonomic ranking were plotted to show

the progression of the eukaryotic communities (Fig. 3.5). The fifth level of identification represents both the class and order levels of taxonomy. Chlorophytes within the classes of *Chlorophyceae* and *Trebouxiophyceae* dominated in all samples. Dominant orders that are defined within the class *Chlorophyceae* include the *Sphaeropleales* and the *Chlamydomonadales* while the *Oedogoniales* is the minor order. Examination of the experimental ponds in 2016 shows that after fertilization, the chlorophytes virtually took over the entire pond's algal community. Contrary to this, 1_F17 shows a diminishing chlorophyte population and undefined ambiguous taxa gain dominance. The *Sphaeropleales* and the *Trebouxiophyceae* appear to be unchanged by the addition of the fertilizer.

Rarifying the samples to an even depth of 22,000 sequences/sample removed two samples and 77 OTUs. The rarefaction plot does not show a plateau of the curves, indicating that more sampling depth would be required to fully sample the entire community (Fig. 3.6). Richness, diversity, and evenness diversity measures (observed OTUs, Shannon, and Pielou's J indices) plotted through the progression of the experiment trended towards a reduction in both the richness and the evenness of each ponds' diversity (Fig. 3.7). Kruskal-Wallis rank sum tests performed on the experimental ponds between each day of the experiment showed significant differences for each of the diversity indices, however, pairwise *post hoc* Nemenyi tests did not show significant differences from one day to another. It is worth noting that lower p-scores are typically observed between days prior to treatment and those post-treatment. (Table A3.2).

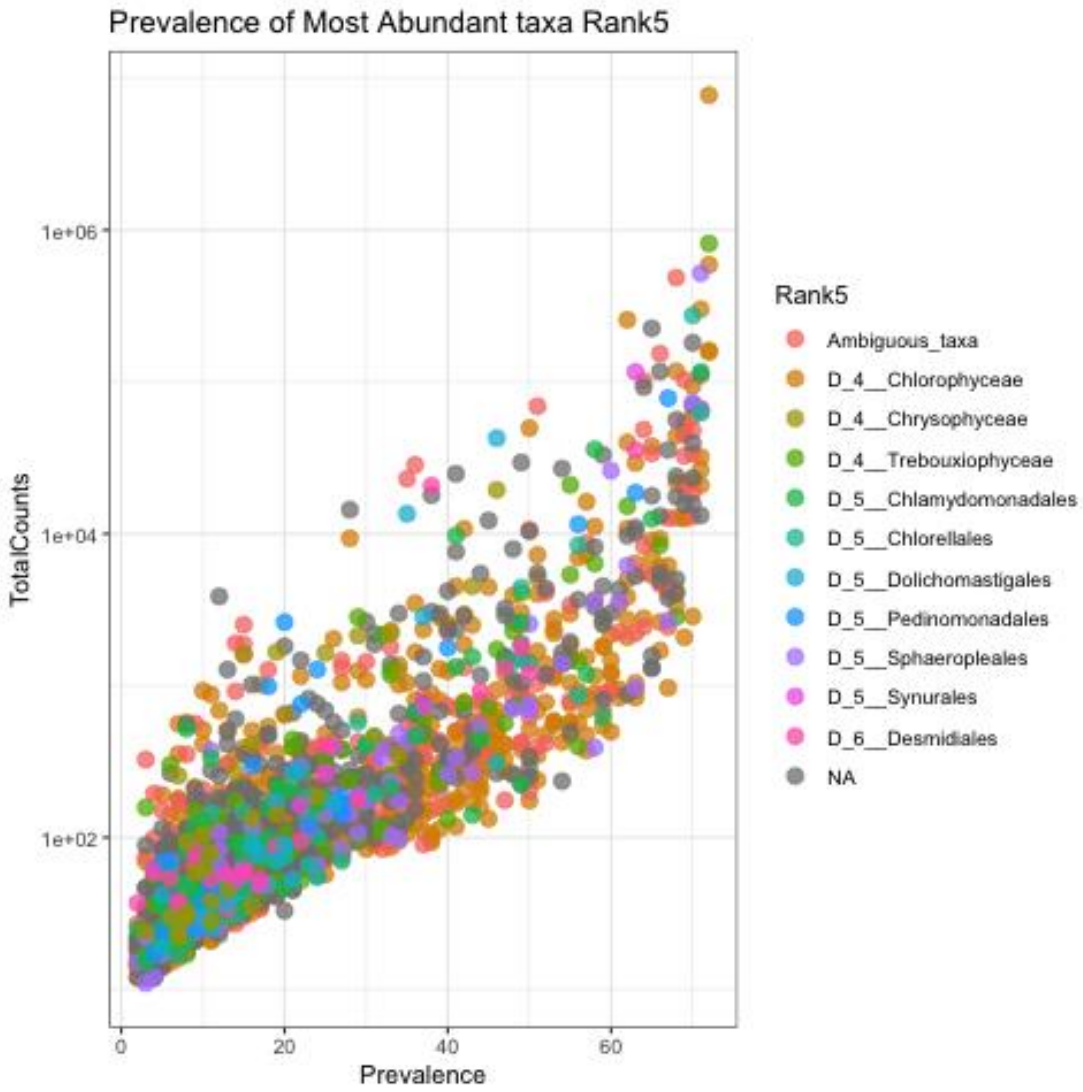

Figure 3.4: Prevalence of the 12 most dominant eukaryotic taxon identified to the deepest identifiable level of classification. The horizontal axis represents the number of samples it occurs in; the y-axis shows the abundance of each individual OTU.

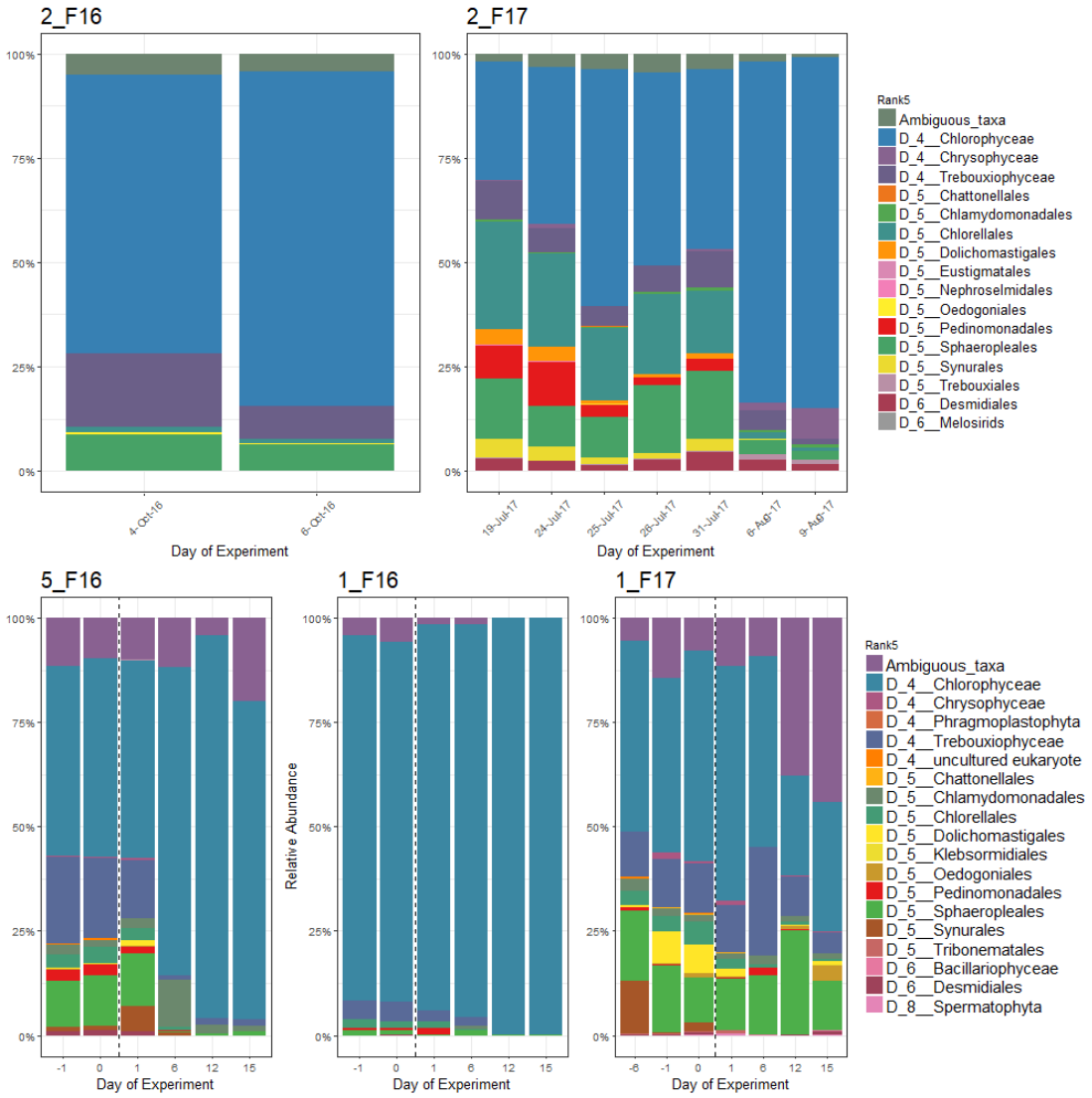

Figure 3.5: Relative abundance of the most dominant eukaryotic taxon. Taxa are identified to the deepest level of identification that represent a minimum of 0.1% of the community in each pond. Charts 2_F16 and 2_F17 represent control ponds that were never fertilized. The date of sampling is provided with percent of the community contributed by each taxon. Experimental ponds are shown in the bottom graphs and the black vertical line represents the time of fertilization.

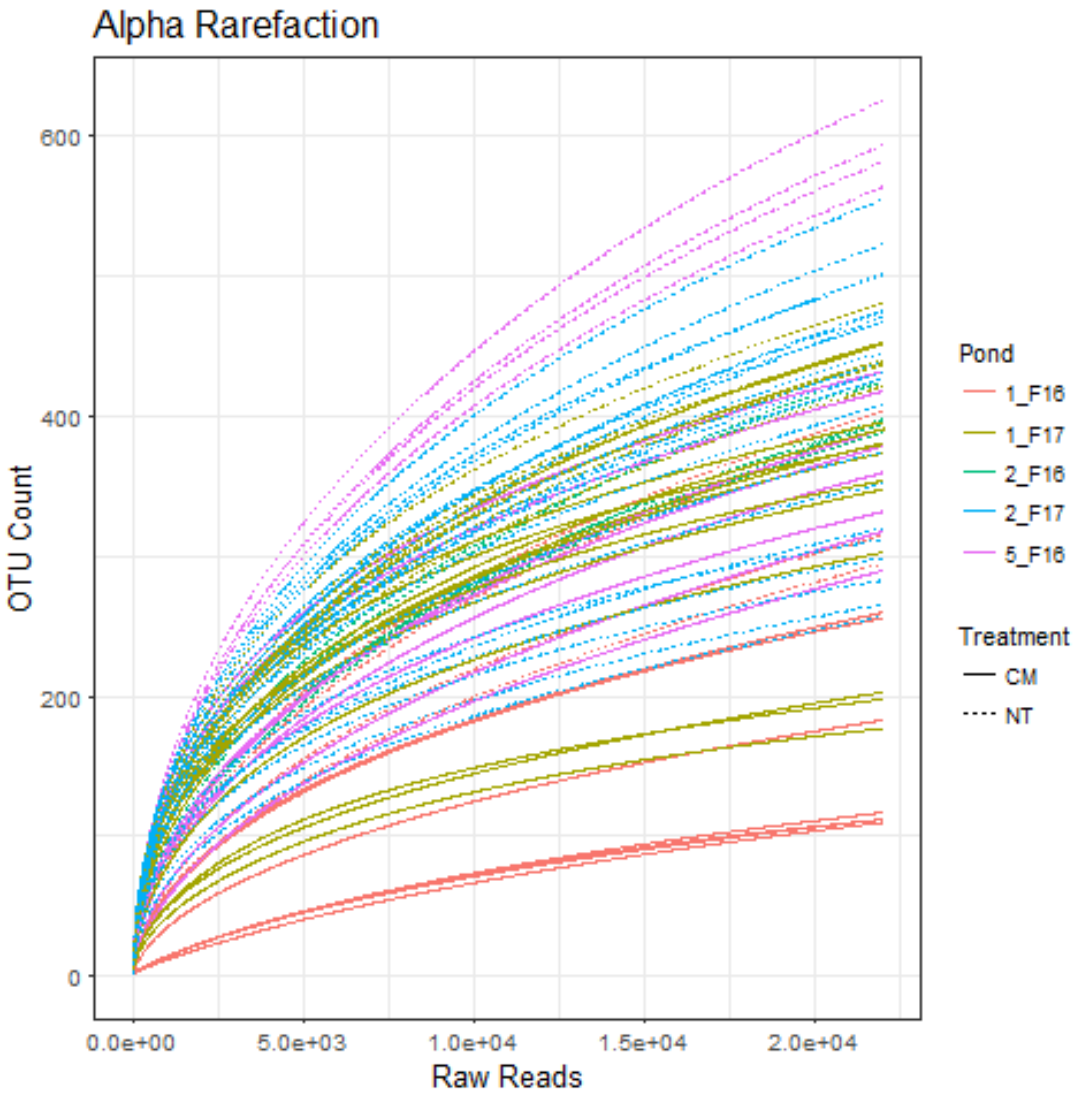

Figure 3.6: Rarefaction of the eukaryotic communities. Colored lines indicate the pond and year from which the sample was collected. Line types indicate the if the sampled water was collected after fertilization (CM) or before fertilization (NT).

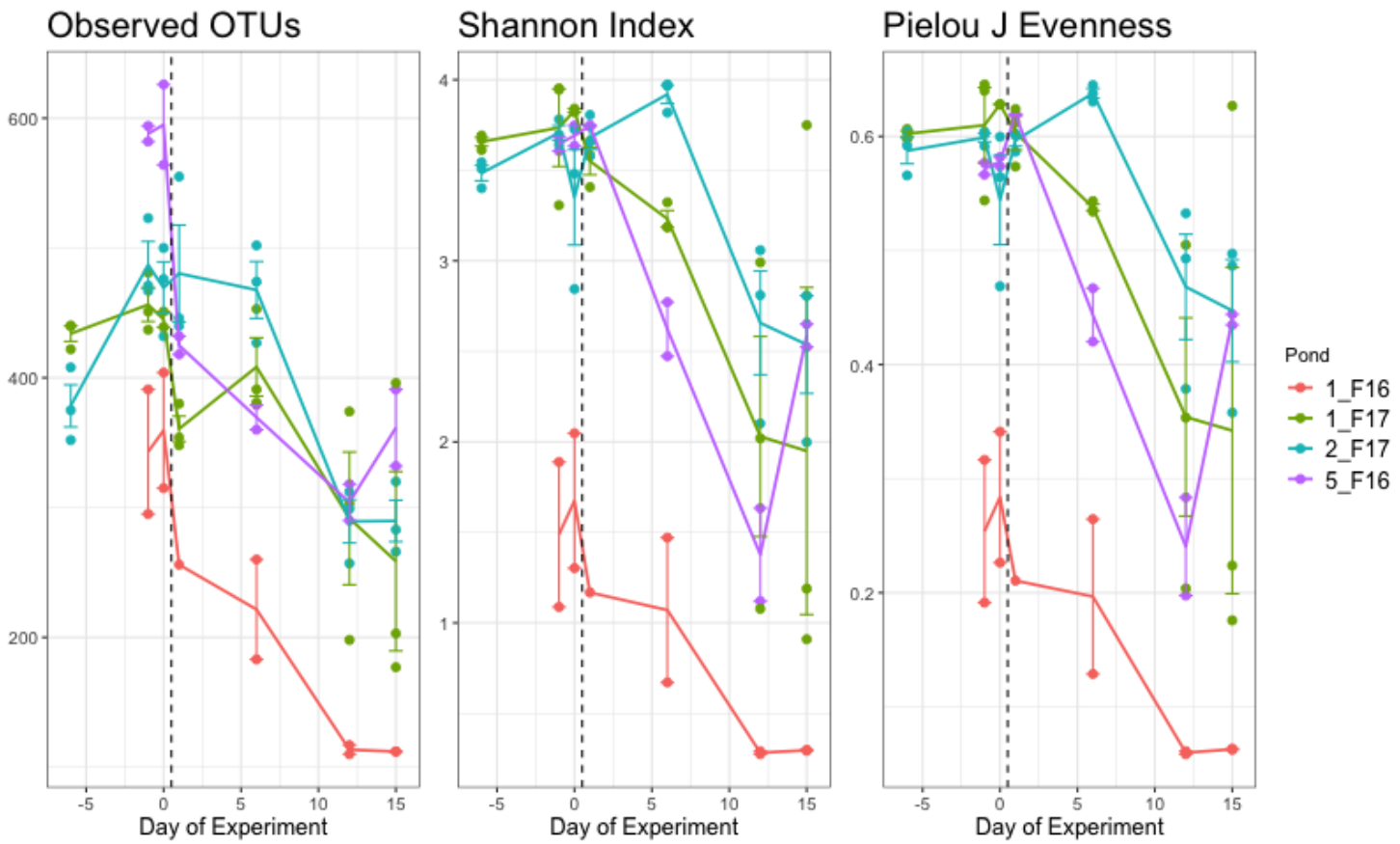

Figure 3.7: Mean alpha diversity measures of the algal community of each pond over time. The black vertical line indicates the time of fertilization. Pond 2_F17 was never fertilized. Error bars indicate the standard error of the mean of each measure. The black vertical dashed-line represents the time of fertilization into ponds 1_F16, 5_F16, and 1_F17.

The Bray-Curtis dissimilarity distance matrix, unweighted UniFrac distance, and weighted UniFrac distance matrices were generated to elucidate the differences between samples in multi-dimensional space (Fig. 3.8). The Bray-Curtis dissimilarities and the weighted UniFrac distance plots appear to be similar to each other, indicating that the abundance of the OTUs present in each pond or treatment is more similar over time. The unweighted UniFrac distances show that, prior to treatment, the samples clustered more closely together and then diverged after fertilization, indicating that the pond communities became more phylogenetically distinct from each other based on the presence or absence of any algal species unique to each pond. In addition to the unweighted UniFrac, the weighted UniFrac metric shows the five pond communities overlapping with each other, implying that the dominant OTUs in each pond are likely shared or phylogenetically related. Clustering designated by the day of the experiment show that the communities consistently shifts as the experiment progresses. However, the clustering within the weighted UniFrac indicate that the dominant communities are closely related.

3.4.5 Community Similarities

The PERMANOVA tests on all the ponds revealed that each sampled pond contributed the greatest portion of differences in the eukaryotic communities (Table 3.1) (ADONIS: $R^2 = 0.460$, $p = 0.001$). ANOSIM confirmed that the origin of the samples shared few similarities ($R = 0.599$, $p = 0.001$). Examination of the naturally occurring communities in the ponds reiterated that there were very few similarities between any of the ponds prior to fertilization (ANOSIM: $R = 0.970$, $p = 0.001$). The experimental ponds were examined separately to explore where their differences lay.

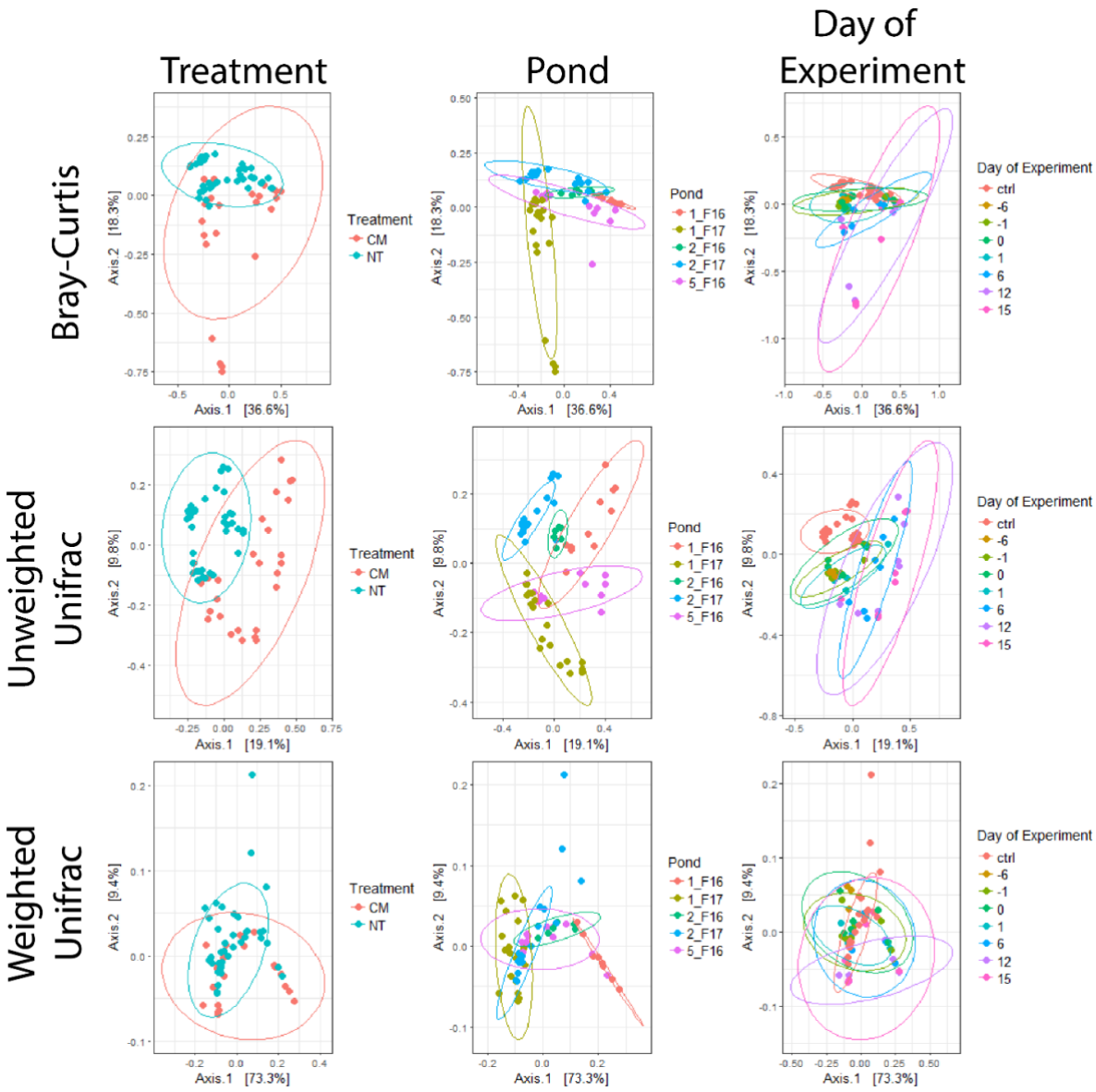

Figure 3.8: Multidimensional scaling/principal coordinate analyses of eukaryotic communities. The top row is distinguished by the Bray-Curtis dissimilarity metric; the middle row shows separation based on unweighted UniFrac distances; the bottom row shows weighted UniFrac distances. Ellipses represent the 95% confidence.

The year when the ponds were sampled explained the greatest amount of variance and was also the most dissimilar group (ADONIS: $R^2 = 0.345$, $p = 0.001$; ANOSIM: $R = 0.703$, $p = 0.001$). Similarly, comparisons within the ponds showed few similarities (ADONIS: $R^2 = 0.161$, $p = 0.006$; ANOSIM: $R = 0.637$, $p = 0.001$). The ANOSIM R statistics between the treatment and the day of the experiment suggest that there are no significant similarities within these groups (Treatment: $R = 0.002$, $p = 0.41$; Day of experiment: $R = -0.101$, $p = 0.761$).

Based on the results of the ANOSIM, SIMPER was run to determine which OTUs were specifically contributing to the dissimilarity between years, ponds, and the day of treatment. The eukaryotic communities in the experimental ponds showed 72% dissimilarity between years. This was explained by only three OTUs that cumulatively contributed to 46.7% of the dissimilarity. Representative sequences of these OTUs were identified as *Gonium pectorale* (17.7%), *Pyrobotrys elongata* (11.6%), and a *Monoraphidium* sp. (4.35%) using the BLAST database. Ponds 1_F16 and 5_F16 were 54.6% dissimilar from each other with two OTUs identified as *G. pectoral* (21.9%) and *Micractinium inermum* (3.7%) contributing to 47% of the differences. *G. pectrorale* and *P. elongata* also explained 26% and 11.8% differences, respectively, between pond 1 in 2016 and pond 1 in 2017, which were 78.7% dissimilar. Pond 5_F16and 1_F17 were 65% dissimilar in their composition which was explained by 5 OTUs; *P. elongata* (11.4%), *G. pectorale* (9.3%), *Monoraphidium* sp. (3.7%), *M. inermum* (3.5%), and *Choricystis* sp. (2.7%).

SIMPER analyses revealed the two untreated dates were the most similar, with 45.9% dissimilarities, and day 1 and day 15 were the most dissimilar (66.2%).

Between all the sampled dates, only 16 OTUs contributed to 50% of the differences between any two of the sampling days. All 16 OTUs were chlorophytes that consisted of 673,348 sequences of the 946,000 sequences in the experimental ponds. Representative sequences from OTU clustering were identified using the BLAST database. The *Gonium* sp. (OTU FR865536.2.2159) appears to be the most stable after fertilization. The *Vitreochlamys* sp. (OTU JX101905.1.1706) did not show any clear enrichment in the ponds. Another OTU (LC093471.1.1704) was identified as *Pyrobotrys,* a genus that is in the order *Chlamydomonadales* (Fig. 3.9). When screening the filter cut-off samples for detection of microalgae, 18S rRNA gene bands that appeared in the 1 μm > x ≥ 0.22 μm fractions were excised, sequenced, and identified with BLAST. These sequences were positively identified as members of the *Chlamydomonadales* order, possibly a *Pyrobotrys* sp. The bands were dominant in 1_F17 and appeared to become more prevalent at the end of the sampling period (Fig A3.4).

Prior to fertilization, *G. pectorale*, *M. inermum*, *Monoraphidium* sp., and *Volvox* sp. dominated the ponds. *G. pectorale* steadily began to proliferate until reaching its peak on day 12. The second most abundant OTU at the start of the experiment, *M. inermum*, was one third as abundant as the *Gonium* sp., on average, and peaked at day 6 until it's abundance declined to its lowest abundance on day 15. By the end of the experiment, the second most abundant species was *P. elongata* which was nearly undetectable on days -1 and 0 but began to display immediate enrichment after fertilization.

Table 3.1: ADONIS and ANOSIM tests describing the explanation of variation in the eukaryotic communities. ANOSIM values describe the similarity between ponds; R values range from 0-1, 1 representing no similarities between the ponds and 0 representing identical communities. * = replicates were not combined due to lack of sample size within comparisons.

Pond			Untreated Water*			Fertilized		
ADONIS	**R^2**	**P**	**ADONIS**	**R^2**	**P**	**ADONIS**	**R^2**	**P**
Pond	0.460	0.001	**Pond**	0.523	0.001	**Pond**	0.119	0.091
Year	0.225	0.002	**Year**	0.278	0.001	**Year**	0.436	0.002
Treatment	0.103	0.008	**Date**	0.590	0.001	**Day of Exp**	0.175	0.801
ANOSIM	**R**	**P**	**ANOSIM**	**R**	**P**	**ANOSIM**	**R**	**P**
Pond	0.599	0.001	**Pond**	0.970	0.001	**Pond**	0.632	0.003
Year	0.392	0.001	**Year**	0.427	0.003	**Year**	0.831	0.002
Treatment	0.173	0.021	**Date**	0.381	0.004	**Day of Exp**	-	0.805

Experimental Ponds (1_F16, 5_F16, 1_F17)		
ADONIS	**R^2**	**P**
Pond	0.161	0.006
Year	0.345	0.001
Treatment	0.078	0.201
Day of Exp	0.204	0.854
ANOSIM	**R**	**P**
Pond	0.637	0.001
Year	0.703	0.001
Treatment	0.002	0.41
Day of Exp	-0.101	0.761

3.5 Discussion

Between 2016 and 2017, three man-made ponds were filled with water from a nearby stream and fertilized with chicken manure to stimulate blooms of phytoplankton that could be harvested to produce biofuel. Due to the nature of the growing facility and process, biofuel production is dependent on the diversity of the native phytoplankton present in the source water and successful growth of high-density polycultures. Traditionally, the production of algal-derived biofuels has been based on strain optimization and manipulation within a relatively controlled industrial growth facility. This study has taken a novel approach in exploring the algal diversity using metagenomic analyses within ponds that have artificially been made eutrophic to encourage growth of natural polycultures.

Microalgal and bacterial cell counts showed an interesting numeric relationship between the photosynthetic microbes (eukaryotic microalgae and cyanobacteria) and heterotrophic bacteria. There was a sharp increase in the microalgae in pond 1_F17 directly after the manure was introduced that appeared to persist through most of the experiment. It was unexpected that the addition of the manure did not sustain high bacterial counts beyond 6 days post-inoculation. On days 12 and 15, the abundance of the microalgal cells and bacterial cells were nearly identical between the fertilized pond and the untreated pond. Despite the individual pattern changes in counts of photosynthetic and heterotrophic microbes, the ratios of bacteria:algae in the untreated and fertilized ponds showed a nearly identical pattern (Fig. 3.1). Observations of the eukaryotic algal diversity (Fig. 3.7) prior to fertilization show that the algal diversity between 1_F17 and 2_F17 was more

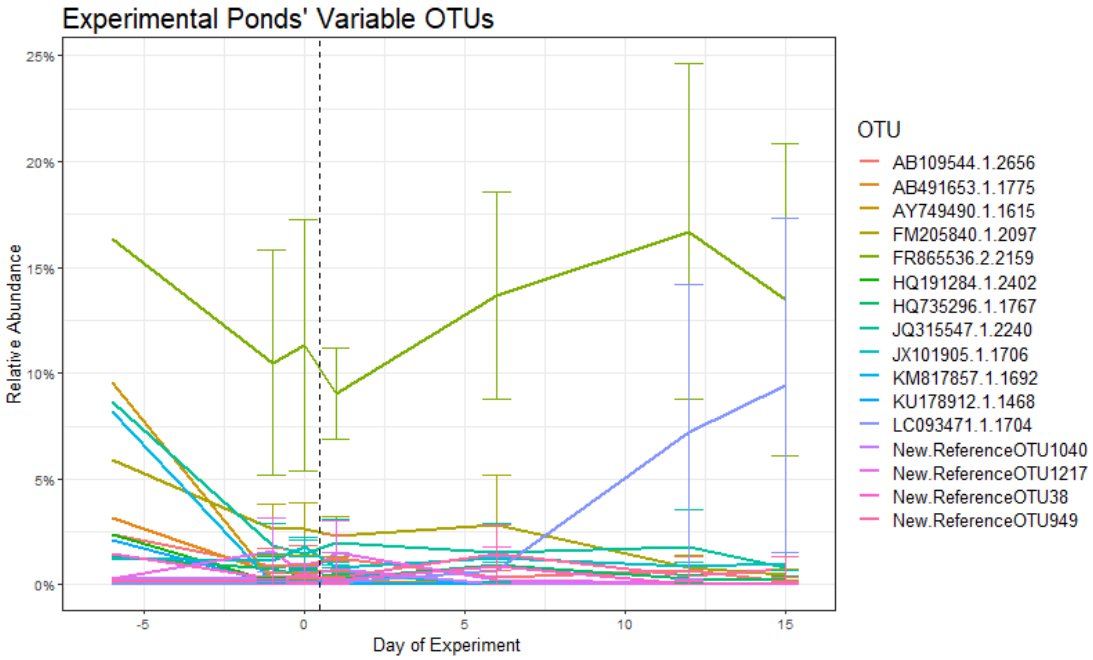

Figure 3.9: Change in relative abundance of the most variable OTUs. The OTUs that explain 50% of the differences between each day plotted over time to show temporal variation in the communities. The percent of the community is based on the normalized sum of each days community abundance. The data from experimental ponds 1_F16, 5_F16, and 1_F17. Error bars represent the standard error of the mean.

similar compared to after 1_F17 fertilization. Together with the algal growth shown in Fig. 3.2, this suggests that the fertilization of the experimental pond resulted in a selection process, allowing fast growing species of eukaryotic algae to flourish for a short time. However, the control pond also appears to be having an increase in the microalgae as well as the bacteria. Through microscopic examination of the pond water, the majority of the microalgal cells seen in pond 2_F17 were cyanobacteria (no differential counts performed), indicating the natural occurrence of a cyanobacterial bloom.

Prior to fertilization, each of the four ponds shared similar concentrations of DOC, TDN, and TDP, but the treated ponds experienced significant shifts in the TDN and TDP concentrations. Ponds that were fertilized with an active nutrient dispersal method (1_F16, 1_F17) had an immediate spike in TDN followed by a steady decline in the mean concentrations of TDN. TDP concentrations also showed an identical spike, but the higher concentrations appeared to be maintained throughout the experiment. The passive nutrient dispersal method pond (5_F16) did not give the same dramatic changes immediately upon fertilization, rather, the mean concentrations of both TDN and TDP gradually increased over subsequent days (Fig. 3.2).

The decreasing concentrations of TDN may be perceived as a desired effect. One issue that has prohibited microalgae-derived biofuels from reaching a commercial product is the lipid production variability within strains of microalgae. Many strains of microalgae produce larger quantities of lipids during times of stress, most notably when nitrogen is a limiting nutrient (37, 211–213). Limitation of nitrogen in microalgae monocultures has shown that it can yield lipid concentrations greater than 2-fold higher in comparison to nutrient sufficient conditions (34, 35, 37, 211, 214). The ability to produce large quantities of lipids is strain specific and cannot be attributed to genus classifications (75). Considering that nitrogen concentrations decrease in the ponds as the abundance of the microalgae increases, it might be surmised that taxa more tolerant or adaptable to eutrophication would be dominant initially. As these taxa exhaust the bioavailable nitrogen supply, the lipid content in the mature bloom may increase. Because HTL is ultimately the end-point biofuel

production strategy lipid content is not as important as in systems where lipids are extracted and converted to biodiesel. Nitrogen limitation resulting in high lipid content may only provide a trivial advantage with the use of a properly optimized HTL system (83–85).

All three of the algae introduced into the synthetic community belonged to the *Chlorophyceae* class of green algae; *Desmodesmus* sp. RAI5 (isolated from homologous ponds; Chapter 4) and *Scenedesmus* sp. HTB1, both belong to the *Scenedesmaceae* family within the *Sphaeropleales* order; and *Chlamydomonas reinhardtii* belongs to the *Chlamydomonadaceae* family within the *Chlamydomonadales* order. Both the Sanger sequencing approach and the Illumina MiSeq sequencing platform yield sequences of similar size, between 250-300 bp and 280 bp, respectively. However, the Next Generation Sequencing data paired with the custom database for OTU clustering and taxonomy assignment revealed the expected values for *Desmodesmus* sp., but the *Chlamydomonas* was over represented ~1.5 times and *Scenedesmus* was only present half as frequently as expected.

The chosen primers, P47R and P73F, were designed to specifically target *Chlorophycea* and Diatoms, and thus have been shown to successfully amplify all tested monocultures (210). Wallace *et al.* (2015) showed the capability of the P47R and P73F primers to resolve as deep as the class level and successfully identify the *Trebouxiophyceae* and the *Chlorophyceae* classes within the *Chlorophyta* phylum (Chlorophytes) (215). They were also able to identify the phylum *Streptophyta* dominated by the *Embryophyta* class (vascular plants). It has been shown that *Scenedesmus* sp. (*Chlorophyceae*) and *Chlorella* sp. (*Trebouxiophyceae*) could be

sequenced and identified through traditional Sanger sequencing and multiple alignment with these primers (216). Although the taxonomic resolution within the chosen database (SILVA128) is not as precise and uniform as desired, molecular identification provides invaluable data as the degree of conservation of 18S rRNA genes can identify differences between closely related groups (217). As mentioned, the chosen primer pair was designed and proven to target microalgae; no research has shown the ability of these primers to amplify or identify eukaryotic algal grazers. This restricts the present research from providing insights into any top-down control imposed by algal predators.

Prevalence data from the pond samples showed that the most dominant OTUs are also the most widely distributed. Three of the most dominant OTUs belonged to the *Chlorophyceae* and the *Trebouxiophyceae*. The representative sequence of these OTUs were aligned with the BLAST database. Two of these were members of the genus *Gonium* and *Vitreochlamys*, of the order *Chlamydomonadales* (also referred to as *Volvocales*), and class *Chlorophyceae.* Another *Trebouxiophyceae* was identified as the genus *Micractinium* of the order *Chlorellales*. The OTUs that represented these genera were also found to be among the most variable in the ponds (Fig. 3.9). Members of the *Chlamydomonadales* have been reported to be associated with eutrophic water (218, 219).

Patterns in the relative abundance data show that the Chlorophytes were the most dominant group in all the ponds. Fertilization of the experimental ponds appear to select for the Chlorophytes while reducing the abundance of the *Trebouxiophyceae* (Fig. 3.5). Enrichment for a select group of species is corroborated by the reduction in

the richness and evenness in the measured alpha-diversity metrics (Fig. 3.7). Canonical correspondence analyses were used to assess the degree of influence of each environmental parameter measured (Fig. 3.3). The TDP of the communities showed the largest vector in the CCA, suggesting that the community structure is most affected by the concentration of TDP. This observation was backed up by Mantel tests that found the 18S rRNA gene community to be most positively correlated with TDP ($\rho_s = 0.326$, $p = 0.001$), followed by TDN ($\rho_s = 0.261$, $p = 0.002$), and water temperature ($\rho_s = 0.189$, $p = 0.001$), but no statistically significant correlation could be found with DOC ($\rho_s = 0.021$, $p = 0.28$). It has been suggested that phytoplankton communities can be used as a bioindicator for water quality and that selective factors may occur within a single environmental variable such as the availability of phosphorous (56, 219). Others have determined that pH, surface-water temperature, and salinity significantly explained variations in microalgae communities (220). The Mantel tests and the CCA suggest that TDN and TDP are indicative of the communities that can adapt to high levels of nutrient, while DOC and water temperature are community drivers in this context.

It is important to note that ANOSIM analyses revealed that the native communities in each of the ponds had almost no similarities with each other (ANOSIM: $R = 0.970$, $p= 0.001$). Analyses of all the sample data showed that the greatest differences were between each ponds' individual community (ANOSIM: $R = 0.599$, $p = 0.001$). However, the fertilized waters showed that the year explained the greatest amount of the variation and the similarities (ADONIS: $R^2 = 0.436$, $p = 0.002$; ANOSIM: $R = 0.831$, $p = 0.002$) (Table 3.1). This may be explained by the uneven

sampling of collecting from one fertilized pond in 2017 and two ponds in 2016, each using different nutrient dispersal systems. The Bray-Curtis and Unweighted UniFrac MDS/PCoA appear to reiterate this observation by showing that the communities within each of the experimental ponds spread in different directions after fertilization. Although the unweighted UniFrac metric showed that there are OTUs within each pond that are phylogenetically unique, weighted UniFrac plots show that the most abundant OTUs in each pond, pre- and post- fertilization, are more phylogenetically related (Fig. 3.8). These observations regarding the diversity indices indicate that species present in the ponds are becoming dominant after fertilization, as shown by the weighted UniFrac plot. On the other hand, the unweighted UniFrac plot shows that samples collected from the fertilized ponds are more diverse, having a higher number of rare-species in the community unique to each pond. Eutrophication has been shown to reduce the species diversity at the microalgae and macrophyte level, in congruence with all measured species diversity metrics in the present study (91–94). It is possible that the phytoplankton community from the source water used to fill the ponds varied between each fill which may have had an effect on the measured diversity of the ponds.

Observations of the 16 OTUs that explained the first 50% of the differences between each sampled day shows two species were most tolerant of eutrophic conditions. Both OTUs are members of the *Chlamydomonadales* (OTU: FR865536.2.2159 and OTU: LC093471.1.1704). OTU FR865536.2.2159 whose representative sequence identified it (Fig. 3.9). In 2017, eukaryotic 18S rRNA gene sequences identified via PCR amplification and Sanger sequencing identified a

Gonium sp. that displayed evidence of increasing concentrations of their 18S rRNA gene sequences (Fig. A3.4). These sequences were aligned against the representative sequence of OTU LC093471.1.1704, showing that they shared >99% identity with a 235 bp match. The reduction in the diversity of each pond, along with the observed discrimination for two specific OTUs indicates the dominant cause for the reduction of the microalgal diversity in the ponds.

Narwani *et al*. (2016) performed direct oil quality analyses based on controlled variations in iterative diversities for polycultures of six strains of microalgae (221). Their findings showed a reduced productivity in the biocrude yield with increasing species diversity compared with biocrude generated from a monoculture. They also found that increasing the microalgal species diversity, though it may reduce productivity, it stabilized the variation between each iteration on the diversity. This appears to be contrary to other studies that show diverse polycultures of algae may be used to improve biomass, productivity, stability, and functionality (90, 222–224). To further investigate the findings of Narwani *et al*, (2016); Godwin *et al*., (2018) used a larger scale and four of the originally tested algae to examine the functionality of the polycultures measured as the mean biomass, mean biocrude yield, mean temporal stability of biomass; mean maximum crash; crash timing; mean maximum of invaders; and invasion timing (225). They were able to determine that polycultures were no better at increasing either the biomass nor the biocrude yield, but they were more resistant to foreign algae invasion and four-species polycultures maintained six of the seven functions over the 70^{th} percentile, where as the best monocultures never performed four of the seven functions over the 60^{th} percentile.

These experiments were performed in a unique mesocosm environment with Bold-3N medium compared with the presented study. The ponds in Frederick, MD are minimally manipulated and filled with natural water from a nearby stream. Any resulting microalgae in these ponds are sourced from either the source water or algae innately present in the pond prior to filling. In these ponds, it has been demonstrated that the microalgae present are a diverse group with far more species of microalgae than the mesocosm. This type of diversity suggests that our systems should outperform the culture systems with only six unique algae, qualifying the natural open pond approach of algae culturing as superior. This claim will require future investigation into the biomass and yield of the microalgae and the resulting biomass and may be improved by using a meta-transcriptomic approach to understand the progressive changes in the physiology of the microbial communities used for biofuel generation.

3.6 Conclusions

Water samples of three man-made ponds were sampled over two consecutive years. Ponds were fertilized with chicken manure to establish a eutrophic state to stimulate algae blooms. Molecular identification methods have described a community of eukaryotic microalgae that appear to be suitably adapted to dealing with high nutrient conditions. Though the chosen database did not have high taxonomic resolution, representative sequences of OTUs could be identified by alternative methods, such as BLAST, to give a better taxonomic profile. Data from these analyses suggests that members of class *Chlorophyceae*, specifically the order *Chlamydomonadales*, become dominant members in the highly eutrophic waters.

Direct microscopic counts of bacteria and autofluorescent cells suggests a ratio that could further be investigated to determine if an ecological ratio of bacteria:algae is consistent across all environments.

This study shows a novel approach for monitoring the total algae community developments in an agricultural growth facility. Members of the *Chlorophyceae* class of eukaryotic microalgae were found to favor the eutrophic waters, specifically the *Gonium* sp. and *Pyrobotrys* sp., of the *Chlamydomonadales* order. Further investigation into the bacterial and microalgal associations could reveal a community of bacterial symbionts that are beneficial for microalgae to proliferate.

Chapter 4: Bacterial-algal interactions and isolation of axenic *Desmodesmus* cultures from artificial ponds using physical isolation and antibiotic treatment

4.1 Abstract

Obtaining an axenic microalgal culture for research purposes is crucial to understand how microalgae respond to their surrounding environment or their nearest neighbors. Due to the diversity of microalgae, there is no definitive method for achieving axenic cultures. Here we isolated seven microalgal strains of the genus *Desmodesmus* which originated from man-made freshwater ponds in Frederick, MD. Each strain was identically handled and isolated from 25 native community samples through both physical isolation as well as treatment with an antibiotic cocktail. *Scenedesmus* sp. HTB1 was grown in co-culture with a panel of bacterial isolates derived from the native environment of its close relative *Desmodesmus* sp. The growth response of the microalga to the bacteria add to the mounting evidence of the diversity of bacteria that can participate in mutualistic interactions with microalgae.

4.2 Introduction

Algae are the result of millions of years of evolution, stemming from the engulfment of an ancient cyanobacterium by a heterotrophic protist in order to harness the cyanobacterium's photosynthetic ability to generate sugars for growth (Chapter 1, 8–10, 15). All eukaryotic life is a result of a series of endosymbiotic events between ancient prokaryotic organisms, indicating that bacterial life plays a

crucial role in the sustainability of eukaryotic organisms. Algae also have close relationships with bacterial symbionts that live in the area around the algal cells, termed the phycosphere. For instance, bacteria can provide nutrients, vitamins, and phytohormones to promote the healthy proliferation of the microalgae (98, 100, 101, 110, 125, 226). Researchers have recently proposed engineering the microbiomes of plants and animals to improve host fitness (129). However, to elucidate the symbiotic interactions between two microorganisms like the microalgae *Scenedesmus obliquus* and the bacterium *Rudanella lutea*, it is best if no other organisms are present as to not confound the experimental results. When bacterial species are systematically added to an axenic culture of microalgae and then paired with multi-omics data, conclusions can be drawn about the mechanisms that are associated with bacterial-microalgal relationships (124, 227).

Identifying bioactive compounds also requires axenic cultures because microalgae are not the only source of many valuable products (228). Being able to identify the source of a valuable compound, whether it is the microalgae or a bacterial symbiont, will affect the marketability of the product (132). After the source of a product is identified, omics tools can be used to explore the underlying genetic mechanisms that express specific products (229). For example, axenic strains of *Nannochloropsis oceanica* were required to characterize and engineer enzymes coded in the microalgal genome that generate high quality precursors for biofuels (230).

Obtaining an axenic culture can be done using many different techniques, as there is not a definitive method for every type of microalgae (229). The process requires two basic steps, the first being the establishment of a unialgal culture by

separating out a microalga from an environmental sample. This can be achieved with techniques such as, but not limited to filtration (to separate cells based on size), centrifugation (to separate cells based on density), or agar methods (to isolate culturable colonies from each other). A combination of these methods will isolate microalgae from their environmental cohorts and reduce the bacterial diversity that may be present in planktonic form. However, microalgae produce extracellular polymeric substances (EPS) that form a protective film around the microalgae. The EPS is rich in nutrients and often has bacteria attached to it (229, 231).

The second step to obtaining axenic cultures is a physical or chemical treatment to remove or kill all the remaining bacteria. Killing the remaining bacteria can be achieved with antibiotics, lysozyme treatment (or other enzymes), or by treatment with detergents like Tween or Triton (229). Chemical treatments are riskier to use on high value strains because some antibiotics or detergents may act indiscriminately and kill everything in a culture.

By combining bacteria that may be identified as having a mutualistic relationship with axenic microalgae, synthetic ecology can be employed to artificially construct a probiotic community. Synthetic ecology is a relatively new area of study that mixes two discrete cell populations to produce co-cultures in order to observe how the communities respond (232, 233). It would be expected that bacteria that co-evolve with microalgae could have a positive effect on the community as a whole, and they do (105). However, it was not until recently that it was shown that species of bacteria and microalgae with a vastly different evolutionary history can still participate in mutualistic interactions in which they exchange carbon and nitrogen

(114). Using synthetic ecology methods to observe the community dynamics of simple and controlled microbial consortia will provide invaluable information into the bacteria that are either essential or preferential partners for microalgae.

In the following study, native communities of microalgae were collected from ponds fertilized with chicken manure to stimulate blooms of microalgae for conversion to biofuel. The microalgal cultures were maintained in liquid media, isolated on agar plates, and treated with antibiotics. Axenic status was assessed using DAPI staining and showed that several axenic cultures were successfully obtained. The resulting microalgae showed heterotrophic characteristics and were identified by 18S rRNA gene sequencing as belonging to the genus *Desmodesmus.* Bacteria from the same ponds were also isolated and screened for symbiotic activities with *Scenedesmus* sp. HTB1 using an algal-underlay assay.

4.3 Methods

4.3.1 Algal and bacterial culturing and isolation

To culture microalgae indigenous to the ponds, water from each replicate from the corresponding day and pond designation was pooled and mixed. The pooled sample was inoculated into BG11 liquid medium [17.65 mM of $NaNO_3$; 229.62 μM of K_2HPO_4; 304.29 μM of $MgSO_4 \cdot 7H_2O$; 244.88 μM of $CaCl_2 \cdot 2H_2O$; 31.23 μM of citric acid; 22.90 μM of ferric ammonium citrate; 2.97 μM of EDTA (disodium salt); 188.70 μM of Na_2CO_3; 46.25 μM of H_3BO_3; 9.15 μM of $MnCl_2 \cdot 4H_2O$; 772.04 nM of $ZnSO_4 \cdot 7H_2O$; 1.61 μM of $NaMoO_4 \cdot 2H_2O$; 494.96 nM of $CuSO_4 \cdot 5H_2O$; 270.03 nM of $Co(NO_3)_2 \cdot 6H_2O$; pH 7.1] to give 25 initial cultures. Initial cultures were

subcultured once a month for two months and then on average every eight days for four weeks. Cultures were subsequently spread onto BG11 agar plates made with 10 g/L of agarose and allowed to grow at ambient temperature and light. Each isolation took place between the second and sixth subculturing. Unique and individual colonies were subsequently isolated onto a BG11 agarose plate and then recovered in liquid BG11 to give 24 isolated cultures. Bacterial and algal counts were performed on the resultant cultures that had been subcultured 13 to 14 times. The isolated algal cultures were subcultured into the antibiotic-containing media circa the seventh passage. The twelve surviving bacterial and algal cultures were counted prior to the third passage, nine of these twelve cultures survived until the eighth passage and had the bacterial and algal counts performed.

To isolate bacterial representatives from the ponds, water from the previously described pooled sample was serially diluted and cultured on R2A plates at 27^{o}C for 48 hours. Individual bacterial colonies forming unique morphologies on plates were isolated from each sampling date. Cultures were cryopreserved at -80^{o}C in a solution of 1:1:2 glycerol:H_2O:R2B within a 96-well plate.

4.3.2 Antibiotic treatment

Isolated cultures in liquid medium were subsequently passed into a fresh aliquot of their respective medium containing 100 U/mL penicillin G, 250 µg/mL streptomycin, 25 U/mL polymyxin B, and 1 µg/mL chloramphenicol (234). Cultures were allowed to grow at ambient light (~10 µE) and temperature (~24^{o}C) in a static vessel for 1 week and then subcultured into fresh, antibiotic-free BG11 medium.

Subsamples were fixed in 4% formaldehyde upon the second and seventh passage to enumerate the bacterial load in each sample.

After the eleventh sub-culturing, 100 µL of the algal cultures were spread onto R2A agar plates and incubated in the dark at 27ºC for 1 week. Algal colonies that appeared after incubation were subsequently cultured into a fresh aliquot of BG11 medium. All cultures were subcultured every 14-21 days.

4.3.3 Bacterial:algal ratios and algal identification

One-week-old cultures were fixed in 2% formaldehyde overnight at 4ºC, stained with 300 µM of DAPI, and filtered onto 0.1 µm black polycarbonate filters. Epifluorescence microscopy was used to enumerate the bacteria and microalgae. Chlorophyll autofluorescence was used to count the primary producing microbes identified as microalgae. The bacteria-to-algae ratio was calculated to determine the bacterial load in each culture. Light microscopy was performed on the re-isolated antibiotic treated cultures to assess if the cultures were a single unialgal isolate. Both the light microscopy and epifluorescent microscopy were performed with a Zeiss AxioPlan microscope. DAPI-stained cells were counted visualizing the staining with Zeiss filter set 49 (G: 365; FT: 395; BP: 445/50). Photosynthetic microalgae were counted on the basis of their morphology and autofluorescence, visualized using Zeiss filter set 43 (BP: 545/20; FT: 570; BP: 605/70).

DNA from cultures visually identified as an algal monoculture was extracted using MoBio PowerPlant™ Pro kits. The 18S rRNA gene was amplified and sequenced using P73F (5'-AATCAGTTATAGTTTATTTGRTGGTACC-3') and P47R (5'-TCTCAGGCTCCCTCTCCGGA-3') (210). The resulting sequences were

aligned with the Basic Local Alignment Search Tool (BLAST) from the National Center for Biotechnology Information (NCBI).

4.3.4 Screen for algal-bacterial interactions

An algal underlay assay was developed to screen for potential symbiotic interactions between bacteria and a model alga. Single well 11.4 x 7.3 cm plates with R2A medium were inoculated with 2.0 x 10^6 cells of *Scenedesmus* sp. HTB1 (2.4 x 10^4 cells/cm) and the algal cells were allowed to adsorb to the agar for 24 hours at room temperature in the light. Isolated bacteria from the ponds were stamped on to the algae plates using a 96-pin replicator. Plates were incubated at room temperature in daylight, exposed to an average of 9.4 µE of light. Each plate was observed daily to monitor bacterial colony development and algal growth. Isolates that were identified as having either a growth enhancing or growth inhibiting effect were photographed and identified with 16S rRNA gene sequencing with the universal 16S primers 27F (5'-AGAGTTTGATCMTGGCTCAG-3') and 1492R (5'-TACGGYTACCTTGTTACGACTT-3').

4.4 Results

4.4.1 Algal culturing and treatment

Direct microscopic counts of each of the subsequent treatments revealed a general trend toward achieving axenic status (Fig. 4.1). Holm's adjusted p-values from a pairwise Wilcoxon rank sum test show the most significant differences occur between the bacteria:algae ratios of the stock cultures and the isolated cultures post-antibiotic treatment passage (Stock:Ab.7 $p = 0.012$; Isolation:Ab.7 $p= 0.012$). Many

cultures could not be recovered after each treatment. The nine remaining cultures, each originating from one of 25 initial cultures, showed an identical pattern to that of the entire culture collection (Fig. 4.2 and Fig 4.3). These remaining samples and their source-stock culture were compared using the Holm's adjusted p-values of a pairwise Wilcoxon rank sum test. The most significant difference was found between isolated cultures and the seventh post-antibiotic treatment passage (Isolation:Ab.7 p= 0.023).

There was also significant reduction between the bacterial load for both the antibiotic cultures and the isolated cultures (isolation:Ab.2 p = 0.0206; isolation:Ab.7 p = 0.0296) (Fig. 4.1). Contrary to expectations, isolating the microalgae appeared to enrich for bacteria as there was a significant increase in the bacterial numbers after isolation (stock:isolation p = 0.0046). Interestingly, Ab.7 cultures had the fewest bacteria in the cultures but was significantly more abundant in algal cells than the laboratory maintained stock culture (stock:Ab.7 p = 0.020).

Of the nine remaining cultures, four samples appeared to be axenic. The surviving cultures were plated onto R2A agar to screen for bacterial colony formation; no colony growth was observed. Green algal colonies forming on the R2A plates were isolated and recovered in BG11 media. These isolated cultures were further characterized by 18S rRNA gene sequencing and aligning with the BLAST NCBI database. Each of the remaining seven cultures were identified to be of the genus *Desmodesmus*. Light microscopy images of the cultures showed several phenotypes, suggesting some strain variation.

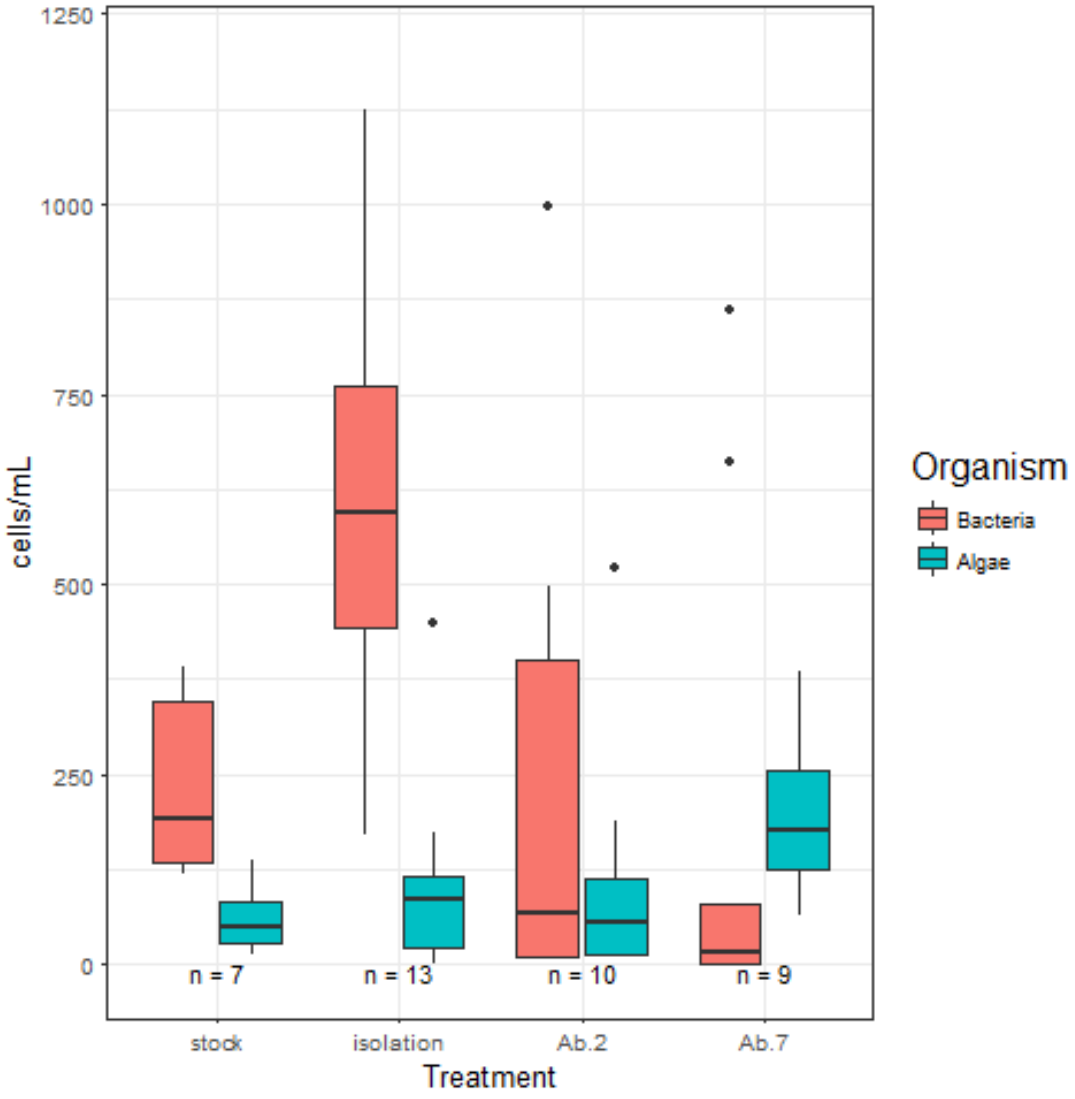

Figure 4.1: Boxplot of bacteria and algae. Counts are given per milliliter for each subsequent treatment of the surviving cultures. "Stock" treatment refers to the culture as it has been maintained in the laboratory with minimal manipulation. "Isolation" treatment refers to a culture that has been isolated on agar plates and subsequently transferred and grown in liquid media. "Ab.2" and "Ab.7" are the cultures that were treated with antibiotics and subcultured 2 or 7 times, respectively.

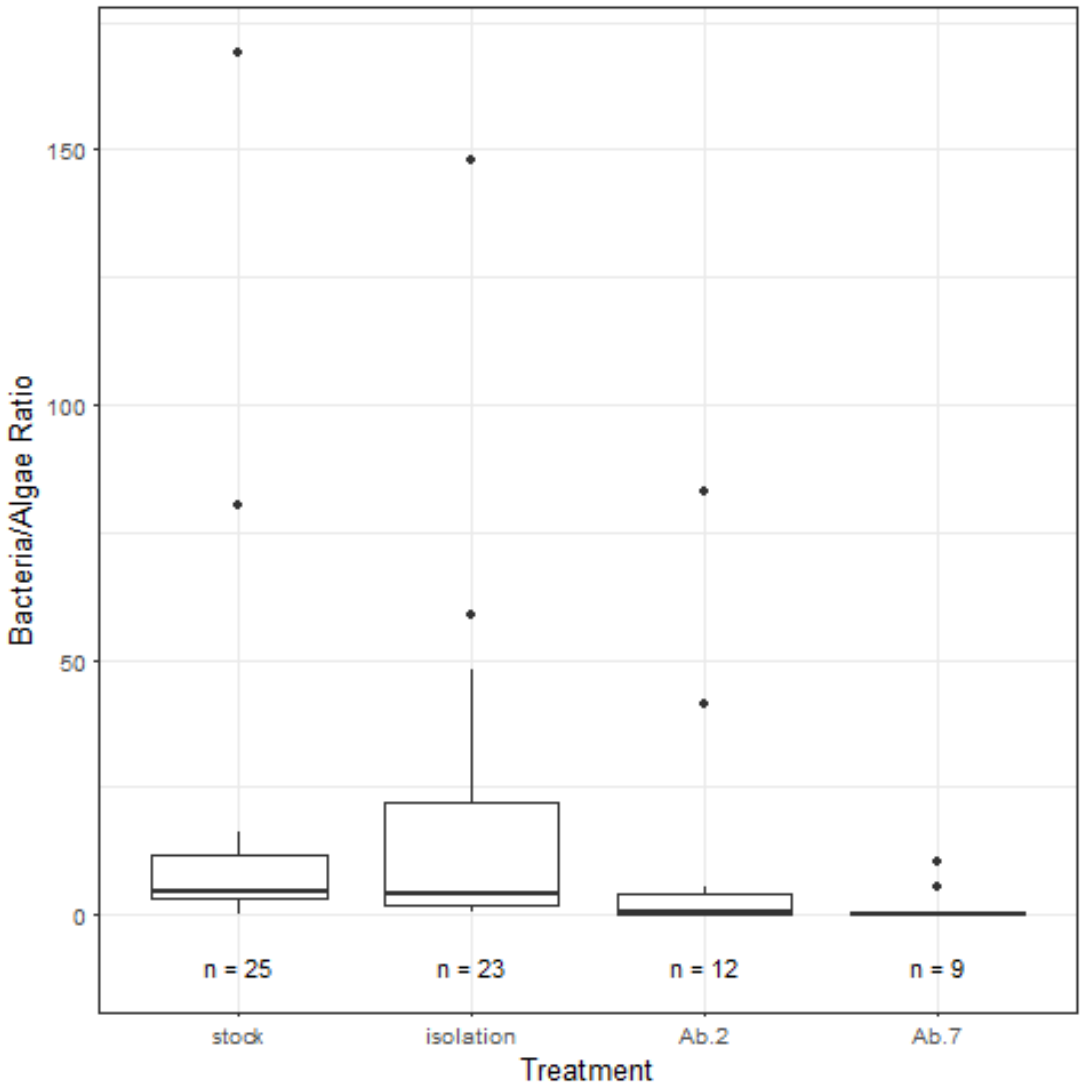

Figure 4.2: Boxplot of bacteria-to-algae ratio of culture collection. Each subsequent treatment are counts of cultures sustained at time of sampling. "Stock" treatment refers to the culture as it has been maintained in the laboratory with minimal manipulation. "Isolation" treatment refers to a culture that has been isolated on agar plates and subsequently transferred and grown in liquid media. "Ab.2" and "Ab.7" are the cultures that were treated with antibiotics and subcultured 2 or 7 times, respectively.

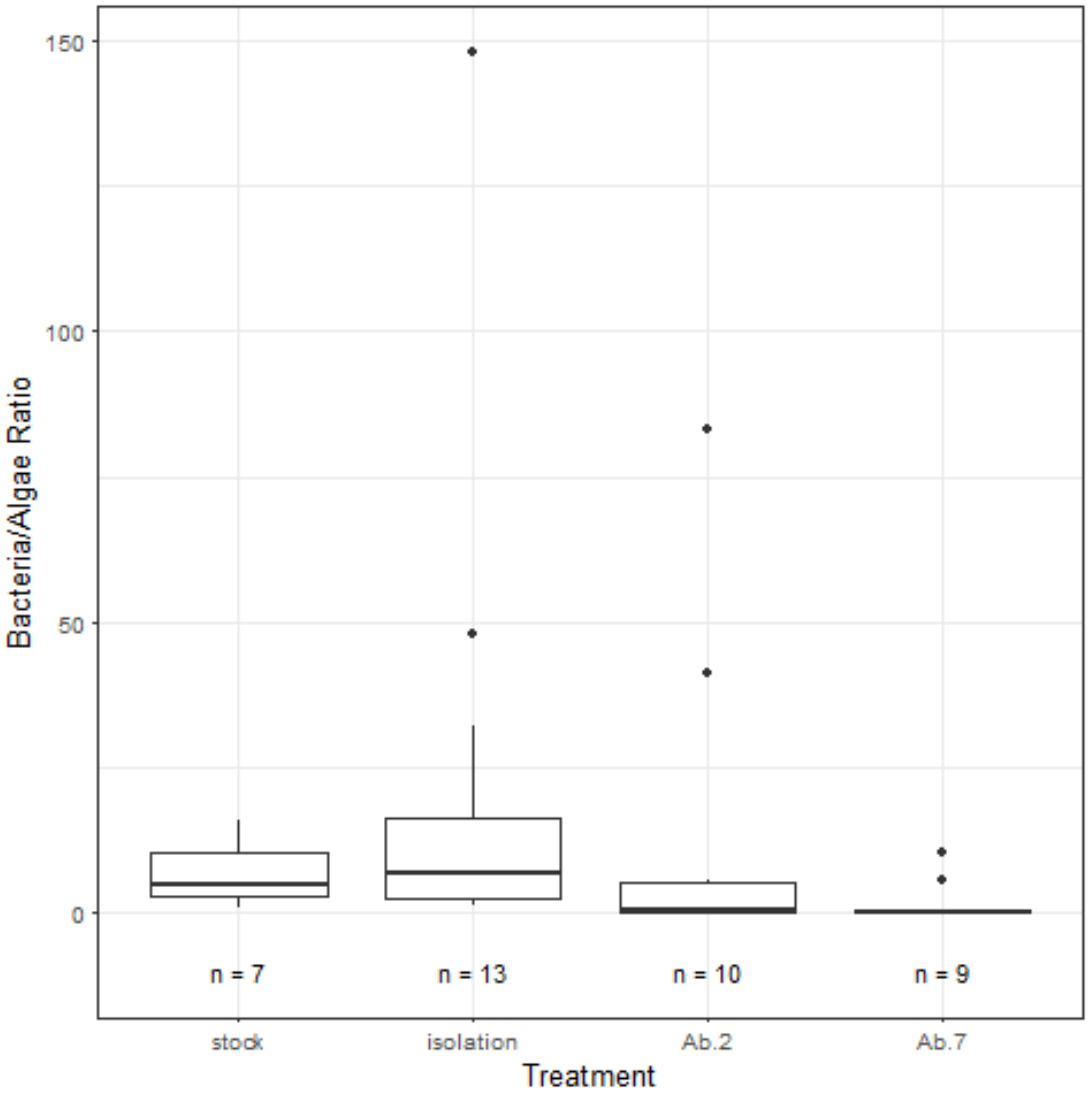

Figure 4.3: **Boxplot of bacteria-to-algae ratio of final cultures.** Each subsequent treatment is a parent of the proceeding culture. "Stock" treatment refers to the culture as it has been maintained in the laboratory with minimal manipulation. "Isolation" treatment refers to a culture that has been isolated on agar plates and subsequently transferred and grown in liquid media. "Ab.2" and "Ab.7" are the cultures that were treated with antibiotics and subcultured 2 or 7 times, respectively.

4.4.2 Screen for algal-bacterial interactions

Plates were incubated for 14 days at room temperature and the growth of the algae showed three patterns in response to the bacteria. The algae growing adjacent to the bacterial colony showed: 1. growth inhibition, shown as a lack of algal growth; 2. growth enhancement, shown as a ring of algae more dense than the surrounding area; or 3. commensal growth, normal growth despite the proximity of the bacterial colony. Using 16S rRNA gene sequencing, three strains that inhibited algal growth were identified as *Rhodobacter* sp., *Chryseobacterium* sp., and *Serratia* sp. Another two strains identified as *Cloacibacterium* sp., and *Rudenella* sp. displayed growth enhancement effects (Fig. 4.4).

4.5 Discussion

All the microalgal cultures that were used in the experiment were isolated from the experimental ponds in 2016. Using culture-based agar methods to separate the microalgae from their bacterial cohorts proved to be ineffective in reducing the bacterial load on the algae. However, it is likely that the isolation process only retained bacteria that are naturally closely associated with the microalgal culture rather than those that are free-living or planktonic. To remove the closely associated bacteria from the microalgae, an antibiotic cocktail containing penicillin G, streptomycin, polymyxin B, and chloramphenicol was prepared in media ready for subculturing the microalgae. This antibiotic cocktail was originally optimized by Tatewaki (1989) to produce axenic cultures of seaweed, a form of macroalgae (234). It has been found that this antibiotic cocktail is sufficient to make cultures axenic or at least to significantly reduce the bacterial contamination in microalgal cultures. The

use of antibiotics is not a novel approach to obtain axenic cultures but has been proven to be an effective tool to remove bacteria from microalgal cultures (229, 235, 236). Antibiotic treatment resulted in a reduction in the ratio of bacterial:algal cells, indicating that the bacteria are more susceptible to the antibiotics, as expected. Antibiotic treatment did not permit many of the cultures to grow, selecting for the microalgal cultures that are most tolerant to these antibiotics or to the lack of bacterial symbionts. The most significant differences were between the initial isolation of stock cultures and the seventh passage after antibiotic treatment followed by the stock cultures and the seventh passage after antibiotic treatment. No differences were found with the second passage after the antibiotic treatment perhaps because bacteria that are not killed or lysed with the antibiotics may still be alive but not actively dividing. The second passage did not dilute out the static bacteria to show a statistically significant difference, likely explaining why a statistically significant difference was found with the seventh passage.

Well-defined green microalgal colonies were present in both types of culture media. No bacterial colonies were visible after the microalgal cultures were plated on BG11 agarose plates nor R2A culture plates to screen for bacterial growth. Green algal colonies were picked off and cultured in BG11 medium. Light microscopy was used to assess if the isolated cultures were monocultures (Table 4.1). Cultures RAI 3, RAI 5, RAI 6, and RAI 7 were considered to be monocultures based on the cellular morphologies. All cultures were then classified based on the 18S rRNA gene sequence and their alignment with NCBI's BLAST database. Results of the BLAST alignment most closely identified each culture as *Desmodesmus* sp. It should be noted

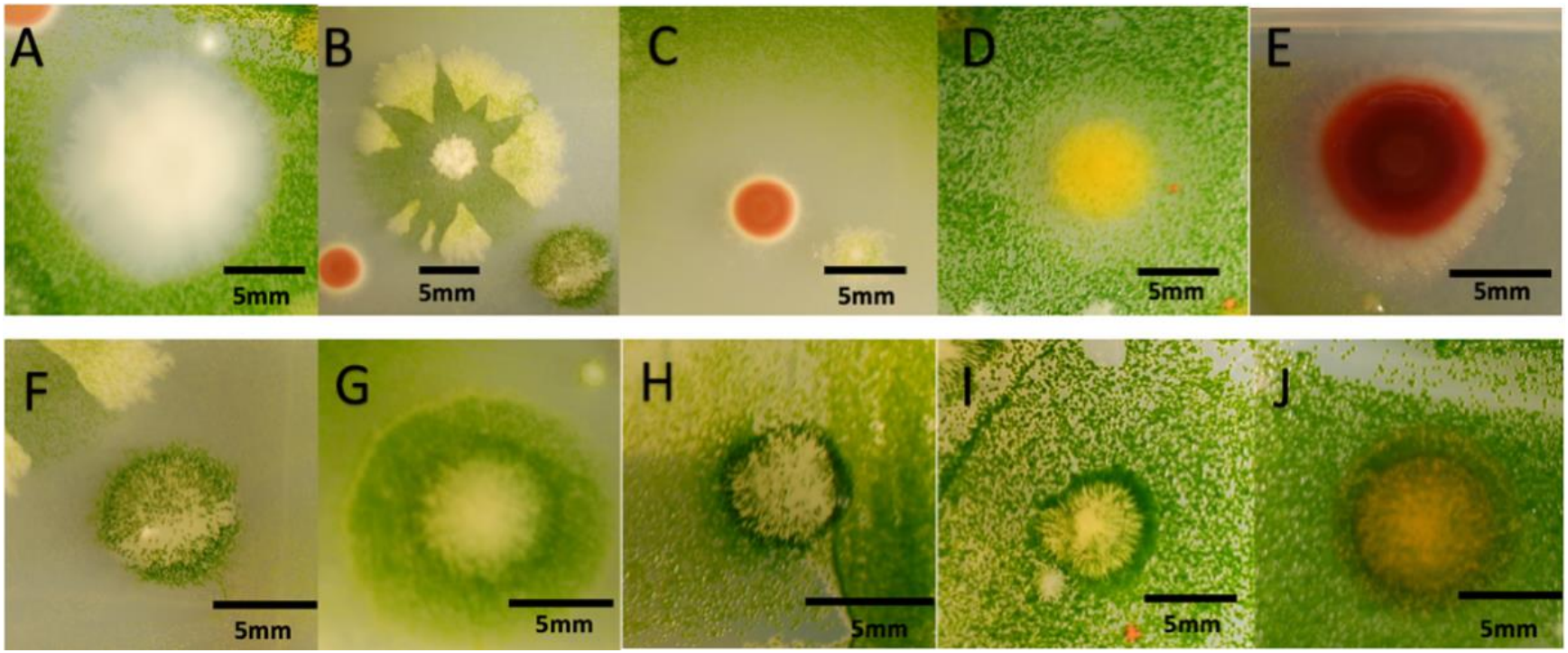

Figure 4.4: Bacterial colonies exemplifying microalgal-bacterial interactions. *Scenedesmus* sp. HTB1 growth inhibition [A-E] and growth enhancing effects [F-J]. The 16S rRNA gene sequence identified [C] as *Rhodobacter* sp., [D] *Chryseobacterium* sp., [E] *Serratia* sp., [F-I] *Cloacibacterium* sp., [J] *Rudanella* sp.

however, that the RAI cultures (antibiotic treated and re-isolated on R2A) became contaminated with bacteria from the laboratory. The contaminating bacteria were not identified but showed identical morphologies when grown on R2A agar to those that could be cultured with a "sterile" media control. Because the cultures were previously identified as having little or no bacterial contaminants; the fact that they were able to persist when exposed to ambient bacteria reveals that the microalgae may be tolerant of foreign bacteria or they may not be adapted to effectively interact with one another.

Desmodesmus is one of very few genera of microalgae that has been known to cause infection in immunocompetent humans as well as become parasitic in marine fish (237, 238). Recent studies have also shown that *Desmodesmus* has many potential biotechnological applications such as producing lutein, mitigating excess nutrients from wastewater, or being harvested for biofuel (239–241). However, characterization of the *Desmodesmus* biomass showed low total fatty acid content around 1.4-9.3% in nitrogen replete conditions but could reach its maximum biomass with anaerobic digestion wastewater in 14 days (240, 241). It has also been reported that two isolates of *Desmodesmus* are heat tolerant and their total lipid content can yield over 50% under nitrogen starvation, making it a potential biofuel feedstock crop (242). Considering that these microalgae were isolated from ponds designated for biofuel production, these novel strains in culture would make the ideal model to test open-pond growth conditions or interactions with bacteria isolated from the algal phycosphere.

Bacterial isolates from ponds were assayed with an algal underlay assay to

Table 4.1: Light microscopy of final isolated cultures. Each culture was molecularly identified as *Desmodesmus* sp. using 18S rRNA gene sequencing.

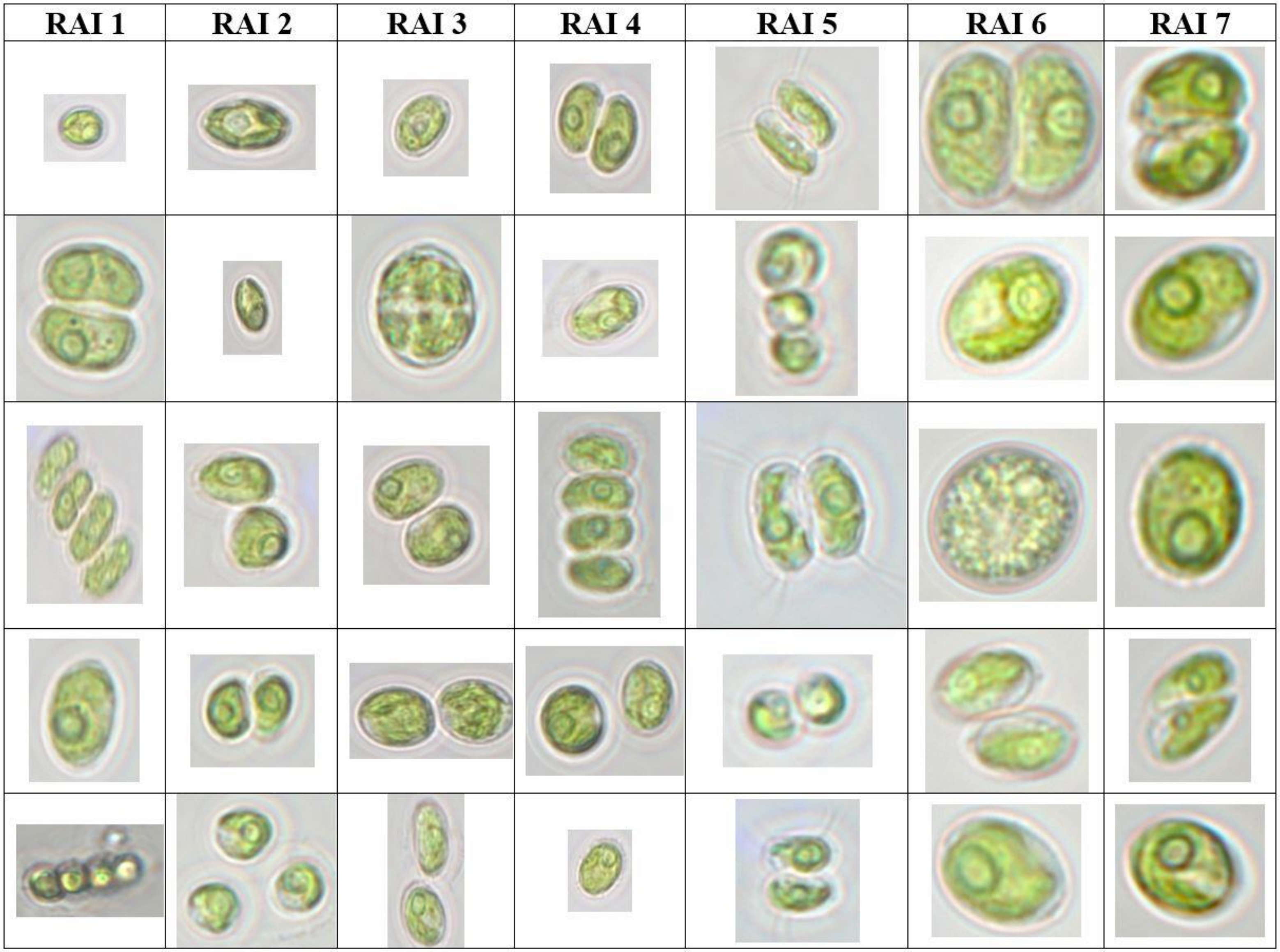

screen for potential growth effects. Two putative algal responses were observed: growth inhibition, classically depicted by a ring of inhibition; and growth enhancement, which characterized by a dense ring of algae around the bacterial colony (Fig. 4.4). 16S rRNA gene sequence analysis was used to successfully identify three of the inhibitory bacteria as *Rhodobacter* sp., *Chryseobacterium* sp., and *Serratia* sp. *Rhodobacter* and *Serratia* are members of the *Proteobacteria* phylum, belonging to the *α-proteobacteria* and the *γ-proteobacteria*, respectively. The *Chryseobacterium* is part of the *Bacteroidetes* phylum and a member of the *Flavobacteriia* class. Mayali and Azam (2004) authored a review of algicidal bacteria in marine ecosystems in which they described four genera of *Gammaproteobacteria* and six genera of *Bacteroidetes* that produced algicidal activity against marine eukaryotic microalgae (243). No reports have been found that describe specific bacterial: algal associations between *Rhodobacter* sp. and *Serratia* sp. However, *Chryseobacterium* sp. had previously been isolated from decomposing algal scum that was collected during an alga bloom in China (244). *Chryseobacterium* sp. have been described to exist as either a free-living bacterium or with a parasitic lifestyle (245). Considering the algal growth effect screen and the occurrence of *Chryseobacterium* sp. in a decomposing algal mass, it is possible that the *Chryseobacterium* is an opportunistic pathogen of microalgae.

Conversely, five isolates were identified as growth enhancing bacteria, four belonging to the *Cloacibacterium* genus, also of the class *Flavobacteriia*, and another strain within the genus *Rudanella* of the class *Cytophaga*. These growth-enhancing isolates are all members of the *Bacteroidetes* phylum. The two genera are relatively novel in the context of microalgae and have only been recently described within the past 12 years. The genus *Rudanella* was originally described in 2008 from an air sample in Korea and was later emended in 2011 (246, 247). No

literature to date has directly examined the associations between a microalga and a *Rudanella* sp. The other growth enhancing bacterial isolate was identified as a free-living bacterium and was isolated from untreated wastewater at a water-treatment plant in Oklahoma, USA (248). *Cloacibacterium* sp. have been found in freshwater lake sediments, within the gut of an abalone, and with coral and their associated algae (249–251). Recent studies of *Cloacibacterium normanense* have shown they produce extracellular polymeric substances that can be used to flocculate wastewater sludge (252, 253). The *Bacteroidetes* found in this assay (*Chryseobacterium* sp., *Cloacibacterium* sp., and *Rudanella* sp.) are all members of the Cytophaga-Flavobacterium-Bacteroides group (CFB). The CFB are frequently associated with freshwater and marine environments, and they are closely associated with suspended particle matter, including microalgae (103, 144, 254–256). Members of the CFB have also been found to be closely associated with the cyanobacterial phycosphere and are likely adapted to degrading bloom associated hepatotoxins (152, 175). Further research to investigate members of these classes will be needed to describe the molecular mechanism whereby the bacteria and algae may be interacting.

4.6 Conclusion

Bacteria isolated from man-made ponds fertilized to stimulate blooms of microalgae were screened for symbiotic interactions with the model alga, *Scenedesmus* sp. HTB1. The CFB group has been found to be closely associated with algae in the aquatic environment. The Cytophage, *Rudanella* sp. showed putative growth enhancing effects, along with four isolates of the *Cloacibacterium* genus. A third member of the CFB group was identified in having growth inhibiting effects on the microalgae. This bacterium is also a member of the family *Flavobacteriaceae* and is identified as a *Chryseobacterium* sp. With the declining costs in

sequencing technology, omic technologies can be used to molecularly model the mechanisms that enable the microalga and the bacterium to interact.

Using culture-based methods to isolate microalgae is not a new or novel approach of obtaining axenic cultures, neither is treatment with antibiotics. However, obtaining a model monoculture or axenic strain of a microalgal species native to a studied system will offer stronger tools to determine symbiotic relationships or genetic mechanisms for survival. Through a process of mechanical separations via isolation streaking and chemically killing bacteria with a cocktail of antibiotics, seven cultures survived being grown on solid media and treatment with antibiotics. Each surviving culture was genetically identified as belonging to the genus *Desmodesmus*. *Desmodesmus* species have been found to have remarkable biotechnological applications from nutraceutical production to biofuel generation. These cultures derived from three different ponds on the same property exhibits the spatial ubiquity of the microalgae; a characteristic that makes it a potentially stable model that is tolerant of microbial community variability. Successfully isolating and showing axenic viability of these microalgae provides an indispensable tool for further research into using open pond cultivation systems to stimulate blooms of native microalgae for biofuel generation.

Chapter 5: Conclusions and future directions

The research that is described in this thesis was in collaboration with Manta Biofuel, LLC., a local biofuel company that harvests microalgae to produce biocrude oil that is currently being used to replace petroleum-based heating oil (personal communication). The algae collected are grown in open-ponds filled with approximately 5 million liters of local stream water. To stimulate blooms of the microalgae, approximately 5 tons of chicken manure (fertilizer) from local farms was introduced into the ponds. As would be expected, the addition of fertilizer significantly increased the nutrient concentrations in the water. By making the ponds eutrophic, the environment around the microalgae (termed the phycosphere) changed dramatically and only a select microbial community was able to flourish, nearly excluding several phyla. Understanding these changes will ultimately allow us to recognize the difference between healthy blooms or blooms that will yield a substandard product. By being able to identify the bacterial community that leads to a highly productive bloom, these bacteria could be harnessed and introduced to stabilize and promote microalgal growth.

These data give us sequential snapshots of both the bacterial and the microalgal community in three different ponds over two years. We were able to see how closely related each of the ponds' native communities were prior to fertilization and then how the communities shifted in response to the spike in the nutrient levels. These snapshots provide invaluable information on the community of bacteria and microalgae that are most tolerant and responsive to high levels of total dissolved nitrogen (TDN), total dissolved phosphorus (TDP), and dissolved organic carbon (DOC). Insights into the community development of a microalgal bloom tells us which bacteria may be most closely associated with the microalgae, suggesting a symbiotic relationship. Although the presence of a bacterium in the same space as a microalga

does not necessarily mean that they are close symbionts or even interact with each other; this is a valuable first step in deducing which bacteria may be beneficial symbionts and therefore have potential as "probiotic" bacteria for enhancing growth of microalgae.

To assess the symbiotic interactions between the two domains, bacteria from the ponds were purified to screen for growth effects on a purified strain of *Scenedesmus* sp. HTB1. Two types of growth effects were apparent with an algal-underlay assay developed in this study. This assay was designed as a medium-throughput method to screen for interactions between microalgae and bacterial isolates. We identified several isolates belonging to the phylum *Bacteroidetes* that were able to promote the growth of HTB1. The cultured bacteria were within a group commonly known as the Cytophaga-Flavobacterium-Bacteroides (CFB). The CFB are a group of bacteria classically associated with microalgal and the cyanobacterial phycosphere, and they have a diverse metabolism to break down a variety of carbon sources (103, 144, 175, 254–256). Throughout the entirety of the experiment the *Bacteroidetes* phylum remained one of the most stable. For these reasons, an additional analysis was performed to look specifically at the *Bacteroidetes* phylum.

Representatives of the *Bacteroidetes* phylum that made up at least 0.5% of a time point's community were extracted from the experimental pond data and tracked from day -1 to day 15. At the family level, two taxa have nearly reciprocal patterns: the *Chitinophagacea* and the *Flavobacteriaceae*. The *Chitinophagacea* family comprises approximately 4% of the communities prior to fertilization but is reduced to less than 2% of the community after fertilization. Changes observed in this family are primarily explained by the reduction in the genus *Sediminibacterium*, the most abundant genus within the family (Fig. 5.1). These bacteria

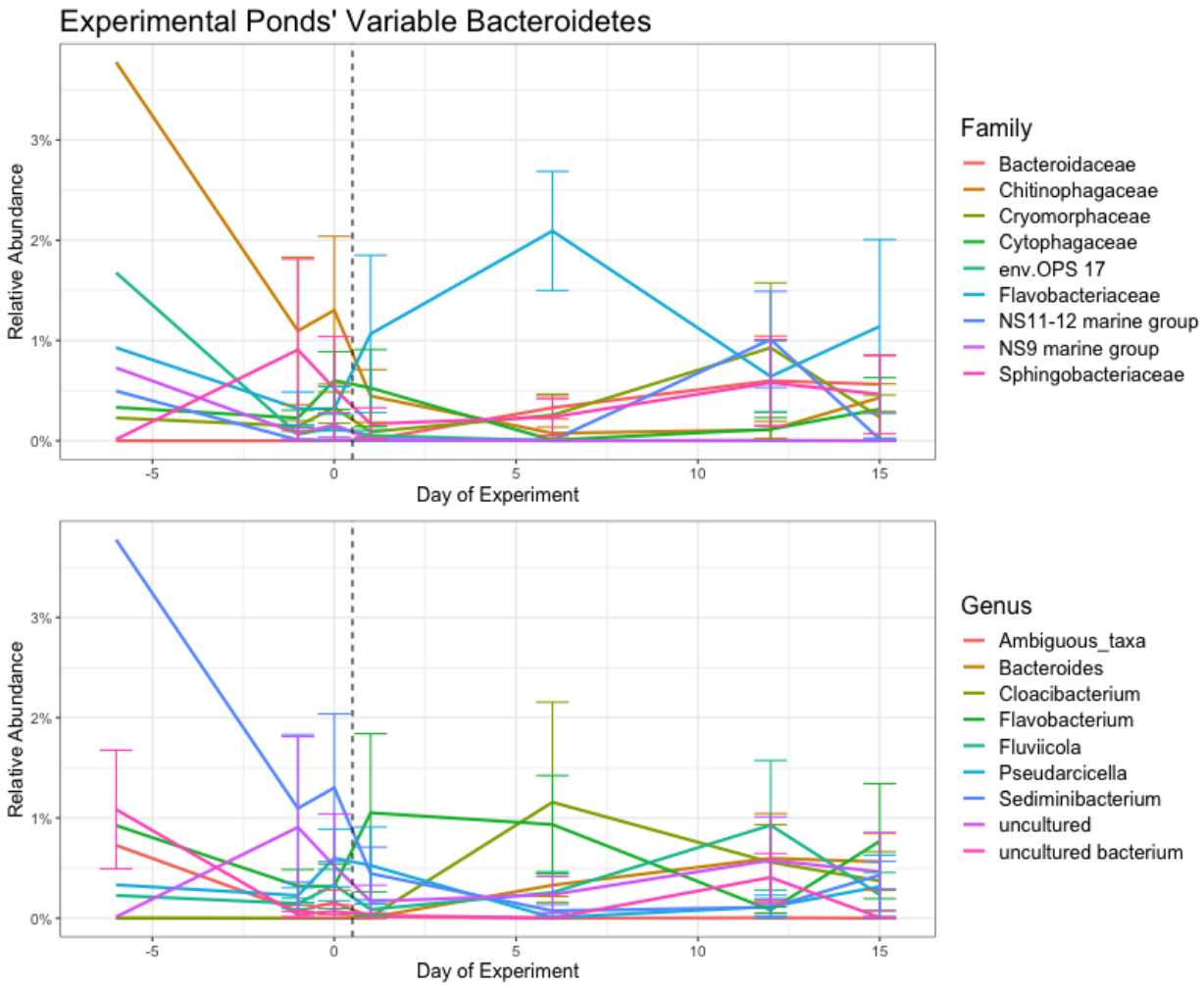

Figure 5.1: Mean percentages of the phylum *Bacteroidetes* in the experimental ponds. The most variable *Bacteroidetes* in the experimental ponds: family (top) and genus (bottom). Error bars represent the standard error of the mean.

have been isolated from soil, eutrophic reservoirs, freshwater reservoirs, and activated sludge (257–260). Recently, three bacterial genomes were sequenced from a non-axenic culture of the cyanobacterium *Tychonema bourrellyi* and identified as belonging to the genera *Pseudomonas*, *Flavobacterium*, and *Sediminibacterium*, suggesting a tight ecological association between cyanobacteria and heterotrophic bacteria (261). In agreement with Pinto *et al.*, we also found that the *Cyanobacteria* became less abundant after the ponds had experienced eutrophication with the fertilizer. However, we saw the *Flavobacteriaceae* become the most dominant family

challenging this suggestion by implying that this family has a general preference for photosynthetic byproducts regardless of the microbial origin. We also observed in the eukaryotic microalgae data that two species representative of the order *Chlamydomonadales* became the most abundant after fertilization. This data may imply that members of the family *Flavobacteriaceae* and some members of the eukaryotic microalgae order *Chlamydomonadales* are more adapted to deal with high levels of nutrients, possibly in concert with each other.

The most dominant genus was the genus *Flavobacterium*, though their abundance varied. *Flavobacterium* was overall more abundant after fertilization but crashed on the sixth day. Considering we were observing blooms of microalgae, we would expect to see increases in the CFB group. The CFB group are frequently found in eutrophic freshwater reservoirs and associated with the algal and cyanobacterial phycosphere (152, 262, 263). We do in fact see increases in the abundance of the genera *Flavobacterium* and *Bacteroides* of the CFB group, particularly at the end of the experiment, but we do not see the genus *Cytophaga* representing more than 0.5% of the community data. However, another relative of *Cytophaga*, *Pseudoarcicella* of the *Cytophagaceae* family, reaches its peak on day 15 post-fertilization.

Importantly, we see family members of the bacteria we have identified as being growth promoting with culture-based methods proliferate in the experimental ponds post-fertilization. The algal-underlay assays identified two genera capable of promoting the growth of a *Scenedesmus* sp. of microalgae, *Cloacibacterium* and *Rudanella*. *Rudanella* is not detected as representing more than 0.5% of the data on any day, but a close relative, *Pseudoarcicella*, became as dominant as the *Flavobacterium* by day 15. The *Cloacibacterium* was observed to be the most dominant on day 6 post-fertilization and then dramatically loses dominance. We collaborated in sequencing the genome of a growth-promoting *Cloacibacterium* and identified

two ammonification systems that putatively explain the growth effect on the model microalgae (264). These systems take nitrate and convert it to ammonium. In the two ponds fertilized using an active-dispersal method, we witnessed the total dissolved nitrogen begin to dramatically decline on the sixth day post-fertilization. This could imply a significant contribution by the *Cloacibacterium* to convert nitrogen species into a more bioavailable compound and suggests a functional redundancy in the bacterial communities. To answer the questions of which genes within the bacterial-algal consortia may be most reactive to the interactions, RNA-seq or qPCR may be employed. This would allow genes of interest, such as the genes in ammonification or those involved in the production of the plant auxin indole-3-acetic acid (IAA), to be monitored and corroborated with growth effects to elucidate the molecular explanation of microbial interactions (110, 265, 266).

"The great plate count anomaly" describes limitations in microbiological culturing techniques that result in culturing approximately 1% of the bacterial cells that can be seen under a microscope (267). Our culturing methods relied on using R2A medium specially formulated to culture bacteria normally inhabiting potable water. In consideration of "the great plate count anomaly", eutrophication of the water, and the observed shifts in the bacterial composition of the ponds, future efforts should utilize a range of culturing media that includes organically complex media (i.e. nutrient agar) and varying pH levels. Using a variety of culture medium will result in culturing a greater diversity of bacteria and microalgae.

The present study provides detailed insight into how the native bacteria and eukaryotic microalgal communities present in the ponds vary over time, before and after nutrient addition. These snapshots give us valuable information into the various taxa that are able to cohabitate the same environment and reveal those that are most suited to thrive in eutrophic conditions.

Analyses have also demonstrated that the bacteria associated with the chicken manure are either intolerant of a freshwater environment or are outcompeted by the native communities. With this knowledge, samples of the microalgae can be taken from the ponds as a bloom develops with minimal concern that a contaminant will skew the bacterial community composition. Efforts to isolate and perform metagenomic analyses on non-axenic monocultures of harvested microalgae will offer greater insights into the specificity of the associations between microalgae and their symbionts. To complement metagenomic approaches, fluorescent in situ hybridization (FISH) should be used to specifically target bacterial groups of interest to identify the frequency with which the bacteria are attached or free-living. Moreover, axenic cultures of representative eukaryotic microalgae from the ponds would be required to elucidate the true molecular mechanisms that explain the symbiotic interactions between the two domains. It is worth noting that bacteria derived from other environments and without sharing a co-evolutionary history have been shown participate in mutualistic interactions (114). Strategic screening of other plant growth-promoting bacteria (PGPB) has great potential to identify foreign mutualistic interactions not found within the microalgal phycosphere.

Several isolates of the chlorophyte genus *Desmodesmus* were cultured, isolated, and treated with antibiotics to reduce the number of bacteria in the cultures. Axenic cultures were transiently achieved, demonstrating the viability of a model microalgae devoid of bacteria that originated from the experimental ponds. *Desmodesmus* was not observed to significantly influence the eukaryotic microalgal communities but research has shown that it can be applied to both wastewater mitigation techniques and/or used for biofuel generation (240, 241). The presence of *Desmodesmus* in these ponds is a useful step towards future studies in which the bacterial-algal interactions between two or more native species can be determined and optimized

to generate blooms of highly productive microalgae. However, due to the nature of the environment in which microalgae are grown in open-ponds, it is important to recognize that increasing the growth rate of microalgae also increases the prey population for microalgal-grazers, potentially leading to culture crashes. Bacteria have been long known to metabolize a broad range of organic compounds but they also produce a variety of compounds that are toxic to other organisms. Using a similar approach to optimizing the growth and productivity of a microalga, bacterial symbionts can be used to protect microalgae from predators. In fact, it has been proposed that the microbiome of plants and animals can be engineered to generate a healthier host.

A new area of study called synthetic ecology can be used to create an artificial community optimized for mutualistic interactions (232, 233). In this way, a collection of bacterial isolates can be described based on their properties and interactions then archived for future use. This type of method would enable researchers or production facilities to create their own custom probiotic based on their specific needs. Ideally, these types of probiotic co-cultures will minimize or eliminate problematic contaminants, improve the growth profile of microalgae, and bioremediate wastewater while producing high-value products (268). Efforts from the current study have already begun screening hundreds of bacteria for growth effects with HTB1 with on-going screening continuing with other microalgal genera.

This research was conducted to parse out the microbial communities that are associated with natural assemblages of microalgae used for the generation of biofuel. The communities were tracked pre- and post-fertilization and revealed that the eutrophication of the ponds resulted in a dramatic decrease in the diversity of both the bacterial and microalgal communities. The caveat of this being that the control communities also experienced a dramatic decrease in the

microbial diversity as well. Our data suggest that the decrease in the diversity of the communities may not only be due to the nutrient influx of the ponds, but blooms of microalgae also decrease the diversity of the community. It has been illustrated that bacterial communities and microalgal communities are influenced by different factors: variability in the bacterial communities were most structured on the total dissolved phosphorus and total dissolved nitrogen; microalgal communities were most explained by total dissolved phosphorus, water temperature, and dissolved organic carbon. It would behoove future studies to take additional parameters such as pH, salinity, and chlorophyll-a measurements. Identification of *Cloacibacterium* sp. and *Rudanella* sp. as microalgal growth promoting bacteria describes a novel and previously unidentified characteristic of these bacteria. Molecular data also identified the genus *Cloacibacterium* and a relative of *Rudanella*, *Pseudoarcicella,* as being at least transiently dominant in the ponds after fertilization. This along with the observed dominance of the *Chlamydomonadales* order suggests a close cooperation for successful proliferation. Though growth effects were only observed with *Scenedesmus* sp. HTB1 (of the order *Sphaeropleales*) and no other microalgae was tested, the relationship between these two algae and the *Cloacibacterium* imply a generalist growth effect that the green-algae can take advantage of. Further growth experiments will be required to positively identify them as part of the PGPB group. Isolation and identification of bacteria that either promote or inhibit growth of microalgae paves the route to properly develop a synthetic community of probiotic bacteria for the use in protecting and promoting microalgal growth for highly productive microalgal culturing systems.

Appendix 1: Supplemental material for Chapter 2

Figure A2.1: Google Maps image of the sampling property in Frederick, MD. [Top] Satellite image of the ponds with annotations marking the ponds and location of each sampling site. [Bottom] Google Maps representations of the relative location of the source water with an arrow annotated to show direction of the water flow.

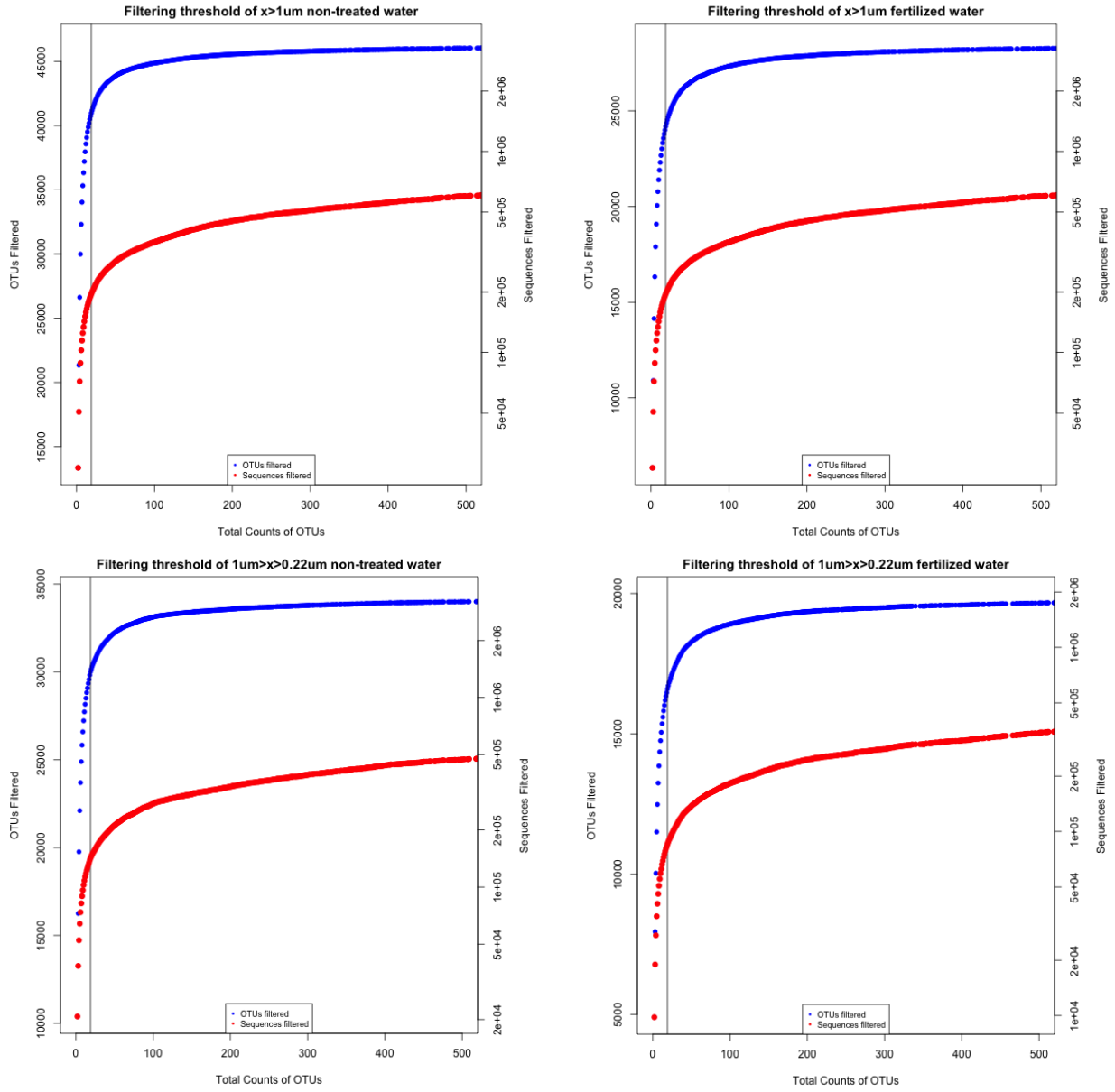

Figure A2.2: Identification of spurious OTUs to be removed. The cumulative number of OTUs (y-axis) with the number of sequences within each OUT (x-axis). The non-treated community (left) and the fertilized community (right). The vertical black line represents filtering threshold. The blue dots are the cumulative sum of the number of OTUs with x or less sequences. The red dots represent the cumulative number of sequences filtered.

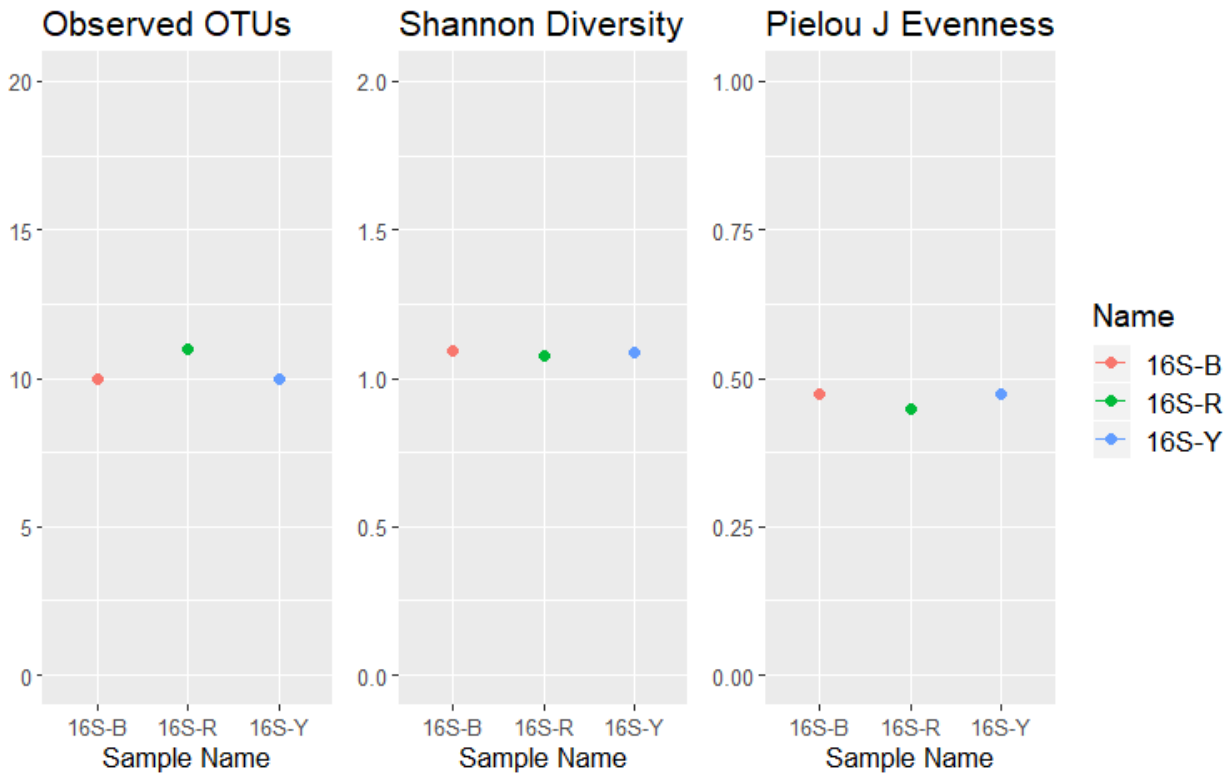

Figure A2.3: Alpha diversity measures of the synthetic mock communities.

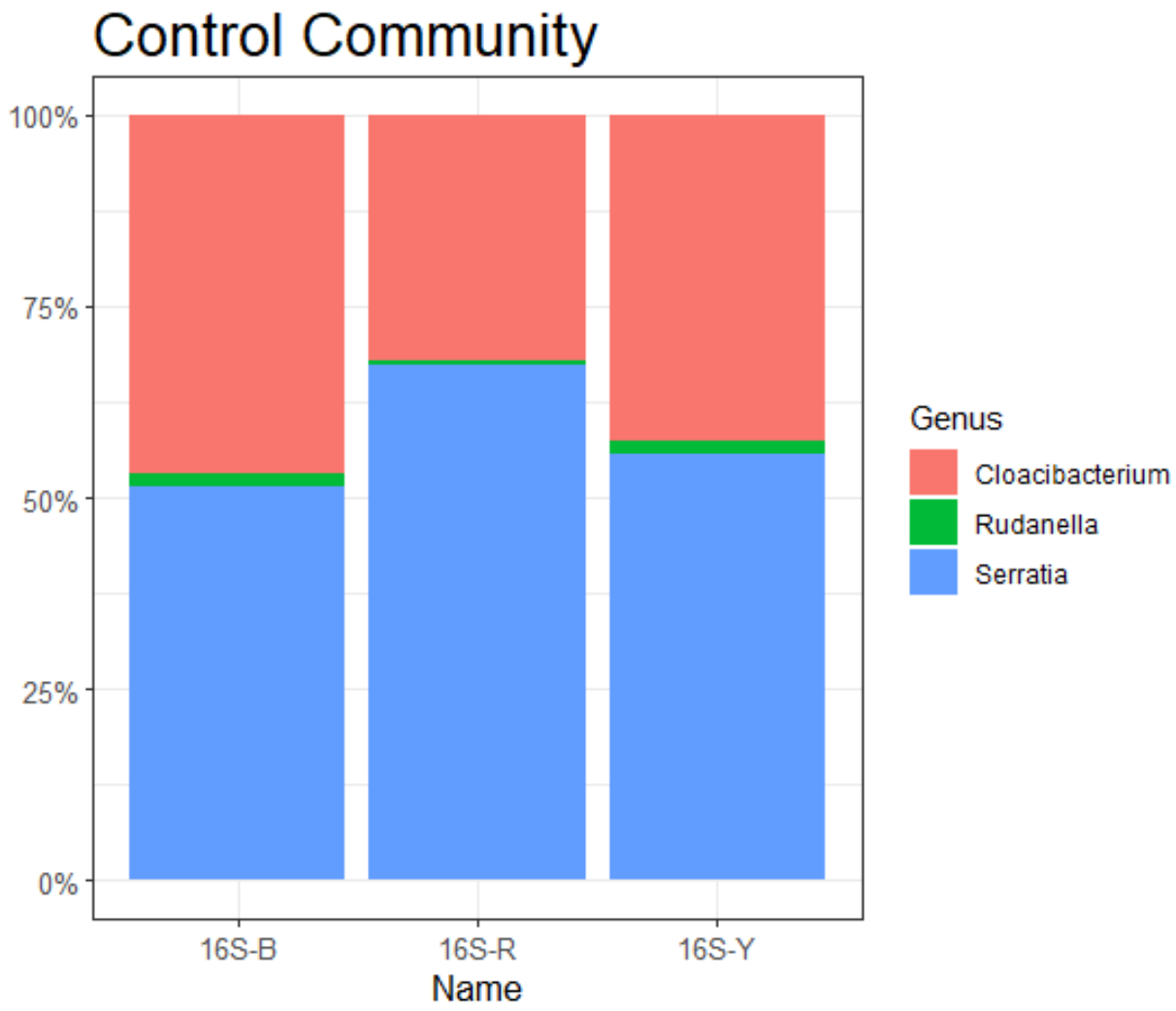

Figure A2.4: Relative abundance of genera representing greater than 0.1% of the synthetic mock communities.

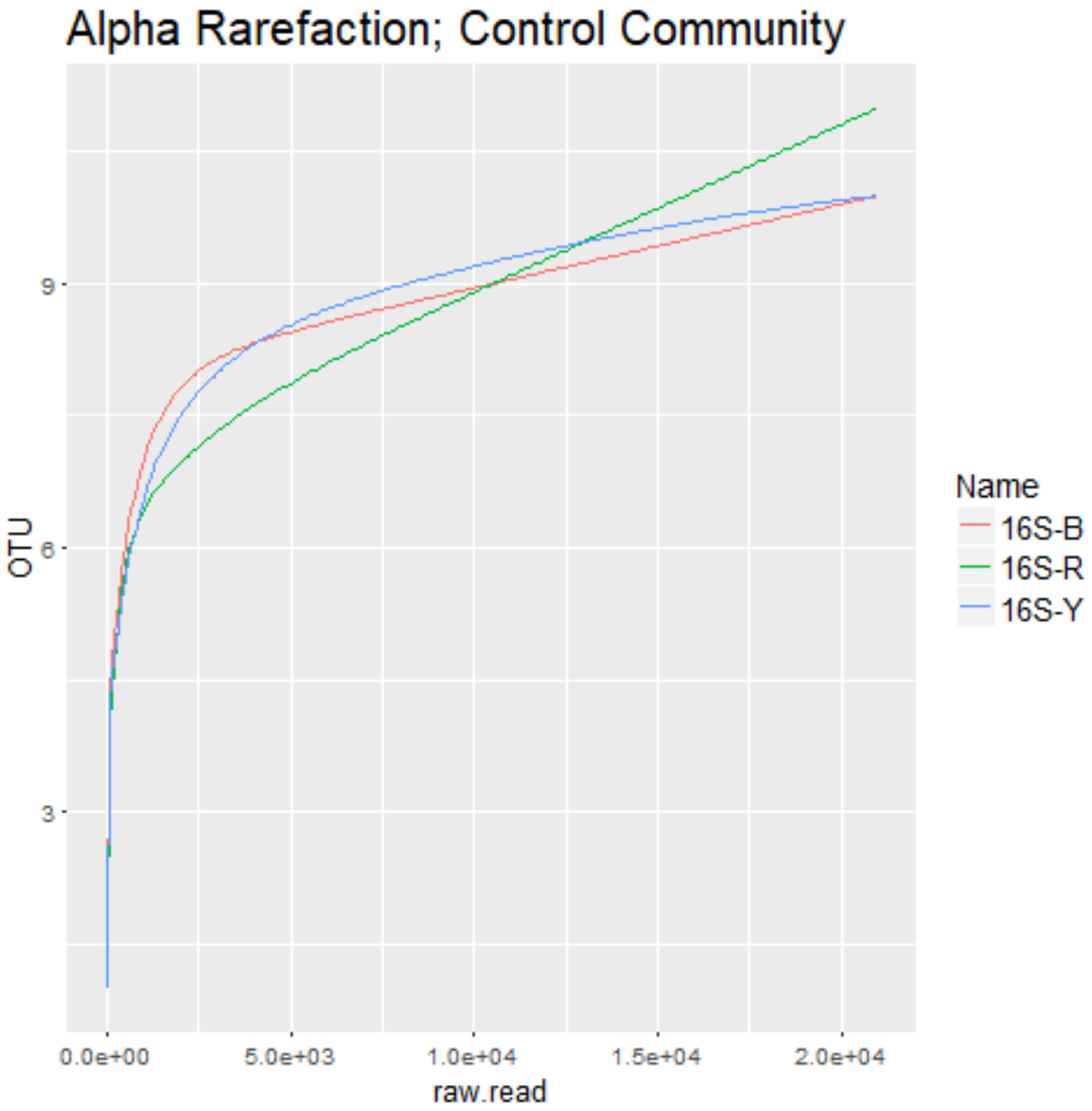

Figure A2.5: Alpha rarefaction plot of synthetic control communities. Rarefaction of the control community showing the sequencing depth of the rarefied community.

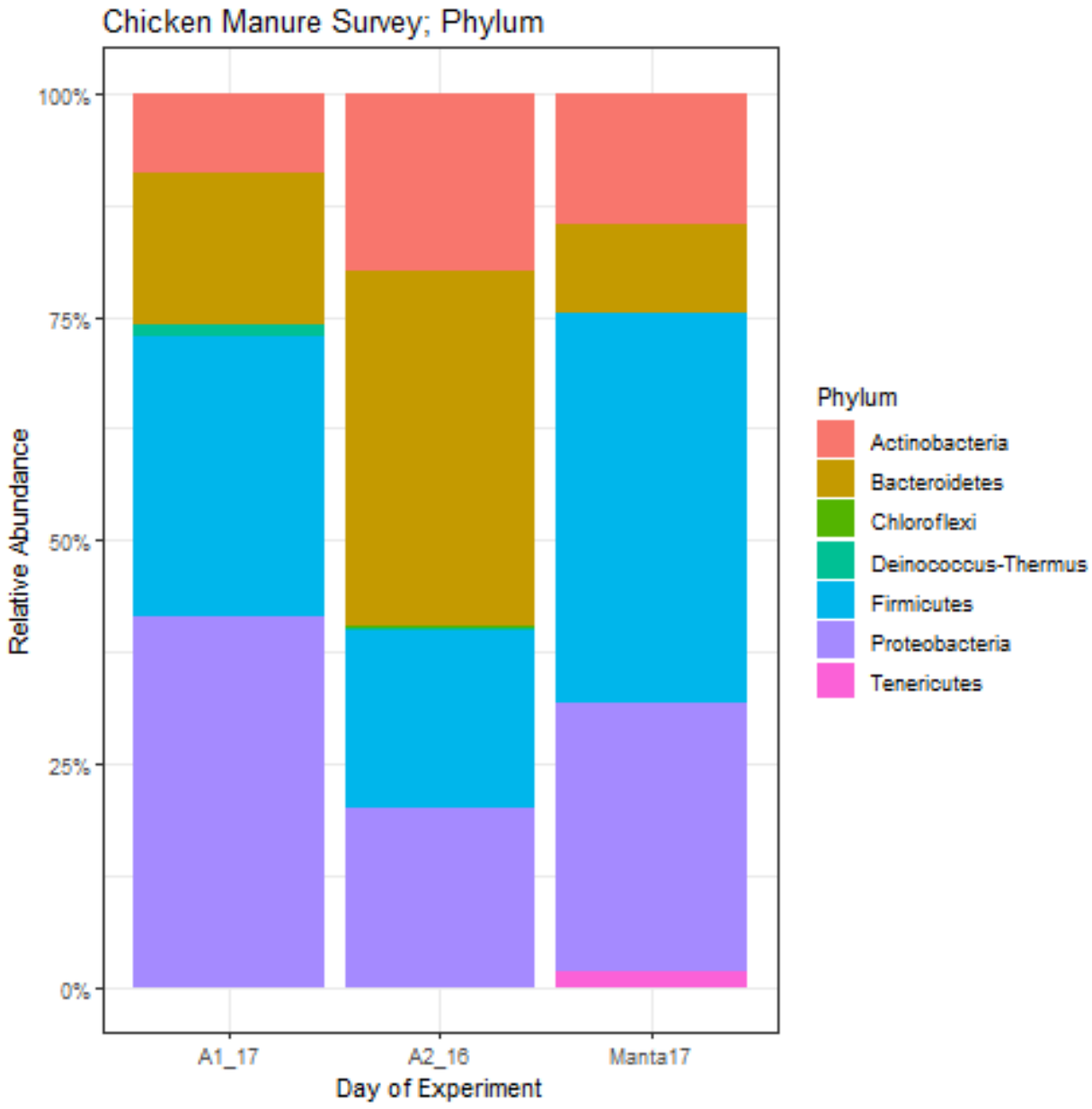

Figure A2.6: Relative abundance of phyla representing greater than 0.1% of the chicken manure communities.

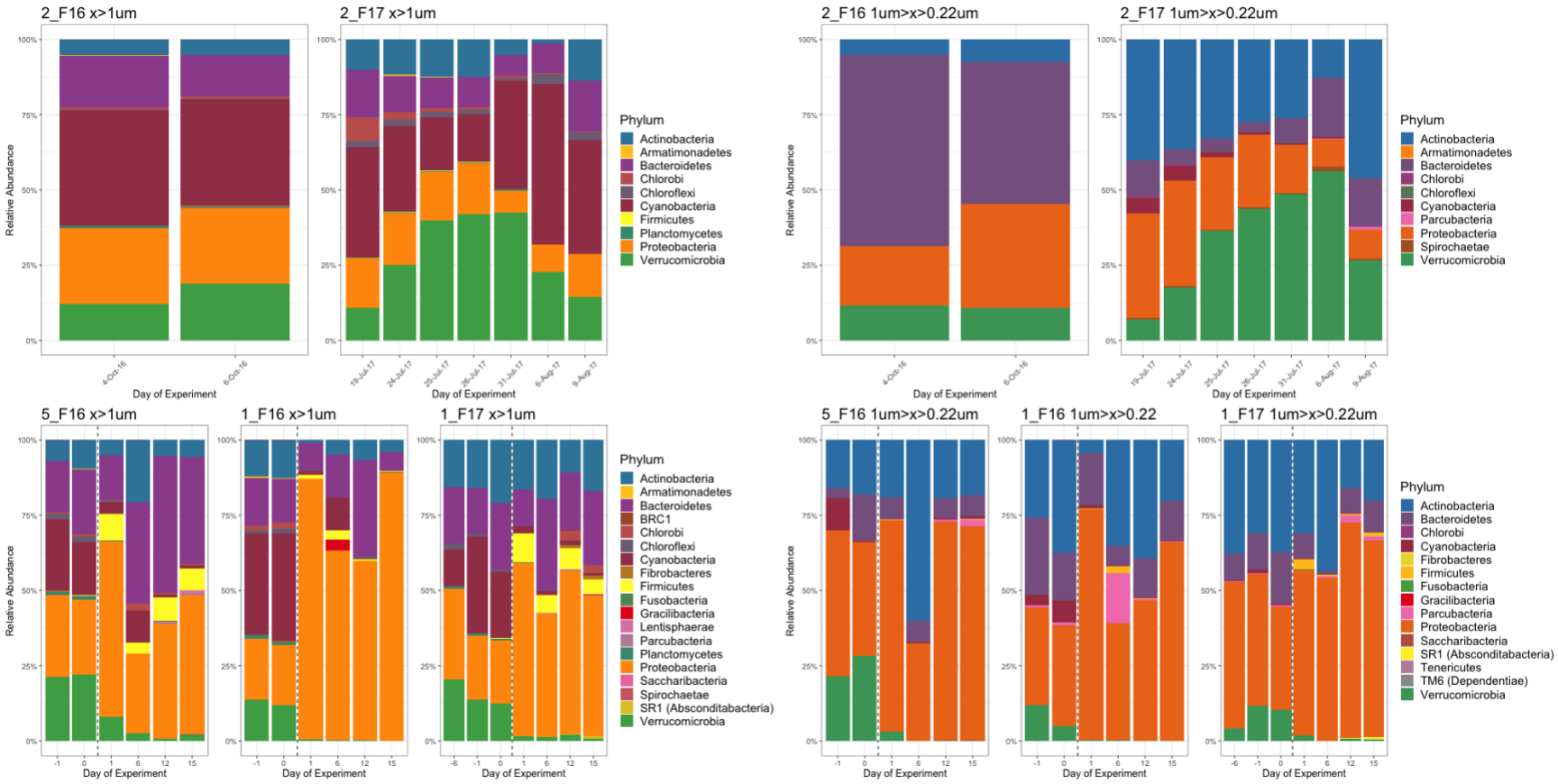

Figure A2.7: Relative abundance of genera representing greater than 0.1% of each filter-fraction size. Phyla that represent a minimum of 0.1% of the community in each pond. Chart 2_F16 and 2_F17 represent control ponds that were never fertilized. The date of sampling is provided with percent of the community contributed by each phylum. Experimental ponds are shown in the bottom graphs and the black vertical line represents the time of fertilization.

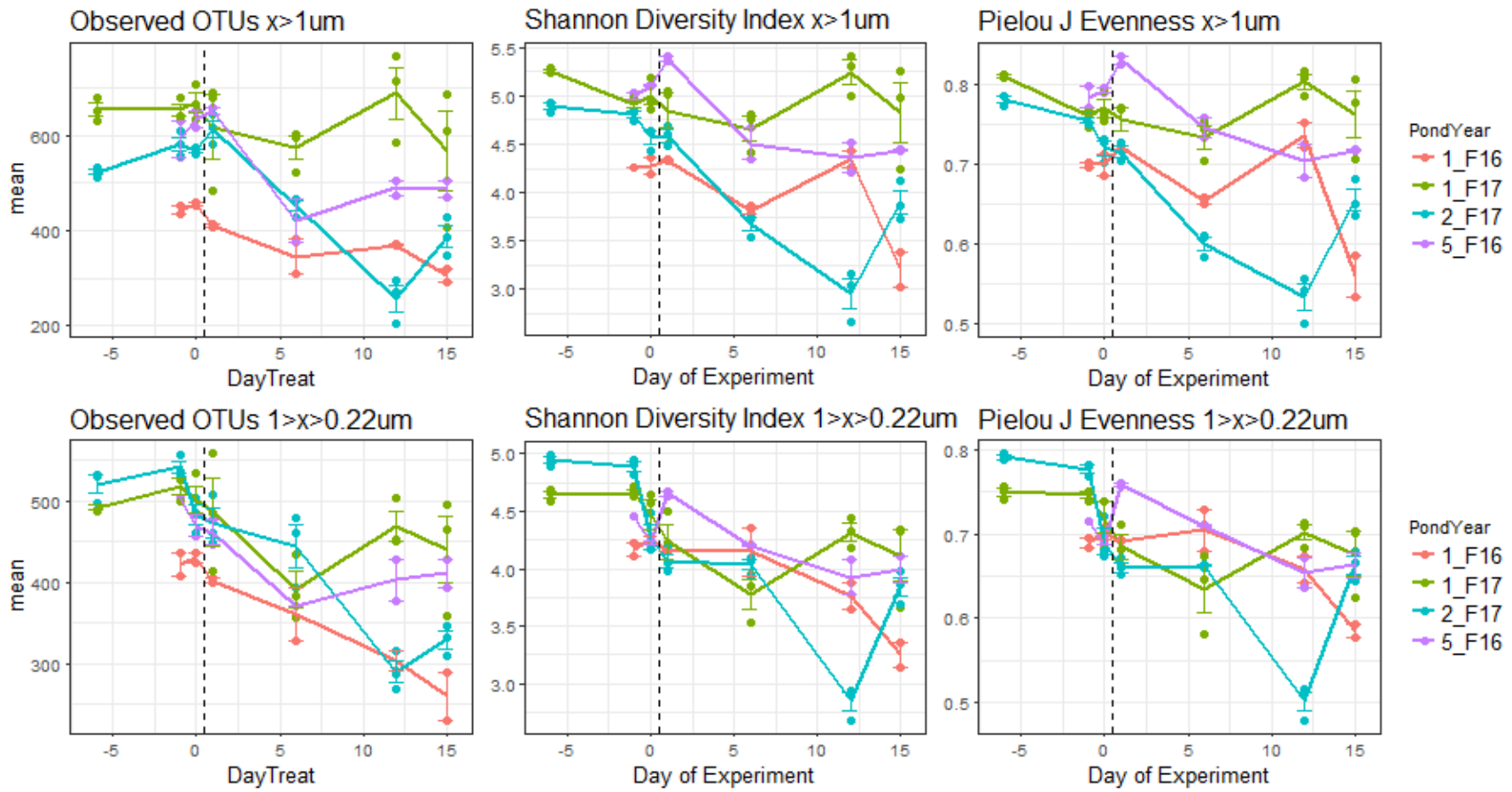

Figure A2.8: Mean alpha diversity measures of the algal community of each pond over time of each filter-fraction size. The black vertical line indicates the time of fertilization. Pond 2_F17 was never fertilized. Error bars indicate the standard error of the mean of each measure. The black vertical dashed-line represents the time of fertilization into ponds 1_F16, 5_F16, and 1_F17.

Table A2.1: Kruskal-Wallis tests with *post hoc* Nemenyi tests of alpha diversity metrics. Significant p values are in bold-face print. Ties in the pairwise *post hoc* Nemeneyi tests were broken with chi-square distributions. Experimental ponds are on the left and the control pond is on the right.

Experimental Ponds

Observed OTUs Kruskal-Wallis Test; pairwise *post hoc* Nemenyi tests

chi-squared = 19.8, df = 6, **p-value = 0.001**

	-6	**-1**	**0**	**1**	**6**	**12**
-1	1	NA	NA	NA	NA	NA
0	1	1	NA	NA	NA	NA
1	0.94	1	1	NA	NA	NA
6	0.17	0.21	0.21	0.56	NA	NA
12	0.65	0.83	0.85	0.99	0.96	NA
15	0.3	0.4	0.41	0.79	0.99	1

Shannon diversity Kruskal-Wallis Test; pairwise *post hoc* Nemenyi tests

chi-squared = 19.4, df = 6, **p-value = 0.003**

	-6	**-1**	**0**	**1**	**6**	**12**
-1	0.93	NA	NA	NA	NA	NA
0	0.84	1	NA	NA	NA	NA
1	0.85	1	1	NA	NA	NA
6	0.11	0.47	0.66	0.63	NA	NA
12	0.41	0.92	0.98	0.98	0.99	NA
15	0.08	0.38	0.57	0.54	1	1

Pielou J index Kruskal-Wallis Test; pairwise *post hoc* Nemenyi tests

chi-squared = 18.7, df = 6, **p-value = 0.004**

	-6	**-1**	**0**	**1**	**6**	**12**
-1	0.88	NA	NA	NA	NA	NA
0	0.72	1	NA	NA	NA	NA
1	0.85	1	1	NA	NA	NA
6	0.14	0.69	0.89	0.73	NA	NA
12	0.38	0.96	0.99	0.97	0.99	NA
15	0.05	0.38	0.62	0.41	0.99	0.94

Control Pond

Observed OTUs Kruskal-Wallis Test; pairwise *post hoc* Nemenyi tests

chi-squared = 32.0, df = 6, **p-value = <0.001**

	-6	**-1**	**0**	**1**	**6**	**12**
-1	0.98	NA	NA	NA	NA	NA
0	1	0.99	NA	NA	NA	NA
1	1	0.99	1	NA	NA	NA
6	0.9	0.42	0.85	0.75	NA	NA
12	0.08	0.0046	0.06	**0.03**	0.74	NA
15	0.38	0.06	0.31	0.21	0.98	0.9945

Shannon diversity Kruskal-Wallis Test; pairwise *post hoc* Nemenyi tests

chi-squared = 15.93, df = 6, **p-value = 0.014**

	-6	**-1**	**0**	**1**	**6**	**12**
-1	1	NA	NA	NA	NA	NA
0	0.99	0.96	NA	NA	NA	NA
1	1	1	0.98	NA	NA	NA
6	0.93	0.97	0.47	0.94	NA	NA
12	0.84	0.73	1	0.82	0.16	NA
15	0.76	0.62	0.99	0.73	0.11	1

Pielou J index Kruskal-Wallis Test; pairwise *post hoc* Nemenyi tests

chi-squared = 36.8, df = 6, **p-value = <0.001**

	-6	**-1**	**0**	**1**	**6**	**12**
-1	0.99	NA	NA	NA	NA	NA
0	0.69	0.96	NA	NA	NA	NA
1	0.35	0.76	0.99	NA	NA	NA
6	**0.02**	0.15	0.75	0.95	NA	NA
12	**0.0003**	**0.005**	0.15	0.42	0.96	NA
15	0.9	0.39	0.95	0.99	0.99	0.79

Table A2.2: Kruskal-Wallis tests with pairwise *post hoc* Nemenyi tests of alpha diversity metrics of x>1µm filter fraction. Significant p values are in bold-face print. Ties in the pairwise *post hoc* Nemeneyi tests were broken with chi-square distributions.

Experimental Ponds x>1um Fraction

Observed OTUs Kruskal-Wallis Test; pairwise *post hoc* Nemenyi tests
chi-squared = 9.1, df = 6, p-value = 0.17

	-6	-1	0	1	6	12
-1						
0						
1						
6						
12						
15						

Shannon diversity Kruskal-Wallis Test; pairwise *post hoc* Nemenyi tests
chi-squared = 11.0, df = 6, p-value = 0.08

	-6	-1	0	1	6	12
-1						
0						
1						
6						
12						
15						

Pielou J index Kruskal-Wallis Test; pairwise *post hoc* Nemenyi tests
chi-squared = 11.9, df = 6, p-value = 0.06

	-6	-1	0	1	6	12
-1						
0						
1						
6						
12						
15						

Control Pond x>1um Fraction

Observed OTUs Kruskal-Wallis Test; pairwise *post hoc* Nemenyi tests
chi-squared = 19.1, df = 6, **p-value = 0.004**

	-6	-1	0	1	6	12
-1	0.98	NA	NA	NA	NA	NA
0	0.99	1	NA	NA	NA	NA
1	0.82	0.99	0.99	NA	NA	NA
6	0.99	0.83	0.92	0.49	NA	NA
12	0.79	0.24	0.36	0.06	0.97	NA
15	0.97	0.56	0.71	0.22	1	0.99

Shannon diversity Kruskal-Wallis Test; pairwise *post hoc* Nemenyi tests
chi-squared = 18.9, df = 6, **p-value = 0.004**

	-6	-1	0	1	6	12
-1	1	NA	NA	NA	NA	NA
0	0.91	0.99	NA	NA	NA	NA
1	0.93	0.99	1	NA	NA	NA
6	0.27	0.51	0.94	0.93	NA	NA
12	0.06	0.17	0.66	0.62	0.99	NA
15	0.43	0.69	0.99	0.98	1	0.98

Pielou J index Kruskal-Wallis Test; pairwise *post hoc* Nemenyi tests
chi-squared = 19.3, df = 6, **p-value = 0.004**

	-6	-1	0	1	6	12
-1	0.99	NA	NA	NA	NA	NA
0	0.93	0.99	NA	NA	NA	NA
1	0.87	0.99	1	NA	NA	NA
6	0.19	0.47	0.87	0.93	NA	NA
12	**0.05**	0.19	0.58	0.69	0.99	NA
15	0.47	0.79	0.99	0.99	0.99	0.97

Table A2.3: Kruskal-Wallis tests with pairwise *post hoc* Nemenyi tests of alpha diversity metrics of 1μm>x>0.22μm filter fraction. Significant p values are in bold-face print. Ties in the pairwise *post hoc* Nemeneyi tests were broken with chi-square distributions.

Experimental Ponds 1um>x>0.22um Fraction

Observed OTUs Kruskal-Wallis Test; pairwise *post hoc* Nemenyi tests

chi-squared = 18.7, df = 6, **p-value = 0.005**

	-6	**-1**	**0**	**1**	**6**	**12**
-1	1	NA	NA	NA	NA	NA
0	1	1	NA	NA	NA	NA
1	0.97	0.97	1	NA	NA	NA
6	0.24	0.12	0.27	0.6	NA	NA
12	0.71	0.62	0.86	0.99	0.97	NA
15	0.52	0.38	0.65	0.91	1	1

Control Pond 1um>x>0.22um Fraction

Observed OTUs Kruskal-Wallis Test; pairwise *post hoc* Nemenyi tests

chi-squared = 17.7, df = 6, **p-value = 0.007**

	-6	**-1**	**0**	**1**	**6**	**12**
-1	0.99	NA	NA	NA	NA	NA
0	0.99	0.92	NA	NA	NA	NA
1	0.98	0.87	1	NA	NA	NA
6	0.92	0.67	0.99	1	NA	NA
12	0.24	0.07	0.67	0.758	0.92	NA
15	0.47	0.187	0.88	0.928	0.99	1

Shannon diversity Kruskal-Wallis Test; pairwise *post hoc* Nemenyi tests

chi-squared = 19.2, df = 6, **p-value = 0.004**

	-6	**-1**	**0**	**1**	**6**	**12**
-1	0.99	NA	NA	NA	NA	NA
0	0.92	1	NA	NA	NA	NA
1	0.87	0.99	1	NA	NA	NA
6	0.22	0.42	0.73	0.84	NA	NA
12	0.28	0.52	0.82	0.9	1	NA
15	0.15	0.28	0.59	0.71	1	1

Shannon diversity Kruskal-Wallis Test; pairwise *post hoc* Nemenyi tests

chi-squared = 18.6, df = 6, **p-value = 0.005**

	-6	**-1**	**0**	**1**	**6**	**12**
-1	1	NA	NA	NA	NA	NA
0	0.97	0.99	NA	NA	NA	NA
1	0.79	0.91	0.99	NA	NA	NA
6	0.66	0.82	0.99	1	NA	NA
12	0.07	0.14	0.54	0.85	0.928	NA
15	0.27	0.43	0.87	0.987	0.99	0.99

Pielou J index Kruskal-Wallis Test; pairwise *post hoc* Nemenyi tests

chi-squared = 17.6, df = 6, **p-value = 0.007**

	-6	**-1**	**0**	**1**	**6**	**12**
-1	0.99	NA	NA	NA	NA	NA
0	0.83	0.99	NA	NA	NA	NA
1	0.89	1	1	NA	NA	NA
6	0.41	0.72	0.98	0.96	NA	NA
12	0.28	0.54	0.93	0.88	1	NA
15	0.11	0.23	0.68	0.57	0.99	1

Pielou J index Kruskal-Wallis Test; pairwise *post hoc* Nemenyi tests

chi-squared = 17.8, df = 6, **p-value = 0.007**

	-6	**-1**	**0**	**1**	**6**	**12**
-1	0.99	NA	NA	NA	NA	NA
0	0.94	0.99	NA	NA	NA	NA
1	0.39	0.73	0.97	NA	NA	NA
6	0.47	0.79	0.98	1	NA	NA
12	**0.05**	0.19	0.54	0.98	0.97	NA
15	0.62	0.89	0.99	1	1	0.91

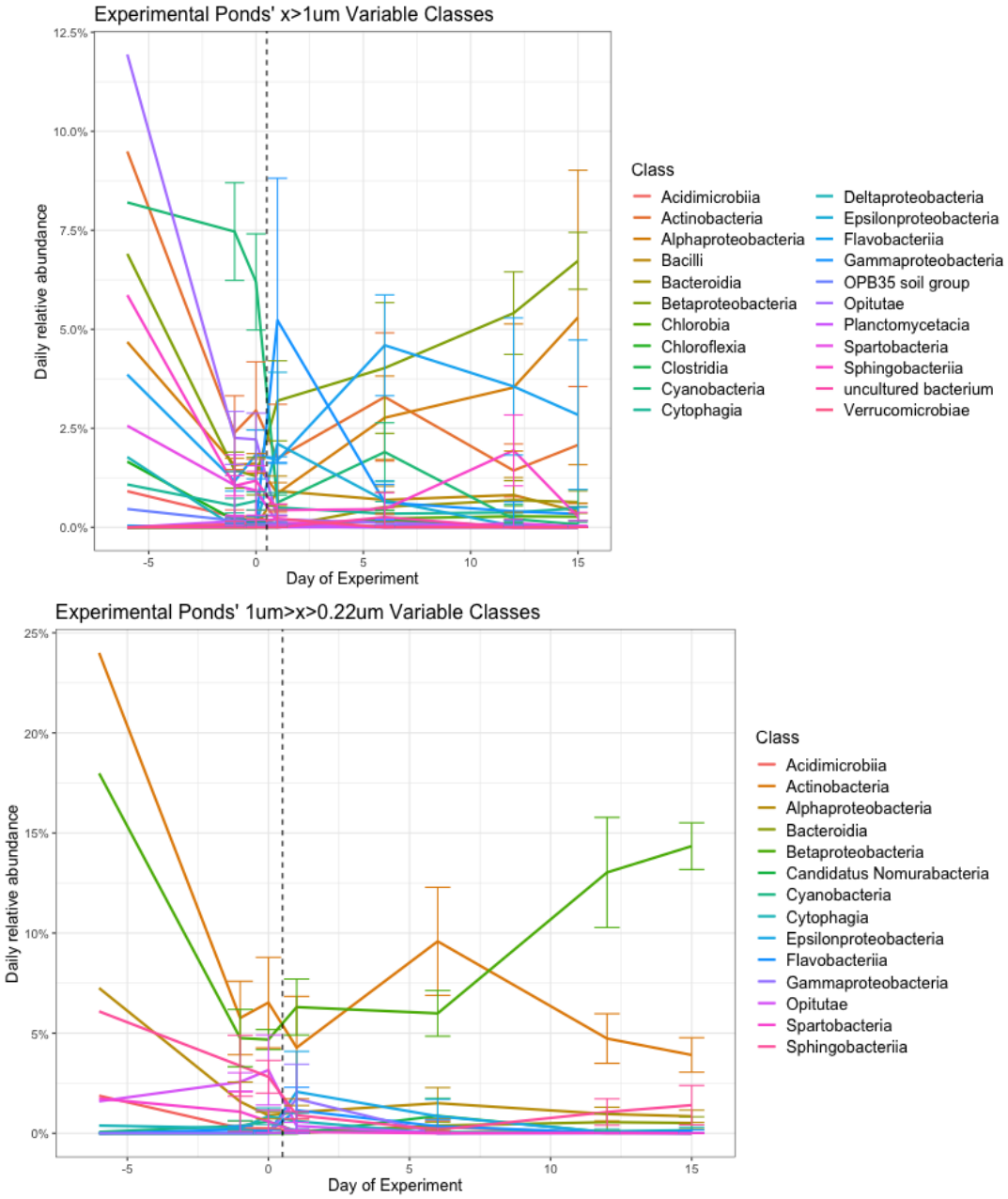

Figure A2.9: Change in relative abundance of the most variable classes captured on each filter size. Classes that explain 50% of the differences between each day plotted over time to show temporal variation in the communities. The percent of the community is based on the normalized sum of each days' community abundance. The data from experimental ponds 1_F16, 5_F16, and 1_F17. Error bars represent the standard error of the mean.

Appendix 2: Supplemental material for Chapter 3

Table A3.1: Pairwise Kruskal-Wallis *post hoc* Nemenyi tests of bacterial and algal counts from 2017. Significant p values are in bold-face print.

Ties in the *post hoc* Nemenyi tests were broken with chi-square distributions.

1_F17

Algae mean Kruskal-Wallis Test; pairwise *post hoc* Nemenyi tests
chi-squared = 12.8, df = 6, p-value = 0.045

	-6	**-1**	**0**	**1**	**6**	**12**
-1	0.85	NA	NA	NA	NA	NA
0	0.85	1	NA	NA	NA	NA
1	0.19	0.93	0.93	NA	NA	NA
6	0.13	0.79	0.79	0.99	NA	NA
12	**0.039**	0.59	0.59	0.99	1	NA
15	0.59	0.99	0.99	0.99	0.94	0.85

Bacteria mean Kruskal-Wallis Test; pairwise *post hoc* Nemenyi tests
chi-squared = 14.3, df = 6, p-value = 0.026

	-6	**-1**	**0**	**1**	**6**	**12**
-1	0.99	NA	NA	NA	NA	NA
0	0.73	0.97	NA	NA	NA	NA
1	**0.025**	0.14	0.64	NA	NA	NA
6	0.32	0.68	0.98	0.99	NA	NA
12	0.19	0.55	0.97	0.99	1	NA
15	0.46	0.85	0.99	0.88	0.99	0.99

Bacteria:Algae ratio Kruskal-Wallis Test; pairwise *post hoc* Nemenyi tests
chi-squared = 13.6, df = 6, p-value = 0.034

	-6	**-1**	**0**	**1**	**6**	**12**
-1	0.59	NA	NA	NA	NA	NA
0	0.88	0.99	NA	NA	NA	NA
1	0.90	0.99	1	NA	NA	NA
6	0.057	0.82	0.55	0.51	NA	NA
12	**0.039**	0.85	0.55	0.51	0.99	NA
15	0.46	0.99	0.99	0.99	0.90	0.93

2_F17

Algae mean
chi-squared = 14.0, df = 6, p-value = 0.029

	-6	**-1**	**0**	**1**	**6**	**12**
-1	0.56	NA	NA	NA	NA	NA
0	1	0.65	NA	NA	NA	NA
1	0.99	0.76	0.99	NA	NA	NA
6	0.45	0.99	0.54	0.65	NA	NA
12	0.099	0.97	0.14	0.19	0.99	NA
15	0.48	1	0.56	0.67	1	0.99

Bacteria mean Kruskal-Wallis Test; pairwise *post hoc* Nemenyi tests
chi-squared = 13.5, df = 6, p-value = 0.035

	-6	**-1**	**0**	**1**	**6**	**12**
-1	0.74	NA	NA	NA	NA	NA
0	0.65	1	NA	NA	NA	NA
1	0.28	0.99	0.99	NA	NA	NA
6	0.39	0.99	0.99	0.99	NA	NA
12	0.99	0.43	0.35	0.099	0.16	NA
15	0.99	0.92	0.87	0.52	0.65	0.98

Bacteria:Algae ratio Kruskal-Wallis Test; pairwise *post hoc* Nemenyi tests
chi-squared = 12.8, df = 6, p-value = 0.046

	-6	**-1**	**0**	**1**	**6**	**12**
-1	0.18	NA	NA	NA	NA	NA
0	0.99	0.61	NA	NA	NA	NA
1	0.84	0.92	0.99	NA	NA	NA
6	**0.039**	0.99	0.24	0.61	NA	NA
12	0.35	0.99	0.81	0.99	0.97	NA
15	0.78	0.96	0.99	1	0.69	0.99

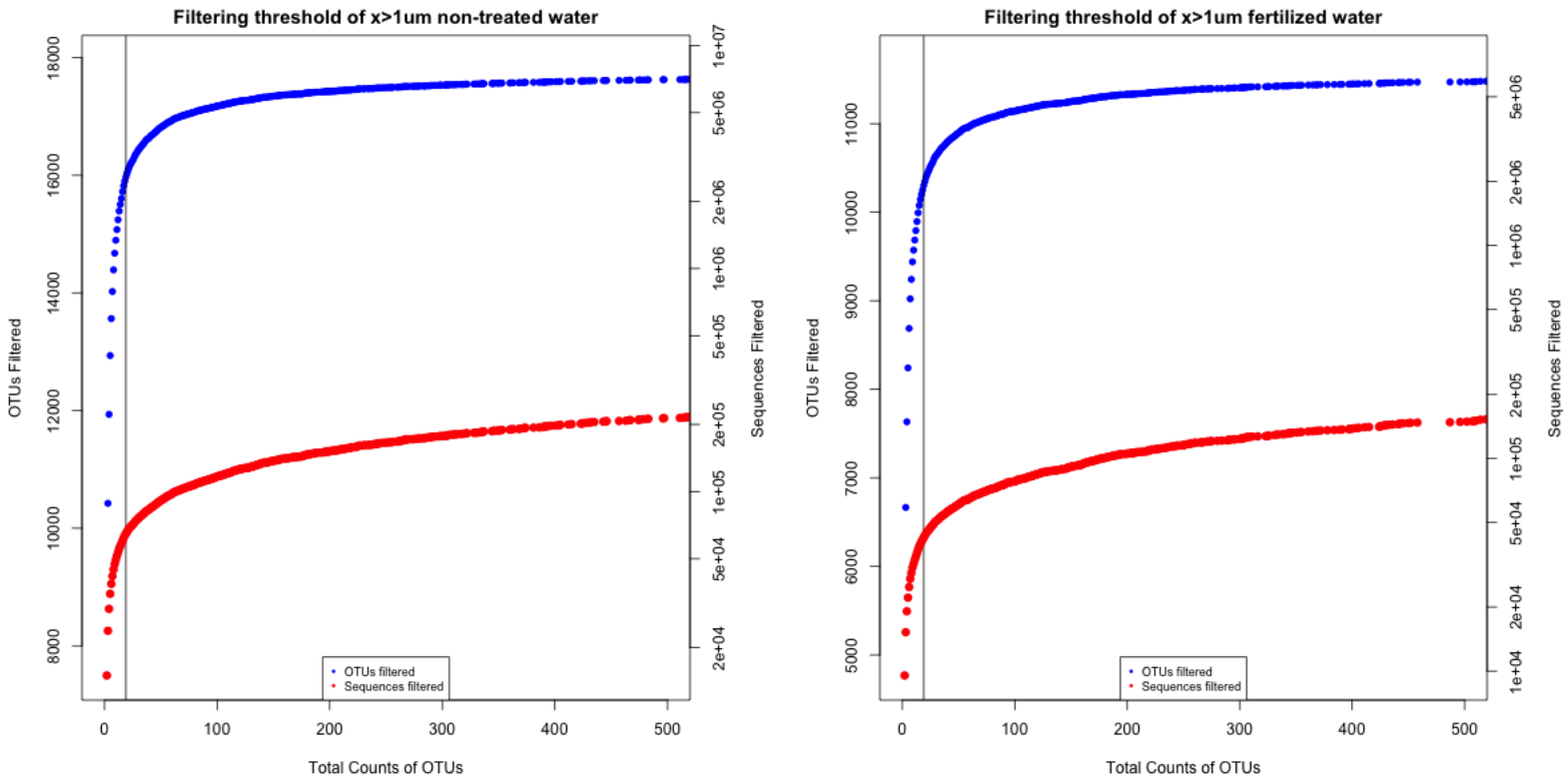

Figure A3.1: Identification of spurious OTUs to be removed. The number of OTUs with the number of sequences within an OUT. The non-treated community (left) and the fertilized community (right). The vertical black line represents filtering threshold. The blue dots are the cumulative sum of the number of OTUs with x or less sequences. The red dots represent the cumulative number of sequences.

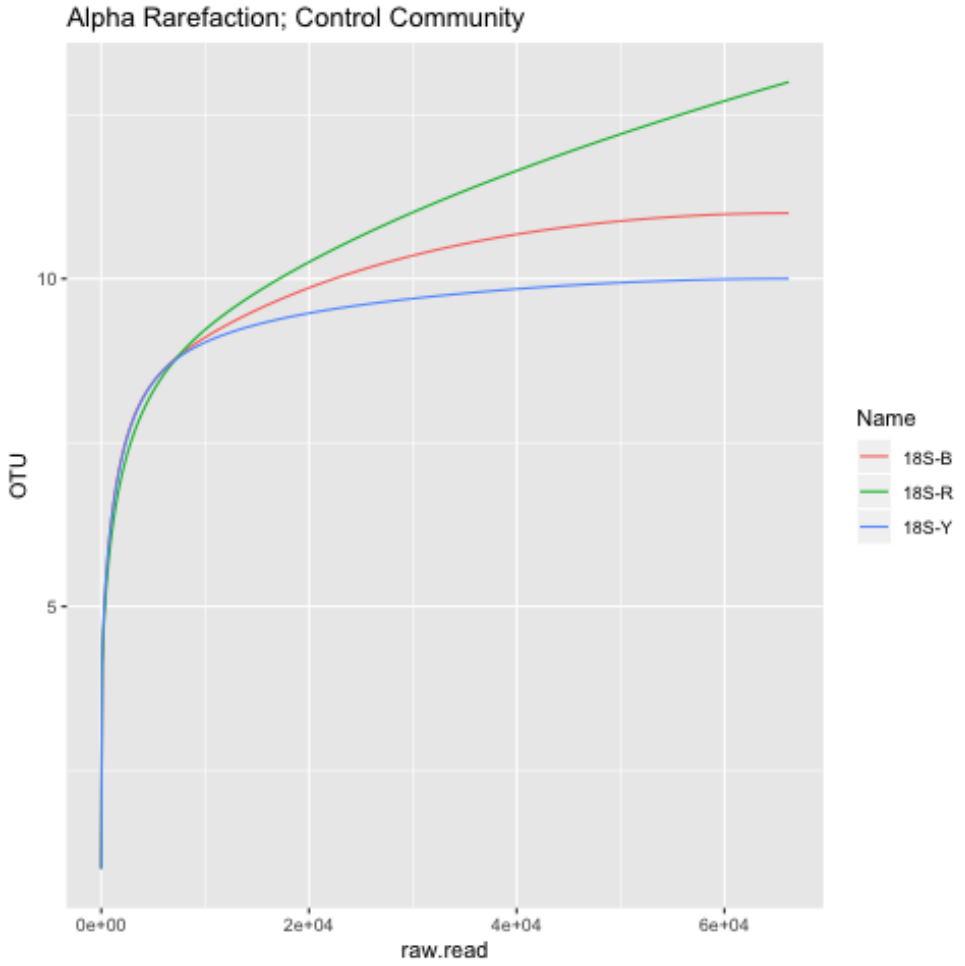

Figure A3.2: Alpha rarefaction plot of algal control communities. Rarefaction of the control community showing the sequencing depth of the rarefied community.

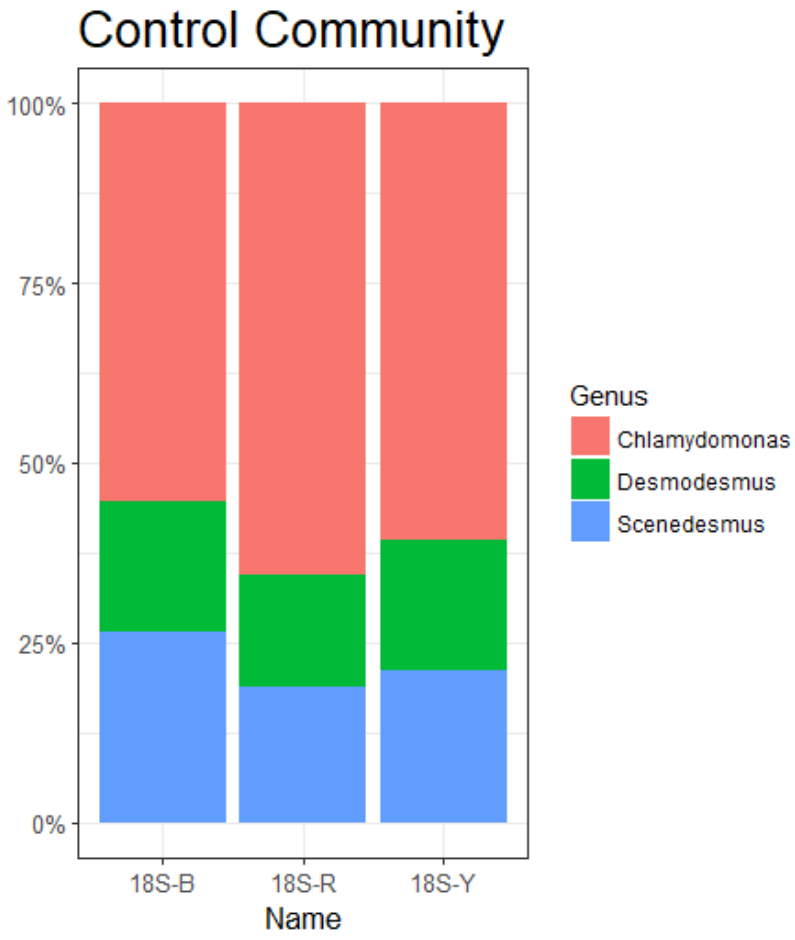

Figure A3.3: Relative abundance of genera representing greater than 0.1% of the synthetic mock communities.

Table A3.2: Pairwise Kruskal-Wallis *post hoc* Nemenyi tests of bacterial and algal counts from 2017. Significant p values are in bold-face print.

Ties in the *post hoc* Nemenyi tests were broken with chi-square distributions.

Experimental Ponds

Observed OTUs Kruskal-Wallis Test; pairwise *post hoc* Nemenyi tests

chi-squared = 21.9, df = 6, p-value = 0.001

	-6	**-1**	**0**	**1**	**6**	**12**
-1	1	NA	NA	NA	NA	NA
0	1	1	NA	NA	NA	NA
1	0.93	0.84	0.87	NA	NA	NA
6	0.91	0.77	0.81	1		NA
12	0.32	0.085	0.12	0.88	0.89	NA
15	0.46	0.17	0.22	0.96	0.96	1

Shannon diversity Kruskal-Wallis Test; pairwise *post hoc* Nemenyi tests

chi-squared = 16.82, df = 6, p-value = 0.009

	-6	**-1**	**0**	**1**	**6**	**12**
-1	1	NA	NA	NA	NA	NA
0	1	1	NA	NA	NA	NA
1	1	1	1	NA	NA	NA
6	0.85	0.92	0.87	0.92	NA	NA
12	0.34	0.31	0.25	0.33	0.95	NA
15	0.63	0.68	0.59	0.68	1	1

Pielou J index Kruskal-Wallis Test; pairwise *post hoc* Nemenyi tests

chi-squared = 16.74, df = 6, p-value = 0.01

	-6	**-1**	**0**	**1**	**6**	**12**
-1	1	NA	NA	NA	NA	NA
0	1	1	NA	NA	NA	NA
1	1	1	1	NA	NA	NA
6	0.83	0.95	0.92	0.8	NA	NA
12	0.34	0.4	0.37	0.21	0.96	NA
15	0.61	0.74	0.71	0.5	1	1

Control Pond

Observed OTUs Kruskal-Wallis Test; pairwise *post hoc* Nemenyi tests

chi-squared = 15.86, df = 6, p-value = 0.014

	-6	**-1**	**0**	**1**	**6**	**12**
-1	0.84	NA	NA	NA	NA	NA
0	0.91	1	NA	NA	NA	NA
1	0.91	1	1	NA	NA	NA
6	0.93	1	1	1	NA	NA
12	0.99	0.36	0.47	0.47	0.51	NA
15	0.99	0.4	0.51	0.51	0.54	1

Shannon diversity Kruskal-Wallis Test; pairwise *post hoc* Nemenyi tests

chi-squared = 15.93, df = 6, p-value = 0.014

	-6	**-1**	**0**	**1**	**6**	**12**
-1	1	NA	NA	NA	NA	NA
0	0.99	0.96	NA	NA	NA	NA
1	1	1	0.98	NA	NA	NA
6	0.93	0.97	0.47	0.94	NA	NA
12	0.84	0.73	1	0.82	0.16	NA
15	0.76	0.62	0.99	0.73	0.11	1

Pielou J index Kruskal-Wallis Test; pairwise *post hoc* Nemenyi tests

chi-squared = 17.32, df = 6, p-value = 0.008

	-6	**-1**	**0**	**1**	**6**	**12**
-1	0.98	NA	NA	NA	NA	NA
0	1	0.99	NA	NA	NA	NA
1	0.99	1	0.99	NA	NA	NA
6	0.65	0.99	0.73	0.98	NA	NA
12	0.99	0.65	0.97	0.69	0.16	NA
15	0.93	0.43	0.89	0.47	0.069	1

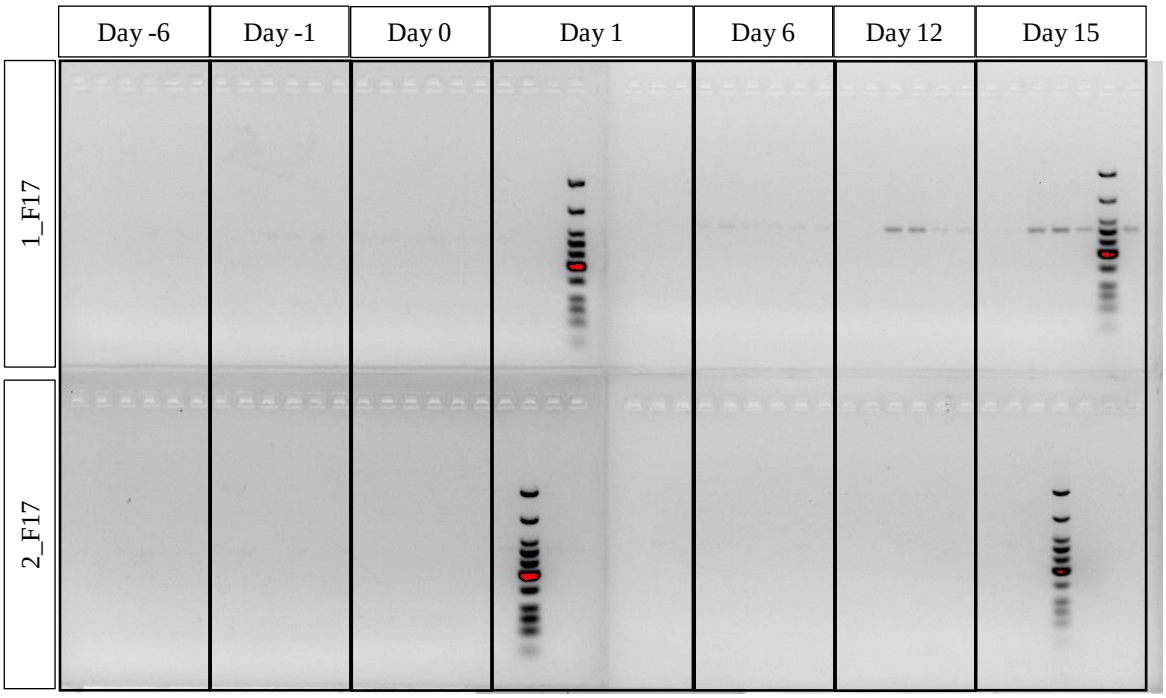

Figure A3.4: 18S rRNA gene PCR for the filter fraction 1 μm > x ≥ 0.22 μm from the 2017 ponds. Pond 1 (top) showed an enrichment for 18S rRNA gene sequence. Bands were excised and sequenced to identify them as belonging to order *Chlamydomonadales*.

Bibliography

1. **Holland, HD**. 2006. The oxygenation of the atmosphere and oceans. Philo Trans R Soc Lond B Biol Sci **361**:903–915.
2. **Rosing, MT, Frei, R**. 2004. U-rich Archaean sea-floor sediments from Greenland–indications of> 3700 Ma oxygenic photosynthesis. Earth and Planet Sci Lett **217**:237–244.
3. **Buick, R**. 2005. Paleontological and geochemical records of early life in Archean rocks from the Pilbara Craton, Australia. **16th Joint Meeting for Earth and Planetary Science, Makuhari, Japan.**
4. **Buick, R**. 2008. When did oxygenic photosynthesis evolve. Philos Trans R Soc Lond B Biol Sci **363**:2731–2743.
5. **Tirichine, L, Bowler, C**. 2011. Decoding algal genomes: tracing back the history of photosynthetic life on Earth. Plant J **66**:45–57.
6. **Shih, PM, Matzke, NJ**. 2013. Primary endosymbiosis events date to the later Proterozoic with cross-calibrated phylogenetic dating of duplicated ATPase proteins. Proc Natl Acad Sci U S A **110**:12355–12360.
7. **McFadden, GI, van Dooren, GG**. 2004. Evolution: red algal genome affirms a common origin of all plastids. Curr Biol **14**:R514–6.
8. **Reyes-Prieto, A, Weber, APM, Bhattacharya, D**. 2007. The origin and establishment of the plastid in algae and plants. Annu Rev Genet **41**:147–168.
9. **Archibald, JM**. 2009. The puzzle of plastid evolution. Curr Biol **19**:R81–8.

10. **Leliaert, F, Smith, DR, Moreau, H, Herron, MD, Verbruggen, H, Delwiche, CF, De Clerck, O**. 2012. Phylogeny and molecular evolution of the green algae. Crit Rev Plant Sci **31**:1–46.

11. **Delwiche, CF**. 1999. Tracing the thread of plastid diversity through the tapestry of life. Am Nat **154**:S164–S177.

12. **Rodríguez-Ezpeleta, N, Brinkmann, H, Burey, SC, Roure, B, Burger, G, Löffelhardt, W, Bohnert, HJ, Philippe, H, Lang, BF**. 2005. Monophyly of primary photosynthetic eukaryotes: green plants, red algae, and glaucophytes. Curr Biol **15**:1325–1330.

13. **Ochoa de Alda, JA, Esteban, R, Diago, ML, Houmard, J**. 2014. The plastid ancestor originated among one of the major cyanobacterial lineages. Nat Commun **5**:4937.

14. **Delwiche, CF, Palmer, JD**. 1997. The origin of plastids and their spread via secondary symbiosis, p. 53–86. *In* Bhattacharya D. (ed), Origins of algae and their plastids, vol 11. Springer, Vienna.

15. **McFadden, GI**. 2001. Primary and secondary endosymbiosis and the origin of plastids. J Phycol **37**:951–959.

16. **Adl, SM, Simpson, AG, Farmer, MA, Andersen, RA, Anderson, OR, Barta, JR, Bowser, SS, Brugerolle, G, Fensome, RA, Fredericq, S, James, TY, Karpov, S, Kugrens, P, Krug, J, Lane, CE, Lewis, LA, Lodge, J, Lynn, DH, Mann, DG, McCourt, RM, Mendoza, L, Moestrup, O, Mozley-Standridge, SE, Nerad, TA, Shearer, CA, Smirnov, AV, Spiegel, FW, Taylor, MF**. 2005.

The new higher level classification of eukaryotes with emphasis on the taxonomy of protists. J Eukaryot Microbiol **52**:399–451.

17. **Cavalier-Smith, T, Allsopp, MT, Chao, EE**. 1994. Chimeric conundra: are nucleomorphs and chromists monophyletic or polyphyletic. Proc Natl Acad Sci U S A **91**:11368–11372.
18. **Archibald, JM**. 2007. Nucleomorph genomes: structure, function, origin and evolution. Bioessays **29**:392–402.
19. **Gibbs, SP**. 1981. The chloroplast endoplasmic reticulum: structure, function, and evolutionary significance, p. 49–99. Int Rev Cytol, vol 72. Acedemic Press.
20. **Douglas, SE, Murphy, CA, Spencer, DF, Gray, MW**. 1991. Cryptomonad algae are evolutionary chimaeras of two phylogenetically distinct unicellular eukaryotes. Nature **350**:148.
21. **Delwiche, CF, Kuhsel, M, Palmer, JD**. 1995. Phylogenetic analysis of tufA sequences indicates a cyanobacterial origin of all plastids. Mol Phylogenet Evol **4**:110–128.
22. **Yoon, HS, Hackett, JD, Bhattacharya, D**. 2002. A single origin of the peridinin-and fucoxanthin-containing plastids in dinoflagellates through tertiary endosymbiosis. Proc Natl Acad Sci U S A **99**:11724–11729.
23. **Yoon, HS, Hackett, JD, Van Dolah, FM, Nosenko, T, Lidie, KL, Bhattacharya, D**. 2005. Tertiary endosymbiosis driven genome evolution in dinoflagellate algae. Mol Biol Evol **22**:1299–1308.
24. **Spolaore, P, Joannis-Cassan, C, Duran, E, Isambert, A**. 2006. Commercial applications of microalgae. J Biosci Bioeng **101**:87–96.

25. **Thao, TY, Linh, DTN, Si, VC, Carter, TW, Hill, RT**. 2017. Isolation and selection of microalgal strains from natural water sources in Viet Nam with potential for edible oil production. Mar Drugs **15**:194.

26. **Jensen, GS**. 2001. Blue-green algae as an immuno-enhancer and biomodulator. J Am Nutraceutical Assoc **3**:24–30.

27. **Richer, S, Stiles, W, Statkute, L, Pulido, J, Frankowski, J, Rudy, D, Pei, K, Tsipursky, M, Nyland, J**. 2004. Double-masked, placebo-controlled, randomized trial of lutein and antioxidant supplementation in the intervention of atrophic age-related macular degeneration: the Veterans LAST study (Lutein Antioxidant Supplementation Trial). J Am Optom Assoc **75**:216–229.

28. **Franklin, SE, Mayfield, SP**. 2004. Prospects for molecular farming in the green alga *Chlamydomonas*. Curr Opin Plant Biol **7**:159–165.

29. **Havaux, M, Niyogi, KK**. 1999. The violaxanthin cycle protects plants from photooxidative damage by more than one mechanism. Proc Natl Acad Sci U S A **96**:8762–8767.

30. **Havaux, M, Kloppstech, K**. 2001. The protective functions of carotenoid and flavonoid pigments against excess visible radiation at chilling temperature investigated in *Arabidopsis* npq and tt mutants. Planta **213**:953–966.

31. **Takaichi, S**. 2011. Carotenoids in algae: distributions, biosyntheses and functions. Mar Drugs **9**:1101–1118.

32. **Sheehan, J, Dunahay, T, Benemann, J, Roessler, P**. 1998. Look back at the US department of energy's aquatic species program: biodiesel from algae. National Renewable Energy Laboratory. Golden, CO.

33. **Chisti, Y**. 2007. Biodiesel from microalgae. Biotechnol Adv **25**:294–306.

34. **Hu, Q, Sommerfeld, M, Jarvis, E, Ghirardi, M, Posewitz, M, Seibert, M, Darzins, A**. 2008. Microalgal triacylglycerols as feedstocks for biofuel production: perspectives and advances. Plant J **54**:621–639.

35. **Rodolfi, L, Chini Zittelli, G, Bassi, N, Padovani, G, Biondi, N, Bonini, G, Tredici, MR**. 2009. Microalgae for oil: strain selection, induction of lipid synthesis and outdoor mass cultivation in a low-cost photobioreactor. Biotechnol Bioeng **102**:100–112.

36. **Tredici, MR**. 2010. Photobiology of microalgae mass cultures: understanding the tools for the next green revolution. Biofuels **1**:143–162.

37. **Pal, D, Khozin-Goldberg, I, Cohen, Z, Boussiba, S**. 2011. The effect of light, salinity, and nitrogen availability on lipid production by *Nannochloropsis* sp. Microb Biotechnol **90**:1429–1441.

38. **Nascimento, IA, Marques, SSI, Cabanelas, ITD, Pereira, SA, Druzian, JI, de Souza, CO, Vich, DV, de Carvalho, GC, Nascimento, MA**. 2013. Screening microalgae strains for biodiesel production: Lipid productivity and estimation of fuel quality based on fatty acids profiles as selective criteria. BioEnergy Research **6**:1–13.

39. **Levitan, O, Dinamarca, J, Hochman, G, Falkowski, PG**. 2014. Diatoms: a fossil fuel of the future. Trends Biotechnol **32**:117–124.

40. **Li, M, Wang, T-G, Lillis, P, Wang, C, Shi, S**. 2012. The significance of 24-norcholestanes, triaromatic steroids and dinosteroids in oils and Cambrian–

Ordovician source rocks from the cratonic region of the Tarim Basin, NW China. Appl Geochem **27**:1643–1654.

41. **Georgianna, DR, Mayfield, SP**. 2012. Exploiting diversity and synthetic biology for the production of algal biofuels. Nature **488**:329–335.

42. **Ferrell, J, Sarisky-Reed, V**. 2010. National algal biofuels technology roadmap. United States. doi:10.2172/1218560

43. **Wang, H, Hill, RT, Zheng, T, Hu, X, Wang, B**. 2016. Effects of bacterial communities on biofuel-producing microalgae: stimulation, inhibition and harvesting. Crit Rev Biotechnol **36**:341–352.

44. **Searchinger, T, Heimlich, R, Houghton, RA, Dong, F, Elobeid, A, Fabiosa, J, Tokgoz, S, Hayes, D, Yu, TH**. 2008. Use of U.S. croplands for biofuels increases greenhouse gases through emissions from land-use change. Science **319**:1238–1240.

45. **Fargione, J, Hill, J, Tilman, D, Polasky, S, Hawthorne, P**. 2008. Land clearing and the biofuel carbon debt. Science **319**:1235–1238.

46. **Dismukes, GC, Carrieri, D, Bennette, N, Ananyev, GM, Posewitz, MC**. 2008. Aquatic phototrophs: Efficient alternatives to land-based crops for biofuels. Curr Opin Biotechnol **19**:235–240.

47. **Carlson, RR**. 1977. A trophic state index for lakes. Limnol Oceanogr **22**:361–369.

48. **Whitman, RL, Shively, DA, Pawlik, H, Nevers, MB, Byappanahalli, MN**. 2003. Occurrence of *Escherichia coli* and enterococci in *Cladophora*

(Chlorophyta) in nearshore water and beach sand of Lake Michigan. Appl Environ Microbiol **69**:4714–4719.

49. **Salmaso, N, Morabito, G, Buzzi, F, Garibaldi, L, Simona, M, Mosello, R**. 2006. Phytoplankton as an indicator of the water quality of the deep lakes south of the Alps. Hydrobiologia **563**:167–187.

50. **Peckol, P, Rivers, JS**. 1995. Physiological responses of the opportunistic macroalgae *Cladophora vagabunda* (L.) van den Hoek and *Gracilaria tikvahiae* (McLachlan) to environmental. J Exp Mar Bio Ecol **190**:1–16.

51. **Anderson, DM, Glibert, PM, Burkholder, JM**. 2002. Harmful algal blooms and eutrophication: Nutrient sources, composition, and consequences. Estuaries **25**:704–726.

52. **O'Neil, JM, Davis, TW, Burford, MA, Gobler, CJ**. 2012. The rise of harmful cyanobacteria blooms: The potential roles of eutrophication and climate change. Harmful Algae **14**:313–334.

53. **Schindler, DW**. 1977. Evolution of phosphorus limitation in lakes. Science **195**:260–262.

54. **Reckhow, KH, Chapra, SC**. 1983. Engineering approaches for lake management. vol 1. Butterworth Publishers.

55. **Correll, DL**. 1998. The role of phosphorus in the eutrophication of receiving waters: A review. J Environ Qual **27**:261–266.

56. **Reynolds, C, Dokulil, M, Padisák, J**. 2000. Understanding the assembly of phytoplankton in relation to the trophic spectrum: Where are we now. Hydrobiologia **424**:147–152.

57. **Ptacnik, R, Solimini, AG, Andersen, T, Tamminen, T, Brettum, P, Lepistö, L, Willén, E, Rekolainen, S**. 2008. Diversity predicts stability and resource use efficiency in natural phytoplankton communities. Proc Natl Acad Sci U S A **105**:5134–5138.

58. **Vollenweider, RA**. 1976. Advances in defining critical loading levels for phosphorus in lake eutrophication. Memorie dell'Istituto Italiano di Idrobiologia **33**:53–83.

59. **Von Liebig, JF**. 1855. Principles of agricultural chemistry: With special reference to the late researches made in England. Walton & Maberly.

60. **De Baar, HJW**. 1994. von Liebig's law of the minimum and plankton ecology (1899–1991). Prog Oceanogr **33**:347–386.

61. **Phillips, G, Pietiläinen, O-P, Carvalho, L, Solimini, A, Solheim, AL, Cardoso, AC**. 2008. Chlorophyll–nutrient relationships of different lake types using a large European dataset. Aquat Ecol **42**:213–226.

62. **Smith, VH, Tilman, GD, Nekola, JC**. 1999. Eutrophication: impacts of excess nutrient inputs on freshwater, marine, and terrestrial ecosystems. Environ Pollut **100**:179–196.

63. **Oswald, WJ, Gotaas, HB**. 1957. Photosynthesis in sewage treatment. Trans A, Soc Civ Eng **1**:73–105.

64. **Borowitzka, MA, Borowitzka, LJ**. 1988. Micro-algal biotechnology. Cambridge University Press, Cambridge.

65. **de la Noue, J, de Pauw, N**. 1988. The potential of microalgal biotechnology: a review of production and uses of microalgae. Biotechnol Adv **6**:725–770.

66. **Douskova, I, Doucha, J, Livansky, K, Machat, J, Novak, P, Umysova, D, Zachleder, V, Vitova, M**. 2009. Simultaneous flue gas bioremediation and reduction of microalgal biomass production costs. Appl Microbiol Biotechnol **82**:179–185.

67. **Lee Jeong, M-J, Gillis, JM, Hwang, J-Y**. 2003. Carbon dioxide mitigation by microalgal photosynthesis. Bull Korean Chem Soc **24**:1763–1766.

68. **Sayre, R**. 2010. Microalgae: The potential for carbon capture. BioScience **60**:722–727.

69. **Höök, M, Tang, X**. 2013. Depletion of fossil fuels and anthropogenic climate change—A review. Energy Policy **52**:797–809.

70. **Rodhe, H**. 1990. A comparison of the contribution of various gases to the greenhouse effect. Science **248**:1217–1219.

71. **Doney, SC, Fabry, VJ, Feely, RA, Kleypas, JA**. 2009. Ocean acidification: the other CO_2 problem. Ann Rev Mar Sci **1**:169–192.

72. **Raven, J, Caldeira, K, Elderfield, H, Hoegh-Guldberg, O, Liss, P, Riebesell, U, Shepherd, J, Turley, C, Watson, A**. 2005. Ocean acidification due to increasing atmospheric carbon dioxide. The Royal Society, London.

73. **Meher, L, Vidya Sagar, D, Naik, SN**. 2006. Technical aspects of biodiesel production by transesterification—a review. Renew Sust Energ Rev **10**:248–268.

74. **Dong, HP, Williams, E, Wang, DZ, Xie, ZX, Hsia, RC, Jenck, A, Halden, R, Li, J, Chen, F, Place, AR**. 2013. Responses of *Nannochloropsis oceanica*

IMET1 to long-term nitrogen starvation and recovery. Plant Physiol **162**:1110–1126.

75. **Hu, Q, Zhang, C, Sommerfeld, M**. 2006. Biodiesel from algae: Lessons learned over the past 60 years and future perspectives. J Phycol **42**:12.

76. **Fukuda, H, Kondo, A, Noda, H**. 2001. Biodiesel fuel production by transesterification of oils. J Biosci Bioeng **92**:405–416.

77. **Trivedi, J, Aila, M, Bangwal, DP, Kaul, S, Garg, MO**. 2015. Algae based biorefinery—How to make sense? Renew Sust Energ Rev **47**:295–307.

78. **Zhou, Y, Schideman, L, Yu, G, Zhang, Y**. 2013. A synergistic combination of algal wastewater treatment and hydrothermal biofuel production maximized by nutrient and carbon recycling. Energ Environ Sci **6**:3765–3779.

79. **Laurens, LML, Nagle, N, Davis, R, Sweeney, N, Van Wychen, S, Lowell, A, Pienkos, PT**. 2015. Acid-catalyzed algal biomass pretreatment for integrated lipid and carbohydrate-based biofuels production. Green Chemistry **17**:1145–1158.

80. **Ross, AB, Biller, P, Kubacki, ML, Li, H, Lea-Langton, A, Jones, JM**. 2010. Hydrothermal processing of microalgae using alkali and organic acids. Fuel **89**:2234–2243.

81. **Peterson, AA, Vogel, F, Lachance, RP, Fröling, M, Antal, J, Michael J., Tester, JW**. 2008. Thermochemical biofuel production in hydrothermal media: A review of sub- and supercritical water technologies. Energ Environ Sci **1**:32.

82. **Toor, SS, Rosendahl, L, Rudolf, A**. 2011. Hydrothermal liquefaction of biomass: A review of subcritical water technologies. Energy **36**:2328–2342.

83. **Yu, G, Zhang, Y, Schideman, L, Funk, TL, Wang, Z**. 2011. Hydrothermal liquefaction of low lipid content microalgae into bio-crude oil. Trans ASABE **54**:239–246.

84. **Li, H, Liu, Z, Zhang, Y, Li, B, Lu, H, Duan, N, Liu, M, Zhu, Z, Si, B**. 2014. Conversion efficiency and oil quality of low-lipid high-protein and high-lipid low-protein microalgae via hydrothermal liquefaction. Bioresour Technol **154**:322–329.

85. **Manandhar-Shrestha, K, Hildebrand, M**. 2015. Characterization and manipulation of a DGAT2 from the diatom *Thalassiosira pseudonana*: Improved TAG accumulation without detriment to growth, and implications for chloroplast TAG accumulation. Algal Res **12**:239–248.

86. **Benemann, J**. 2013. Microalgae for biofuels and animal feeds. Energies **6**:5869–5886.

87. **Striebel, M, Behl, S, Stibor, H**. 2009. The coupling of biodiversity and productivity in phytoplankton communities: consequences for biomass stoichiometry. Ecology **90**:2025–2031.

88. **Smith, VH, Sturm, BS, Denoyelles, FJ, Billings, SA**. 2010. The ecology of algal biodiesel production. Trends Ecol Evol **25**:301–309.

89. **Power, LD, Cardinale, BJ**. 2009. Species richness enhances both algal biomass and rates of oxygen production in aquatic microcosms. Oikos **118**:1703–1711.

90. **Stockenreiter, M, Graber, A-K, Haupt, F, Stibor, H**. 2012. The effect of species diversity on lipid production by micro-algal communities. J Appl Phycol **24**:45–54.

91. **Hillebrand, H, Sommer, U**. 2000. Diversity of benthic microalgae in response to colonization time and eutrophication. Aquat Bot **67**:221–236.

92. **Chase, JM, Leibold, MA**. 2002. Spatial scale dictates the productivity-biodiversity relationship. Nature **416**:427–430.

93. **Worm, B, Lotze, HK**. 2006. Effects of eutrophication, grazing, and algal blooms on rocky shores. Limnol Oceanogr **51**:569–579.

94. **Chase, JM**. 2010. Stochastic community assembly causes higher biodiversity in more productive environments. Science **328**:1388–1391.

95. **Smith, VH, Sturm, BBS, Billings, SA**. 2010. The ecology of algal biofuel production. Trends Ecol Evol **25**:301–309.

96. **McBride, RC, Lopez, S, Meenach, C, Burnett, M, Lee, PA, Nohilly, F, Behnke, C**. 2014. Contamination management in low cost open algae ponds for biofuels production. Ind Biotechnol **10**:221–227.

97. **Grossart, HP, Simon, M**. 2007. Interactions of planktonic algae and bacteria: Effects on algal growth and organic matter dynamics. Aquat Microb Ecol **47**:163–176.

98. **Croft, MT, Lawrence, AD, Raux-Deery, E, Warren, MJ, Smith, AG**. 2005. Algae acquire vitamin B_{12} through a symbiotic relationship with bacteria. Nature **438**:90–93.

99. **Helliwell, KE, Wheeler, GL, Leptos, KC, Goldstein, RE, Smith, AG**. 2011. Insights into the evolution of vitamin B_{12} auxotrophy from sequenced algal genomes. Mol Biol Evol **28**:2921–2933.

100. **Kazamia, E, Czesnick, H, Nguyen, TT, Croft, MT, Sherwood, E, Sasso, S, Hodson, SJ, Warren, MJ, Smith, AG**. 2012. Mutualistic interactions between vitamin B_{12} -dependent algae and heterotrophic bacteria exhibit regulation. Environ Microbiol **14**:1466–1476.

101. **Amin, SA, Parker, MS, Armbrust, EV**. 2012. Interactions between diatoms and bacteria. Microbiol Mol Biol Rev **76**:667–684.

102. **Goecke, F, Thiel, V, Wiese, J, Labes, A, Imhoff, JF**. 2013. Algae as an important environment for bacteria – phylogenetic relationships among new bacterial species isolated from algae. Phycologia **52**:14–24.

103. **Grossart, HP, Levold, F, Allgaier, M, Simon, M, Brinkhoff, T**. 2005. Marine diatom species harbour distinct bacterial communities. Environ Microbiol **7**:860–873.

104. **Bagatini, IL, Eiler, A, Bertilsson, S, Klaveness, D, Tessarolli, LP, Vieira, AA**. 2014. Host-specificity and dynamics in bacterial communities associated with Bloom-forming freshwater phytoplankton. PLoS One **9**:e85950.

105. **Watanabe, K, Takihana, N, Aoyagi, H, Hanada, S, Watanabe, Y, Ohmura, N, Saiki, H, Tanaka, H**. 2005. Symbiotic association in *Chlorella* culture. FEMS Microbiol Ecol **51**:187–196.

106. **Rosenberg, G, Paerl, HW**. 1981. Nitrogen fixation by blue-green algae associated with the siphonous green seaweed *Codium decorticatum*: Effects on ammonium uptake. Mar Biol **61**:151–158.

107. **Foster, RA, Kuypers, MM, Vagner, T, Paerl, RW, Musat, N, Zehr, JP**. 2011. Nitrogen fixation and transfer in open ocean diatom-cyanobacterial symbioses. ISME J **5**:1484–1493.

108. **Cooper, MB, Smith, AG**. 2015. Exploring mutualistic interactions between microalgae and bacteria in the omics age. Curr Opin Plant Biol **26**:147–153.

109. **Gonzalez, LE, Bashan, Y**. 2000. Increased growth of the microalga *Chlorella vulgaris* when coimmobilized and cocultured in alginate beads with the plant-growth-promoting bacterium *Azospirillum brasilense*. Appl Environ Microbiol **66**:1527–1531.

110. **de-Bashan, LE, Antoun, H, Bashan, Y**. 2008. Involvement of indole-3-acetic acid produced by the growth-promoting bacterium *Azospirillum* spp. in promoting growth of *Chlorella vulgaris*. J Phycol **44**:938–947.

111. **Meza, B, de-Bashan, LE, Bashan, Y**. 2015. Involvement of indole-3-acetic acid produced by Azospirillum brasilense in accumulating intracellular ammonium in *Chlorella vulgaris*. Res Microbiol **166**:72–83.

112. **Natrah, FMI, Bossier, P, Sorgeloos, P, Yusoff, FM, Defoirdt, T**. 2014. Significance of microalgal-bacterial interactions for aquaculture. Rev Aquac **6**:48–61.

113. **Palacios, OA, Bashan, Y, Schmid, M, Hartmann, A, De-Bashan, LE**. 2016. Enhancement of thiamine release during synthetic mutualism between *Chlorella*

sorokiniana and *Azospirillum brasilense* growing under stress conditions. J Appl Phycol **28**:1521–1531.

114. **de-Bashan, LE, Mayali, X, Bebout, BM, Weber, PK, Detweiler, AM, Hernandez, J-P, Prufert-Bebout, L, Bashan, Y**. 2016. Establishment of stable synthetic mutualism without co-evolution between microalgae and bacteria demonstrated by mutual transfer of metabolites (NanoSIMS isotopic imaging) and persistent physical association (Fluorescent in situ hybridization). Algal Res **15**:179–186.
115. **Zablotowicz, RM, Tipping, EM, Lifshitz, R, Kloepper, JW**. 1991. Plant growth promotion mediated by bacterial rhizosphere colonizers, p. 315–326. *In* Keister, DL, Cregan PB (eds), The Rhizosphere and Plant Growth. Beltsville Symposia in Agricultural Research, vol 14. Springer, Dorecht.
116. **Bell, W, Mitchell, R**. 1972. Chemotactic and growth responses of marine bacteria to algal extracellular products. Biol Bull **143**:265–277.
117. **Bashan, Y, Holguin, G**. 1998. Proposal for the division of plant growth promoting rhizobacteria into two classifications: Biocontrol PGPB (plant growth-promoting bacteria) and PGPB. Soil Biol Biochem **30**:1225–1228.
118. **Kloepper, JW, Leong, J, Teintze, M, Schroth, MN**. 1980. Enhanced plant-growth by siderophores produced by plant growth-promoting rhizobacteria. Nature **286**:885–886.
119. **Ramanan, R, Kim, BH, Cho, DH, Oh, HM, Kim, HS**. 2016. Algae-bacteria interactions: Evolution, ecology and emerging applications. Biotechnol Adv **34**:14–29.

120. **Barea, JM, Navarro, E, Montoya, E**. 1976. Production of plant growth regulators by rhizosphere phosphate-solubilizing bacteria. J Appl Bacteriol **40**:129–134.

121. **Weller, DM**. 1988. Biological control of soilborne plant pathogens in the rhizosphere with bacteria. Annu Rev Phytopathol **26**:379–407.

122. **Teplitski, M, Rajamani, S**. 2011. Signal and nutrient exchange in the interactions between soil algae and bacteria, p 413-426. *In* Witzany G (ed), Biocommunication in Soil Microorganisms. Springer, Berlin, Heidelberg.

123. **Kuo, RC, Lin, S**. 2013. Ectobiotic and endobiotic bacteria associated with *Eutreptiella* sp. isolated from Long Island Sound. Protist **164**:60–74.

124. **Amin, SA, Hmelo, LR, van Tol, HM, Durham, BP, Carlson, LT, Heal, KR, Morales, RL, Berthiaume, CT, Parker, MS, Djunaedi, B, Ingalls, AE, Parsek, MR, Moran, MA, Armbrust, EV**. 2015. Interaction and signalling between a cosmopolitan phytoplankton and associated bacteria. Nature **522**:98–101.

125. **Meza, B, De-Bashan, LE, Bashan, Y**. 2015. Involvement of indole-3-acetic acid produced by *Azospirillum brasilense* in accumulation of intracellular ammonium in *Chlorella vulgaris*. Res Microbiol **166**:72–83.

126. **Sharifah, EN, Eguchi, M**. 2011. The phytoplankton *Nannochloropsis oculata* enhances the ability of *Roseobacter* clade bacteria to inhibit the growth of fish pathogen *Vibrio anguillarum*. PLoS One **6**:e26756**.**

127. **Cho, D-H, Ramanan, R, Heo, J, Lee, J, Kim, B-H, Oh, H-M, Kim, H-S**. 2015. Enhancing microalgal biomass productivity by engineering a microalgal–bacterial community. Bioresour Technol **175**:578–585.

128. **Neuhauser, C, Fargione, JE**. 2004. A mutualisim-parasitism continuum model and its application to plant-mycorrhizae interactions. Ecol Modell **177**:337–352.

129. **Mueller, UG, Sachs, JL**. 2015. Engineering microbiomes to improve plant and animal health. Trends Microbiol **23**:606–617.

130. **Smith, FB**. 1944. The occurrence and distribution of algae in soils. Proceedings of the Florida Academy of Sciences **7**:44–49.

131. **Quispel, A**. 1946. The mutual relations between algae and fungi in lichens. Recueil des Travaux Botaniques Néerlandais **1**:413–541.

132. **Borowitzka, MA**. 2013. High-value products from microalgae-their development and commercialisation. J Appl Phycol **25**:743–756.

133. **Watson, E**. 2015. Algae oil: The next big healthy cooking oil? Products have a cleaner taste than other cooking oils, report consumers. www.foodnavigator-usa.com

134. **Herlemann, DP, Labrenz, M, Jürgens, K, Bertilsson, S, Waniek, JJ, Andersson, AF**. 2011. Transitions in bacterial communities along the 2000 km salinity gradient of the Baltic Sea. ISME J **5**:1571–1579.

135. **Klindworth, A, Pruesse, E, Schweer, T, Peplies, J, Quast, C, Horn, M, Glöckner, FO**. 2013. Evaluation of general 16S ribosomal RNA gene PCR primers for classical and next-generation sequencing-based diversity studies. Nucleic Acids Res **41**:e1.

136. **Caporaso, JG, Kuczynski, J, Stombaugh, J, Bittinger, K, Bushman, FD, Costello, EK, Fierer, N, Peña, AG, Goodrich, JK, Gordon, JI, Huttley, GA, Kelley, ST, Knights, D, Koenig, JE, Ley, RE, Lozupone, CA, McDonald, D, Muegge, BD, Pirrung, M, Reeder, J, Sevinsky, JR, Turnbaugh, PJ, Walters, WA, Widmann, J, Yatsunenko, T, Zaneveld, J, Knight, R**. 2010. QIIME allows analysis of high-throughput community sequencing data. Nat Methods **7**:335–336.

137. **Edgar, RC**. 2010. Search and clustering orders of magnitude faster than BLAST. Bioinformatics **26**:2460–2461.

138. **Quast, C, Pruesse, E, Yilmaz, P, Gerken, J, Schweer, T, Yarza, P, Peplies, J, Glöckner, FO**. 2013. The SILVA ribosomal RNA gene database project: improved data processing and web-based tools. Nucleic Acids Res **41**:D590–6.

139. **McMurdie, PJ, Holmes, S**. 2013. phyloseq: an R package for reproducible interactive analysis and graphics of microbiome census data. PLoS One **8**:e61217.

140. **Bray, JR, Curtis, JT**. 1957. An ordination of the upland forest communities of southern Wisconsin. Ecol Monogr **27**:325–349.

141. **Lozupone, C, Knight, R**. 2005. UniFrac: a new phylogenetic method for comparing microbial communities. Appl Environ Microbiol **71**:8228–8235.

142. **Oksanen, J, Blanchet, FG, Kindt, R, Legendre, P, Minchin, PR, O'hara, RB, Simpson, GL, Solymos, P, Stevens, MHH, Wagner, H**. 2013. Package 'vegan'. Community ecology package, version **2**

143. **Newton, RJ, Jones, SE, Eiler, A, McMahon, KD, Bertilsson, S**. 2011. A guide to the natural history of freshwater lake bacteria. Microbiol Mol Biol Rev **75**:14–49.

144. **Riemann, L, Winding, A**. 2001. Community dynamics of free-living and particle-associated bacterial assemblages during a freshwater phytoplankton bloom. Microb Ecol **42**:274–285.

145. **Eiler, A, Bertilsson, S**. 2004. Composition of freshwater bacterial communities associated with cyanobacterial blooms in four Swedish lakes. Environ Microbiol **6**:1228–1243.

146. **Llirós, M, Inceoğlu, Ö, García-Armisen, T, Anzil, A, Leporcq, B, Pigneur, LM, Viroux, L, Darchambeau, F, Descy, JP, Servais, P**. 2014. Bacterial community composition in three freshwater reservoirs of different alkalinity and trophic status. PLoS One **9**:e116145.

147. **Fisher, JC, Newton, RJ, Dila, DK, McLellan, SL**. 2015. Urban microbial ecology of a freshwater estuary of Lake Michigan. Elementa (Wash D C) **3**

148. **Abia, ALK, Alisoltani, A, Keshri, J, Ubomba-Jaswa, E**. 2018. Metagenomic analysis of the bacterial communities and their functional profiles in water and sediments of the Apies River, South Africa, as a function of land use. Sci Total Environ **616-617**:326–334.

149. **Caiola, MG, Pellegrini, S**. 1984. Lysis of *Microcystis aeruginosa* (Kutz.) by *Bdellovibrio*-like bacteria. J Phycol **20**:471–475.

150. **Cottrell, MT, Kirchman, DL**. 2000. Natural assemblages of marine proteobacteria and members of the Cytophaga-Flavobacter cluster consuming

low- and high-molecular-weight dissolved organic matter. Appl Environ Microbiol **66**:1692–1697.

151. **Davidov, Y, Jurkevitch, E**. 2004. Diversity and evolution of *Bdellovibrio*-and-like organisms (BALOs), reclassification of *Bacteriovorax starrii* as *Peredibacter starrii* gen. nov., comb. nov., and description of the *Bacteriovorax-Peredibacter* clade as *Bacteriovoracaceae* fam. nov. Int J Syst Evol Microbiol **54**:1439–1452.
152. **Berg, KA, Lyra, C, Sivonen, K, Paulin, L, Suomalainen, S, Tuomi, P, Rapala, J**. 2009. High diversity of cultivable heterotrophic bacteria in association with cyanobacterial water blooms. ISME J **3**:314–325.
153. **Wei, S, Morrison, M, Yu, Z**. 2013. Bacterial census of poultry intestinal microbiome. Poult Sci **92**:671–683.
154. **Falkinham, JO, George, KL, Parker, BC**. 1989. Epidemiology of infection by nontuberculous mycobacteria: VIII. Absence of mycobacteria in chicken litter. Am Rev Respir Dis **139**:1347–1349.
155. **Lu, J, Sanchez, S, Hofacre, C, Maurer, JJ, Harmon, BG, Lee, MD**. 2003. Evaluation of broiler litter with reference to the microbial composition as assessed by using 16S rRNA and functional gene markers. Appl Environ Microbiol **69**:901–908.
156. **Cotta, MA, Whitehead, TR, Collins, MD, Lawson, PA**. 2004. *Atopostipes suicloacale* gen. nov., sp. nov., isolated from an underground swine manure storage pit. Anaerobe **10**:191–195.

157. **Wadud, S, Michaelsen, A, Gallagher, E, Parcsi, G, Zemb, O, Stuetz, R, Manefield, M**. 2012. Bacterial and fungal community composition over time in chicken litter with high or low moisture content. Br Poult Sci **53**:561–569.

158. **Pan, D, Yu, Z**. 2014. Intestinal microbiome of poultry and its interaction with host and diet. Gut Microbes **5**:108–119.

159. **Dahiru, M, Enabulele, OI**. 2015. *Acinetobacter baumannii* in birds' feces: A public health threat to vegetables and irrigation farmers. Adv Microbiol **5**:693–698.

160. **Davies, CM, Evison, LM**. 1991. Sunlight and the survival of enteric bacteria in natural waters. J Appl Bacteriol **70**:265–274.

161. **Joux, F, Jeffrey, WH, Lebaron, P, Mitchell, DL**. 1999. Marine bacterial isolates display diverse responses to UV-B radiation. Appl Environ Microbiol **65**:3820–3827.

162. **Lozupone, CA, Knight, R**. 2007. Global patterns in bacterial diversity. Proc Natl Acad Sci U S A **104**:11436–11440.

163. **Ma, L, Mao, G, Liu, J, Gao, G, Zou, C, Bartlam, MG, Wang, Y**. 2016. Spatial-temporal changes of bacterioplankton community along an Exhorheic River. Front Microbiol **7**:250.

164. **Eiler, A, Langenheder, S, Bertilsson, S, Tranvik, LJ**. 2003. Heterotrophic bacterial growth efficiency and community structure at different natural organic carbon concentrations. Appl Environ Microbiol **69**:3701–3709.

165. **Gasol, JM, Comerma, M, García, JC, Armengol, J, Casamayor, EO, Kojecká, P, Šimek, K**. 2002. A transplant experiment to identify the factors

controlling bacterial abundance, activity, production, and community composition in a eutrophic canyon-shaped reservoir. Limnol Oceanogr **47**:62–77.

166. **Pinhassi, J, Berman, T**. 2003. Differential growth response of colony-forming alpha- and gamma-proteobacteria in dilution culture and nutrient addition experiments from Lake Kinneret (Israel), the eastern Mediterranean Sea, and the Gulf of Eilat. Appl Environ Microbiol **69**:199–211.
167. **Haukka, K, Kolmonen, E, Hyder, R, Hietala, J, Vakkilainen, K, Kairesalo, T, Haario, H, Sivonen, K**. 2006. Effect of nutrient loading on bacterioplankton community composition in lake mesocosms. Microb Ecol **51**:137–146.
168. **Simek, K, Hornák, K, Jezbera, J, Nedoma, J, Vrba, J, Straskrábová, V, Macek, M, Dolan, JR, Hahn, MW**. 2006. Maximum growth rates and possible life strategies of different bacterioplankton groups in relation to phosphorus availability in a freshwater reservoir. Environ Microbiol **8**:1613–1624.
169. **Eiler, A, Bertilsson, S**. 2007. Flavobacteria blooms in four eutrophic lakes: linking population dynamics of freshwater bacterioplankton to resource availability. Appl Environ Microbiol **73**:3511–3518.
170. **Watanabe, K, Komatsu, N, Ishii, Y, Negishi, M**. 2009. Effective isolation of bacterioplankton genus *Polynucleobacter* from freshwater environments grown on photochemically degraded dissolved organic matter. FEMS Microbiol Ecol **67**:57–68.

171. **Hutalle-Schmelzer, KM, Zwirnmann, E, Krüger, A, Grossart, HP**. 2010. Enrichment and cultivation of pelagic bacteria from a humic lake using phenol and humic matter additions. FEMS Microbiol Ecol **72**:58–73.

172. **Jones, SE, Newton, RJ, McMahon, KD**. 2009. Evidence for structuring of bacterial community composition by organic carbon source in temperate lakes. Environ Microbiol **11**:2463–2472.

173. **Barbeyron, T, L'Haridon, S, Corre, E, Kloareg, B, Potin, P**. 2001. *Zobellia galactanovorans* gen. nov., sp. nov., a marine species of *Flavobacteriaceae* isolated from a red alga, and classification of [Cytophaga] *uliginosa* (ZoBell and Upham 1944) Reichenbach 1989 as *Zobellia uliginosa* gen. nov., comb. nov. Int J Syst Evol Microbiol **51**:985–997.

174. **Miyashita, M, Fujimura, S, Nakagawa, Y, Nishizawa, M, Tomizuka, N, Nakagawa, T, Nakagawa, J**. 2010. *Flavobacterium algicola* sp. nov., isolated from marine algae. Int J Syst Evol Microbiol **60**:344–348.

175. **Cai, H, Jiang, H, Krumholz, LR, Yang, Z**. 2014. Bacterial community composition of size-fractioned aggregates within the phycosphere of cyanobacterial blooms in a eutrophic freshwater lake. PLoS One **9**:e102879.

176. **Nedashkovskaya, OI, Kim, SB, Han, SK, Rhee, MS, Lysenko, AM, Rohde, M, Zhukova, NV, Frolova, GM, Mikhailov, VV, Bae, KS**. 2004. *Algibacter lectus* gen. nov., sp. nov., a novel member of the family *Flavobacteriaceae* isolated from green algae. Int J Syst Evol Microbiol **54**:1257–1261.

177. **Mann, AJ, Hahnke, RL, Huang, S, Werner, J, Xing, P, Barbeyron, T, Huettel, B, Stüber, K, Reinhardt, R, Harder, J, Glöckner, FO, Amann, RI,**

Teeling, H. 2013. The genome of the alga-associated marine flavobacterium *Formosa agariphila* KMM 3901T reveals a broad potential for degradation of algal polysaccharides. Appl Environ Microbiol **79**:6813–6822.

178. **Jezbera, J, Hornák, K, Simek, K**. 2005. Food selection by bacterivorous protists: insight from the analysis of the food vacuole content by means of fluorescence in situ hybridization. FEMS Microbiol Ecol **52**:351–363.
179. **Simek, K, Kasalicky, V, Jezbera, J, Jezberová, J, Hejzlar, J, Hahn, MW**. 2010. Broad habitat range of the phylogenetically narrow R-BT065 cluster, representing a core group of the Betaproteobacterial genus *Limnohabitans*. Appl Environ Microbiol **76**:631–639.
180. **Kasalický, V, Jezbera, J, Hahn, MW, Šimek, K**. 2013. The diversity of the *Limnohabitans* genus, an important group of freshwater bacterioplankton, by characterization of 35 isolated strains. PLoS One **8**:e58209.
181. **Zeng, Y, Kasalický, V, Šimek, K, Koblížeka, M**. 2012. Genome sequences of two freshwater betaproteobacterial isolates, *Limnohabitans* species strains Rim28 and Rim47, indicate their capabilities as both photoautotrophs and ammonia oxidizers. J Bacteriol **194**:6302–6303.
182. **Horňák, K, Kasalický, V, Šimek, K, Grossart, HP**. 2017. Strain-specific consumption and transformation of alga-derived dissolved organic matter by members of the *Limnohabitans*-C and *Polynucleobacter*-B clusters of *Betaproteobacteria*. Environ Microbiol **19**:4519–4535.

183. **Tsuneda, S, Miyauchi, R, Ohno, T, Hirata, A**. 2005. Characterization of denitrifying polyphosphate-accumulating organisms in activated sludge based on nitrite reductase gene. J Biosci Bioeng **99**:403–407.

184. **Schumann, P, Zhang, DC, Redzic, M, Margesin, R**. 2012. *Alpinimonas psychrophila* gen. nov., sp. nov., an actinobacterium of the family *Microbacteriaceae* isolated from alpine glacier cryoconite. Int J Syst Evol Microbiol **62**:2724–2730.

185. **Batut, J, Andersson, SG, O'Callaghan, D**. 2004. The evolution of chronic infection strategies in the alpha-proteobacteria. Nat Rev Microbiol **2**:933–945.

186. **Hahn, MW, Moore, ER, Höfle, MG**. 1999. Bacterial filament formation, a defense mechanism against flagellate grazing, is growth rate controlled in bacteria of different phyla. Appl Environ Microbiol **65**:25–35.

187. **Salcher, MM, Pernthaler, J, Psenner, R, Posch, T**. 2005. Succession of bacterial grazing defense mechanisms against protistan predators in an experimental microbial community. Aquat Microb Ecol **38**:215–229.

188. **Pagan, JD, Child, JJ, Scowcroft, WR, Gibson, AH**. 1975. Nitrogen fixation by *Rhizobium* on a defined medium. Nature **256**:406–407.

189. **O'gara, F, Shanmugam, KT**. 1976. Control of synbiotic nitrogen fixation in *Rhizobia*. Regulation of NH4+ assimilation. Biochim Biophys Acta **451**:342–352.

190. **Jones, KM, Kobayashi, H, Davies, BW, Taga, ME, Walker, GC**. 2007. How rhizobial symbionts invade plants: the Sinorhizobium-Medicago model. Nat Rev Microbiol **5**:619–633.

191. **Badri, DV, Weir, TL, van der Lelie, D, Vivanco, JM**. 2009. Rhizosphere chemical dialogues: plant-microbe interactions. Curr Opin Biotechnol **20**:642–650.

192. **Manhart, JR, Palmer, JD**. 1990. The gain of two chloroplast tRNA introns marks the green algal ancestors of land plants. Nature **345**:268–270.

193. **Kenrick, P, Crane, PR**. 1997. The origin and early evolution of plants on land. Nature **389**:33–39.

194. **Ellis, RJ**. 1979. The most abundant protein in the world. Trends Biochem Sci **4**:241–244.

195. **Spreitzer, RJ, Salvucci, ME**. 2002. Rubisco: structure, regulatory interactions, and possibilities for a better enzyme. Annu Rev Plant Biol **53**:449–475.

196. **Badger, MR, Kaplan, A, Berry, JA**. 1980. Internal inorganic carbon pool of *Chlamydomonas reinhardtii*: Evidence for a carbon dioxide-concentrating mechanism. Plant Physiol **66**:407–413.

197. **Spalding, MH**. 2008. Microalgal carbon-dioxide-concentrating mechanisms: Chlamydomonas inorganic carbon transporters. J Exp Bot **59**:1463–1473.

198. **Jansson, C, Northen, T**. 2010. Calcifying cyanobacteria--the potential of biomineralization for carbon capture and storage. Curr Opin Biotechnol **21**:365–371.

199. **Zhu, XG, Long, SP, Ort, DR**. 2008. What is the maximum efficiency with which photosynthesis can convert solar energy into biomass. Curr Opin Biotechnol **19**:153–159.

200. **Haystead, A, Robinson, R, Stewart, WD**. 1970. Nitrogenase activity in extracts of heterocystous and non-heterocystous blue-green algae. Arch Mikrobiol **74**:235–243.

201. **Gallon, JR**. 1981. The oxygen sensitivity of nitrogenase: a problem for biochemists and micro-organisms. Trends Biochem Sci **6**:19–23.

202. **Mouget, JL, Dakhama, A, Lavoie, MC, de la Noüe, J**. 1995. Algal growth enhancement by bacteria: Is consumption of photosynthetic oxygen involved? FEMS Microbiol Ecol **18**:35–43.

203. **Gurung, TB, Urabe, J, Nakanishi, M**. 1999. Regulation of the relationship between phytoplankton Scenedesmus acutus and heterotrophic bacteria by the balance of light and nutrients. Aquat Microb Ecol **17**:27–35.

204. **Shen, Y, Yuan, W, Pei, ZJ, Wu, Q, Mao, E**. 2009. Microalgae mass production methods. Trans ASABE **52**:1275–1287.

205. **Amer, L, Adhikari, B, Pellegrino, J**. 2011. Technoeconomic analysis of five microalgae-to-biofuels processes of varying complexity. Bioresour Technol **102**:9350–9359.

206. **Pulz, O**. 2001. Photobioreactors: Production systems for phototrophic microorganisms. Appl Microbiol Biotechnol **57**:287–293.

207. **Richmond, A**. 2004. Biological principles of mass cultivation, p 125-177. *In* Richmond A (ed). Handbook of Microalgae culture: biotechnology and applied physiology. Blackwell Publishing Ltd.

208. **Carvalho, AP, Meireles, LA, Malcata, FX**. 2006. Microalgal reactors: a review of enclosed system designs and performances. Biotechnol Prog **22**:1490–1506.

209. **Jorquera, O, Kiperstok, A, Sales, EA, Embiruçu, M, Ghirardi, ML**. 2010. Comparative energy life-cycle analyses of microalgal biomass production in open ponds and photobioreactors. Bioresour Technol **101**:1406–1413.

210. **Bérard, A, Dorigo, U, Humbert, JF, Martin-Laurent, F**. 2005. Microalgae community structure analysis based on 18S rDNA amplification from DNA extracted directly from soil as a potential soil bioindicator. Agron Sustain Dev **25**:285–291.

211. **Thompson, GA**. 1996. Lipids and membrane function in green algae. Biochim Biophys Acta **1302**:17–45.

212. **Zhekisheva, M, Boussiba, S, Khozin-Goldberg, I, Zarka, A, Cohen, Z**. 2002. Accumulation of oleic acid in *Haematococcus pluvialis* (Chloryceae) under nitrogen starvation or high lughr is correlated with that of astaxanthin esters. J Phycol **38**:325–331.

213. **Li, J, Han, D, Wang, D, Ning, K, Jia, J, Wei, L, Jing, X, Huang, S, Chen, J, Li, Y, Hu, Q, Xu, J**. 2014. Choreography of transcriptomes and lipidomes of *Nannochloropsis* reveals the mechanisms of oil synthesis in microalgae. Plant Cell **26**:1645–1665.

214. **Li, Y, Han, D, Sommerfeld, M, Hu, Q**. 2011. Photosynthetic carbon partitioning and lipid production in the oleaginous microalga

Pseudochlorococcum sp. (Chlorophyceae) under nitrogen-limited conditions. Bioresour Technol **102**:123–129.

215. **Wallace, J, Champagne, P, Hall, G, Yin, Z, Liu, X**. 2015. Determination of algae and macrophyte species distribution in three wastewater stabilization ponds using metagenomics analysis. Water **7**:3225–3242.
216. **Gour, RS, Chawla, A, Singh, H, Chauhan, RS, Kant, A**. 2016. Characterization and screening of native *Scenedesmus* sp. isolates suitable for biofuel feedstock. PLoS One **11**:e0155321.
217. **Hoshina, R, Kamako, SI, Imamura, N**. 2004. Phylogenetic position of endosymbiotic green algae in *Paramecium bursaria* Ehrenberg from Japan. Plant Biol (Stuttg) **6**:447–453.
218. **Arauzo, M, Colmenarejo, MF, Martínez, E, García, MG**. 2000. The role of algae in a deep wastewater self-regeneration pond. Water Res **34**:3666–3674.
219. **Salmaso, N, Morabito, G, Buzzi, F, Garibaldi, L, Simona, M, Mosello, R**. 2006. Phytoplankton as an indicator of the water quality of the deep lakes south of the Alps. Hydrobiologia **563**:167–187.
220. **Weckstrom, J, Korhola, A, Blom, T**. 1997. The relationship between diatoms and water temperature in thirty subarctic Fennoscandian lakes. Arctic and Alpine Research **29**:75–92.
221. **Narwani, A, Lashaway, AR, Hietala, DC, Savage, PE, Cardinale, BJ**. 2016. Power of plankton: Effects of algal biodiversity on biocrude production and stability. Environ Sci Technol **50**:13142–13150.

222. **Shurin, JB, Abbott, RL, Deal, MS, Kwan, GT, Litchman, E, McBride, RC, Mandal, S, Smith, VH**. 2013. Industrial-strength ecology: trade-offs and opportunities in algal biofuel production. Ecol Lett **16**:1393–1404.

223. **Lefcheck, JS, Byrnes, JE, Isbell, F, Gamfeldt, L, Griffin, JN, Eisenhauer, N, Hensel, MJ, Hector, A, Cardinale, BJ, Duffy, JE**. 2015. Biodiversity enhances ecosystem multifunctionality across trophic levels and habitats. Nat Commun **6**:6936.

224. **Smith, VH, McBride, RC**. 2015. Key ecological challenges in sustainable algal biofuels production. J Plankton Res **37**:671–682.

225. **Godwin, CM, Lashaway, AR, Hietala, DC, Savage, PE, Cardinale, BJ**. 2018. Biodiversity improves the ecological design of sustainable biofuel systems. Glob Change Biol Bioenergy.

226. **Amin, SA, Green, DH, Hart, MC, Küpper, FC, Sunda, WG, Carrano, CJ**. 2009. Photolysis of iron-siderophore chelates promotes bacterial-algal mutualism. Proc Natl Acad Sci U S A **106**:17071–17076.

227. **Ramanan, R, Kim, BH, Cho, DH, Oh, HM, Kim, HS**. 2016. Algae-bacteria interactions: Evolution, ecology and emerging applications. Elsevier **34**:14–29.

228. **Demain, AL**. 2007. The business of biotechnology. Ind Biotechnol **3**:269–283.

229. **Vu, CHT, Lee, HG, Chang, YK, Oh, HM**. 2018. Axenic cultures for microalgal biotechnology: Establishment, assessment, maintenance, and applications. Biotechnol Adv **36**:380–396.

230. **Xin, Y, Lu, Y, Lee, YY, Wei, L, Jia, J, Wang, Q, Wang, D, Bai, F, Hu, H, Hu, Q, Liu, J, Li, Y, Xu, J**. 2017. Producing designer oils in industrial

microalgae by rational modulation of co-evolving type-2 diacylglycerol acyltransferases. Mol Plant **10**:1523–1539.

231. **Xiao, R, Zheng, Y**. 2016. Overview of microalgal extracellular polymeric substances (EPS) and their applications. Biotechnol Adv **34**:1225–1244.
232. **Dunham, MJ**. 2007. Synthetic ecology: A model system for cooperation. Proc Natl Acad Sci U S A **104**:1741–1742.
233. **Shou, W, Ram, S, Vilar, JM**. 2007. Synthetic cooperation in engineered yeast populations. Proc Natl Acad Sci U S A **104**:1877–1882.
234. **Tatewaki, M**. 1989. A simple method of seaweed axenic culture. Korean J Phycol **4**:183–189.
235. **Jones, K, Rhodes, ME, Evans, SC**. 1973. The use of antibiotics to obtain axenic cultures of algae. Br Phycol J **8**:185–196.
236. **Shishlyannikov, SM, Zakharova, YR, Volokitina, NA, Mikhailov, IS, Petrova, DP, Likhoshway, YV**. 2011. A procedure for establishing an axenic culture of the diatom *Synedra acus* subsp. radians (Kütz.) Skabibitsch. from Lake Baikal. Limnol Oceanogr: Methods **9**:478–484.
237. **Westblade, LF, Ranganath, S, Dunne, WM, Burnham, CA, Fader, R, Ford, BA**. 2015. Infection with a chlorophyllic eukaryote after a traumatic freshwater injury. N Engl J Med **372**:982–984.
238. **Koike, K, Akai, N, Liao, LM, Ikeda, S, Yoshimatsu, S**. 2013. Chlorophycean parasite on a marine fish, *Sillago japonica* (Japanese sillago). Parasitol Int **62**:586–589.

239. **Xie, Y, Ho, SH, Chen, CN, Chen, CY, Ng, IS, Jing, KJ, Chang, JS, Lu, Y**. 2013. Phototrophic cultivation of a thermo-tolerant *Desmodesmus* sp. for lutein production: effects of nitrate concentration, light intensity and fed-batch operation. Bioresour Technol **144**:435–444.

240. **Samorì, G, Samorì, C, Guerrini, F, Pistocchi, R**. 2013. Growth and nitrogen removal capacity of *Desmodesmus communis* and of a natural microalgae consortium in a batch culture system in view of urban wastewater treatment: part I. Water Res **47**:791–801.

241. **Ji, F, Liu, Y, Hao, R, Li, G, Zhou, Y, Dong, R**. 2014. Biomass production and nutrients removal by a new microalgae strain *Desmodesmus* sp. in anaerobic digestion wastewater. Bioresour Technol **161**:200–207.

242. **Pan, YY, Wang, ST, Chuang, LT, Chang, YW, Chen, CN**. 2011. Isolation of thermo-tolerant and high lipid content green microalgae: oil accumulation is predominantly controlled by photosystem efficiency during stress treatments in *Desmodesmus*. Bioresour Technol **102**:10510–10517.

243. **Mayali, X, Azam, F**. 2004. Algicidal bacteria in the sea and their impact on algal blooms. J Eukaryot Microbiol **51**:139–144.

244. **Wu, YF, Wu, QL, Liu, SJ**. 2013. *Chryseobacterium taihuense* sp. nov., isolated from a eutrophic lake, and emended descriptions of the genus *Chryseobacterium*, *Chryseobacterium taiwanense*, *Chryseobacterium jejuense* and *Chryseobacterium indoltheticum*. Int J Syst Evol Microbiol **63**:913–919.

245. **Vandamme, P, Bernardet, J-F, Segers, P, Kersters, K, Holmes, B**. 1994. New perspectives in the classification of the Flavobacteria: Description of

Chryseobacterium gen. nov., *Bergeyella* gen. nov., and *Empedobacter* nom. rev. Int J Syst Evol Microbiol **44**:827–831.

246. **Weon, HY, Noh, HJ, Son, JA, Jang, HB, Kim, BY, Kwon, SW, Stackebrandt, E**. 2008. *Rudanella lutea* gen. nov., sp. nov., isolated from an air sample in Korea. Int J Syst Evol Microbiol **58**:474–478.

247. **Filippini, M, Svercel, M, Laczko, E, Kaech, A, Ziegler, U, Bagheri, HC**. 2011. *Fibrella aestuarina* gen. nov., sp. nov., a filamentous bacterium of the family *Cytophagaceae* isolated from a tidal flat, and emended description of the genus *Rudanella* Weon et al. 2008. Int J Syst Evol Microbiol **61**:184–189.

248. **Allen, TD, Lawson, PA, Collins, MD, Falsen, E, Tanner, RS**. 2006. *Cloacibacterium normanense* gen. nov., sp. nov., a novel bacterium in the family *Flavobacteriaceae* isolated from municipal wastewater. Int J Syst Evol Microbiol **56**:1311–1316.

249. **Cao, SJ, Deng, CP, Li, BZ, Dong, XQ, Yuan, HL**. 2010. *Cloacibacterium rupense* sp. nov., isolated from freshwater lake sediment. Int J Syst Evol Microbiol **60**:2023–2026.

250. **Barott, KL, Rodriguez-Brito, B, Janouškovec, J, Marhaver, KL, Smith, JE, Keeling, P, Rohwer, FL**. 2011. Microbial diversity associated with four functional groups of benthic reef algae and the reef-building coral *Montastraea annularis*. Environ Microbiol **13**:1192–1204.

251. **Hyun, DW, Shin, NR, Kim, MS, Kim, JY, Kim, PS, Oh, SJ, Whon, TW, Bae, JW**. 2014. *Cloacibacterium haliotis* sp. nov., isolated from the gut of an abalone, *Haliotis discus hannai*. Int J Syst Evol Microbiol **64**:72–77.

252. **Nouha, K, Kumar, RS, Tyagi, RD**. 2016. Heavy metals removal from wastewater using extracellular polymeric substances produced by *Cloacibacterium normanense* in wastewater sludge supplemented with crude glycerol and study of extracellular polymeric substances extraction by different methods. Bioresour Technol **212**:120–129.

253. **Nouha, K, Hoang, HV, Song, Y, Tyagi, RD, Surampalli, R**. 2016. Characterization of extracellular polymeric substances (EPS) produced by *Cloacibacterium normanense* isolated from wastewater sludge for sludge settling and dewatering. J Civil Environ Eng **5**:191.

254. **Stewart, JR, Brown, RM**. 1969. Cytophaga that kills or lyses algae. Science **164**:1523–1524.

255. **Glöckner, FO, Fuchs, BM, Amann, R**. 1999. Bacterioplankton compositions of lakes and oceans: a first comparison based on fluorescence in situ hybridization. Appl Environ Microbiol **65**:3721–3726.

256. **Kirchman, DL**. 2002. The ecology of Cytophaga-Flavobacteria in aquatic environments. FEMS Microbiol Ecol **39**:91–100.

257. **Qu, JH, Yuan, HL**. 2008. *Sediminibacterium salmoneum* gen. nov., sp. nov., a member of the phylum *Bacteroidetes* isolated from sediment of a eutrophic reservoir. Int J Syst Evol Microbiol **58**:2191–2194.

258. **Kim, YJ, Nguyen, NL, Weon, HY, Yang, DC**. 2013. *Sediminibacterium ginsengisoli* sp. nov., isolated from soil of a ginseng field, and emended descriptions of the genus *Sediminibacterium* and of *Sediminibacterium salmoneum*. Int J Syst Evol Microbiol **63**:905–912.

259. **Kang, H, Kim, H, Lee, BI, Joung, Y, Joh, K**. 2014. *Sediminibacterium goheungense* sp. nov., isolated from a freshwater reservoir. Int J Syst Evol Microbiol **64**:1328–1333.

260. **Ayarza, JM, Figuerola, EL, Erijman, L**. 2014. Draft genome sequences of type strain *Sediminibacterium salmoneum* NJ-44 and *Sediminibacterium* sp. strain C3, a novel strain isolated from activated sludge. Genome Announc **2**: e01073-13.

261. **Pinto, F, Tett, A, Armanini, F, Asnicar, F, Boscaini, A, Pasolli, E, Zolfo, M, Donati, C, Salmaso, N, Segata, N**. 2018. Draft genome sequences of novel *Pseudomonas*, *Flavobacterium*, and *Sediminibacterium* species strains from a freshwater ecosystem. Genome Announc **6**: e00009-18

262. **Dumestre, JF, Casamayor, EO, Massana, R, Pedrós-Alió, C**. 2002. Changes in bacterial and archaeal assemblages in an equatorial river induced by the water eutrophication of Petit Saut dam reservoir (French Guiana). Aquat Microb Ecol **26**:209–221.

263. **Trusova, MY, Gladyshev, MI**. 2002. Phylogenetic diversity of winter bacterioplankton of eutrophic siberian reservoirs as revealed by 16S rRNA gene sequence. Microb Ecol **44**:252–259.

264. **Singh, SK, Major, SR, Cai, H, Chen, F, Hill, RT, Li, Y**. 2018. Draft genome sequences of *Cloacibacterium normanense* IMET F, a microalgal growth-promoting bacterium, and *Aeromonas jandaei* IMET J, a microalgal growth-inhibiting bacterium. Genome Announc **6**: e00503-18

265. **Steenhoudt, O, Vanderleyden, J**. 2000. *Azospirillum*, a free-living nitrogen-fixing bacterium closely associated with grasses: Genetic, biochemical and ecological aspects. FEMS Microbiol Rev **24**:487–506.

266. **Somers, E, Ptacek, D, Gysegom, P, Srinivasan, M, Vanderleyden, J**. 2005. *Azospirillum brasilense* produces the auxin-like phenylacetic acid by using the key enzyme for indole-3-acetic acid biosynthesis. Appl Environ Microbiol **71**:1803–1810.

267. **Staley, JT, Konopka, A**. 1985. Measurement of in situ activities of nonphotosynthetic microorganisms in aquatic and terrestrial habitats. Annu Rev Microbiol **39**:321–346.

268. **Padmaperuma, G, Kapoore, RV, Gilmour, DJ, Vaidyanathan, S**. 2018. Microbial consortia: a critical look at microalgae co-cultures for enhanced biomanufacturing. Criti Rev Biotechnol **38**:690–703.